THE ANATOMICAL ORGANIZATION OF MUSCARINIC RECEPTOR SUBTYPES IN THE HUMAN EYE

by

NEERU GUPTA

MD., The University of Manitoba, 1986

A THESIS SUBMITTED IN PARTIAL FULFILLMENT OF

THE REQUIREMENTS FOR THE DEGREE OF

DOCTOR OF PHILOSOPHY

in

THE FACULTY OF GRADUATE STUDIES

(Department of Pathology)

We accept this thesis as conforming
to the required standard

THE UNIVERSITY OF BRITISH COLUMBIA
JUNE 1991

In presenting this thesis in partial fulfilment of the requirements for an advanced degree at the University of British Columbia, I agree that the Library shall make it freely available for reference and study. I further agree that permission for extensive copying of this thesis for scholarly purposes may be granted by the head of my department or by his or her representatives. It is understood that copying or publication of this thesis for financial gain shall not be allowed without my written permission.

Department of Pathology

The University of British Columbia
Vancouver, Canada

Date June 4th, 1991

Abstract

To help determine the sites of action of cholinergic drugs in man, for the first time, in vitro autoradiographic techniques were employed to characterize the anatomical distributions of muscarinic acetylcholine binding sites and three different muscarinic receptor subtypes in the post-mortem human eye. Additional studies included in situ hybridization localization of one of the muscarinic receptor subtypes, and the examination of the distributions of two second messenger molecules of the inositol phosphate pathway to which several muscarinic receptor subtypes are believed to be coupled . To localize non-subtype specific muscarinic receptor binding sites, in vitro autoradiography was performed on anatomically intact sections of the human eye using the radioligand [^{3}H]quinuclydinyl benzylate (QNB). Muscarinic binding sites were detected in the ocular smooth muscles and the ciliary epithelium in the anterior segment of the eye, but not in the cornea. They were also localized in the retina, retinal pigment epithelium and choroid of the posterior segment. These qualitative results were consistent among all the different eye specimens studied, however there were marked variations in the quantitative densitometric measurements of the relative amounts of binding between different donor eyes.

To specifically localize M1, M2, and M3 muscarinic receptor subtype binding sites, [^{3}H]pirenzipine, [^{3}H]oxotremorine, and [^{3}H]4-diphenylacetoxy-N-methyl-piperidine methiodide ([^{3}H]4DAMP) were used respectively. In the anterior segment, [^{3}H]pirenzipine binding sites (M1) were found in the iris, ciliary muscle, and ciliary epithelium while [^{3}H]oxotremorine binding sites (M2) were specifically localized only in the longitudinal portion of the ciliary muscle. The distribution of M3 binding sites determined indirectly by [^{3}H]DAMP competition with pirenzipine was in all structures labelled by [^{3}H]QNB, and in addition, was detected in both the corneal epithelium and the actively dividing cells of the lens epithelium. In the posterior segment, both

[^{3}H]pirenzipine and [^{3}H]oxotremorine binding sites were specific for the retina only, in contrast to the M3 binding sites found in the retina, retinal pigment epithelium, and choroid.

As the distribution of M3 binding sites was determined indirectly by [^{3}H]DAMP competition with pirenzipine, this subtype was further explored at the mRNA level. Northern Blot Hybridization on total RNA extracted from the human eye anterior segment was performed using a [^{32}P] m3 oligonucleotide, and detected a single transcript. By *in situ* hybridization, using an [^{35}S] m3 oligonucleotide, the m3 mRNA was localized in the same structures identified as having M3 binding sites, and in addition, was detected in the trabecular meshwork and corneal endothelium.

Two second messenger molecules, IP3 receptor and PKC were localized by in vitro autoradiographic studies with [^{3}H]inositol (1,4,5) triphosphate and [^{3}H]phorbol-12, 13-dibutyrate. They were found in all of the structures found to localize M1 and M3 muscarinic receptor subtypes.

Muscarinic receptor subtypes were localized by in vitro autoradiography and in situ hybridization. The results may be valuable to understanding the effects and side effects of cholinergic drug therapy, to the rationalization of new therapeutic strategies in diseases of the eye, and to the further research of these and other receptors in normal and pathologically affected human donor eyes.

TABLE OF CONTENTS

Abbreviations and Symbols

Ach	acetylcholine
B_{max}	total number of bound sites
BSA	bovine serum albumin
^{o}C	degrees celsius
Ca^{++}	calcium
$CaCl_2$	calcium chloride
Ci/mmol	curies per millimole
cDNA	complementary deoxyribonucleic acid
cm	centimetre
cpm	counts per minute
DNA	deoxyribonucleic acid
dpm	disintegrations per minute
EDTA	ethylenediaminetetraacetic acid disodium salt
Fig.	figure
fmol/mg	femtomoles per milligram
G proteins	guanine nucleotide-binding regulatory proteins
gm	gram
$[^3H]$	tritium-labelled
HEPES	N-2-hydroxyethylpiperazine-N'-2-ethanesulfonic acid
IP3	inositol triphosphate
K^+	potassium
K_D	affinity constant
Kb	kilobase
K_{+1}	association constant

K_{-1}	dissociation constant
Mg	magnesium
mg	milligram
min.	minutes
ml	millilitre
mM	millimole
mm	millimetre
MOPS	3-(N-morphoino) propanesulphonic acid
mRNA	messenger ribonucleic acid
Na	sodium
nM	nanomolar
OD	optical density
PBS	phosphate buffered saline
PKC	protein kinase C
pM	picamolar
PMSF	phenylmethylsulfonylchloride
QNB	quinuclidinyl benzilate
RNA	ribonucleic acid
RPE	retinal pigment epithelium
rpm	revolutions per minute
SA	radiolabel specific activity
SDS	sodium dodecyl sulfate
S.E.	standard error
Tris-HCL	Trizma-Hydrochloride
TEA	triethanolamine
µl	microlitre
µm	micrometre

List of Tables

List of Figures

Acknowledgements

I would like to dedicate this thesis to those people who donated their precious eyes to research, without whom this work could not have been possible. For initiating the opportunity to pursue this Ph.D., and for his continued consistent support and watchfulness throughout the course of this work, I thank Dr. J. Rootman. I am grateful to Dr. M.S. Cynader for his guidance and enthusiasm for the project, and to Dr. S.M. Drance for his continued interest. For their assistance during various stages of the work, I thank Dr. C. Shaw, Rob McAllister and Dr. S. Prasad. For their helpful suggestions, I would like to thank my committee members: Dr. A. Autor, Dr. J.C. Hogg, Dr. R.S. Molday and Dr. V.White, and Dr. P. Kaufman with the University of Wisconsin. For their loving support, I am indebted to my parents, to Kaypee and Sonya, and to my friends.

It is to Dr. C.K. Gupta and Dr. N.D. Gupta that I owe my inspiration.

CHAPTER 1: INTRODUCTION

" What are the distributions of muscarinic receptor subtype binding sites in the human eye ?" has been the question that has driven this thesis work. In order to understand the nature of the ocular cholinergic system in the eye, it is important to be familiar with its neurochemical organization. The anatomical localization of the specific receptors with which cholinergic drugs interact, is fundamental to determining their primary sites of action in the eye. Recent technological advances in pharmacology and molecular biology have provided the tools with which to localize muscarinic receptor binding sites in post-mortem eye tissue, and have also expanded previous knowledge about muscarinic receptor subtypes. In order that the reader understand the initial and ongoing interest behind the experimental work undertaken to describe the anatomical organization of muscarinic receptor subtypes in the human eye, I would like to start this thesis with some general background information. The main topics to be covered include: advances and importance of receptor identification and localization, the general functional diversity of muscarinic receptors, the muscarinic cholinergic system in the eye and its exploitation in ophthalmological conditions including glaucoma, pharmacological and molecular biological evidence for muscarinic receptor diversity, second messenger systems in general, muscarinic receptor subtypes coupling to second messengers, and the importance of localizing muscarinic receptor subtypes in the human eye.

Background

Much of modern pharmacology derives from attempts to understand and to exploit the regulatory proteins involved in the translation of extracellular signals into intracellular physiological events. Many of these proteins are components of plasma membranes and serve as receptors for neurotransmitters, hormones, and a multitude of drugs. The capacity of cells to discriminate between numerous extracellular chemical stimuli is through the presence of highly selective receptors, which recognize a given chemical signal. This is the first step in the signal transduction process through which cell responses are mediated.

The elucidation of physiological receptors in the eye depends heavily on pharmacological tools such as drugs and ligands. Thus, much of our understanding of the regulation of ocular pharmacology comes from observations of functional ocular responses to the actions of drugs. In spite of this, the functions of ocular cells types in the eye are poorly understood with respect to underlying molecular mechanisms. This has hampered interpretations of both therapeutic and adverse ocular drug effects, and the ability to rationally design new pharmacological strategies.

Before the mid 1970's, there were few ways in which to study the interaction of neurotransmitters, hormones, or drugs with cells. The most widely used approach was to observe the functional response to applied agonists and antagonists in an intact isolated organ, for example, the ciliary muscle. This method has provided an important wealth of information

regarding the efficacy and functional activity of agonists on various tissues in the eye. The experimental approach to the study of receptors was improved substantially in the mid-1970's with the introduction of direct radioligand binding (1,2), a technique that uses labelled drugs with high specific radioactivity, and a high affinity for the receptor, allowing the identification and study of receptors directly. Since then, receptors have become a central focus of investigation of drug effects and their mechanisms of action.

The cholinergic system of the eye regulates numerous functions, including the lowering of intraocular pressure. This is the therapeutic goal of medical therapy in the treatment of glaucoma. However, the exact mechanisms by which most normal ocular events occur in response to cholinomimetics are far from understood.

Acetylcholine and Muscarinic Receptors

In the eye, acetylcholine is the neurotransmitter of the parasympathetic division of the autonomic nervous system, and in general, regulates the activities of structures that are not under voluntary control. To describe those neurons which liberate Ach, Dale in 1954, proposed the terms *cholinergic*. He further classified "cholinoceptive" postjunctional sites acted upon by Ach into muscarinic-like and nicotinic-like, based on the effects of two alkaloids, muscarine and nicotine (3). By convention, the

cholinomimetic effects of Ach and related drugs at autonomic effector cells are referred to as muscarinic effects. These effects are initiated by their interaction with muscarinic receptors.

Muscarinic receptors found in many different cell types (4), are involved in numerous physiological processes. They are involved in nerve-to-nerve transmission, and a variety of neurons in both the central and peripheral nervous systems express muscarinic receptors (5). Most smooth muscles contain muscarinic receptors that in general mediate contraction (6, 7). In cardiac muscle, muscarinic receptors decrease the rate and strength of contraction (8). Most endocrine cells have muscarinic innervation, (9), and muscarinic receptors are also found on exocrine gland cells throughout the body (10, 11). Various cell types in the lung (12) and gastrointestinal tract (7, 10) also have muscarinic receptors. As will be shown later, muscarinic receptors are also found on many ocular structures.

The identification and localization of muscarinic receptors in these systems has been an important step toward increasing the clinical usefulness of muscarinic receptor agonists and antagonists in many pathological processes. Those agonists and antagonists have been used therapeutically for many years (3), and although the list is exhaustive, their numerous applications in various organ systems include anti-tremor treatment in Parkinsonian patients, the stimulation of contraction in urinary bladder hypotonia, the reduction of airway resistance in patients with chronic obstructive lung disease, the reduction of acid secretion in peptic ulcer disease, and the lowering of intraocular pressure in glaucoma.

Although the presence of muscarinic receptors in tissues throughout the body often lends the same drugs to numerous clinical uses, this usefulness is at the same time limited, because often the therapeutic effects in one tissue are accompanied by undesired effects in others.

Cholinergic System of the Eye

The presence in the human eye of all the elements of a strong cholinergic input is supported by a wealth of experimental data. Its rich parasympathetic innervation has been histologically studied, with the nerve fibres originating predominantly from the Edinger-Westphal nucleus, localized in the postero-superior part of the oculomotor complex in the midbrain, and synapsing in the ciliary ganglion. Most of the continuing postganglionic parasympathetic fibers terminate in the ciliary muscle and the iris. Acetylcholine has been detected in many different ocular structures, including the cornea, iris, ciliary body, retina, choroid, retinal pigment epithelium, and retina (13-19). Biochemical binding techniques (1,2) have identified muscarinic receptors in the eyes of many non-human species.

The functional responses of the smooth muscles, the iris sphincter and the ciliary muscle, to topically or systemically applied muscarinic agonists and antagonists, can be predicted from their neuroanatomy. When bound by muscarinic agonists, muscarinic receptors located on these muscle cells

transduce the chemical signal and the effects are pupillary constriction (miosis), cyclotonia, and accomodation. Accordingly, antimuscarinic agents induce mydriasis, cycloplegia, and loss of accomodation. In the clinical setting, these agents are used daily in the diagnosis and treatment of variety of ophthalmic disorders.

Pupillary constriction in response to Ach instillation into the eye was first noted in 1949 (20), and since then, miotic therapy with cholinomimetics has had wide applications in ophthalmologic settings. The clinical use of Ach was first reported in routine cataract extraction post-operatively (21) and today, muscarinic agonists are routinely used for their miotic effects in the post-operative management of numerous ocular procedures. In addition, miotics are often alternated with mydriatics in order to break or prevent the development of adhesions between the iris and the lens that form as a result of inflammatory conditions such as iritis. Cholinergic agents are also useful in overcoming the effects of a previously administered mydriatic such as atropine.

Atropine effectively and reversibly blocks the activation of muscarinic receptors in parasympathetically innervated ocular structures. An extract of the plant Atropa belladonna, this alkaloid was used during the Renaissance to dilate pupils for cosmetic purposes, and thus its name belladonna (Italian, " beautiful lady "). Administered topically, or in ointment form, antimuscarinics are widely used in the practice of ophthalmology, and for the most part, the smooth muscles of the anterior segment of the eye are the targets of their therapeutic actions. Ciliary

muscle paralysis is often indicated in the case of young patients in whom accurate measurement of refractive error is desired. When prolonged effect is indicated, as in inflammatory conditions such as uveitis and iritis for the prevention of synechiae formation between the lens and iris, antimuscarinics are used to paralyze the iris sphincter muscle resulting in pupillary dilatation (mydriasis).

Apart from the benefits of miotic therapy brought about by the direct action of muscarinic agonists on iris smooth muscle, these agents also lower intraocular pressure. Historically, this has been exploited in the treatment of chronic open-angle glaucoma. Thus cholinergic agents are a mainstay of therapy in glaucoma today. Although the mechanism by which this occurs has long been speculative, it is now known that muscarinic agonists lower intraocular pressure by enhancing aqueous outflow. The topical administration of muscarinic agonists in the monkey and human increases outflow facility (22, 23), while muscarinic antagonists have the opposite effect (24, 25, 26). In addition, voluntary accomodation in the human (27)., and electrical stimulation of the cat third nerve have both been shown to increase outflow facility (28, 29).

Although these studies suggest that the intrinsic ocular smooth muscles are involved in the lowering of intraocular pressure, recent investigations to determine the respective contributions of the iris and of the ciliary muscle, have shown that the ciliary muscle and not the iris is responsible for enhancing the outflow of aqueous humour (30, 31, 32, 33). It is now well accepted that indeed ciliary muscle contraction increases the outflow

facility seen after cholinergic drug administration, in the absence of an apparent direct effect on the trabeculum, and thus, the ciliary muscle is the therapeutic target of cholinergic therapy in glaucoma. Predicted by the anatomy of ciliary muscle attachment to the trabecular meshwork, the proposed mechanism is the contraction of a specific bundle of fibres located most anteriorly within the muscle, and referred to as the longitudinal ciliary muscle. The tendons of these fibres insert into the trabecular meshwork (Figure 1). The mechanism of augmented bulk outflow is considered to be an alteration of the anatomical disposition of the trabecular meshwork; however, how and where this modification occurs is unknown.

Although it is clear that cholinergic therapy has numerous applications in the clinical setting, it is often limited by the general effects that it produces. For example, in conditions in which constriction of the pupil is desired, cholinomimetics prove very useful. However, in the treatment of open angle glaucoma, the miotic effect of these agents is undesirable, and is considered a "side effect". The decrease in vision secondary to miosis may preclude the use of these agents in elderly patients with already decompensated vision due to lens changes. The commonest causes of treatment failure in the young are the often severe local side effects such as accomodative spasm. Although less common deleterious effects of these agents have been documented, it is likely that many other intraocular processes are affected, the nature of which is as yet unknown.

Additional problems arise in situations where long-term cholinergic maintenace therapy is required, as in chronic open-angle glaucoma. As a

Figure 1

Diagram of the ciliary muscle and the relationship of the longitudinal portion to the trabecular meshwork. Contraction of this muscle improves outflow of aqueous humour.

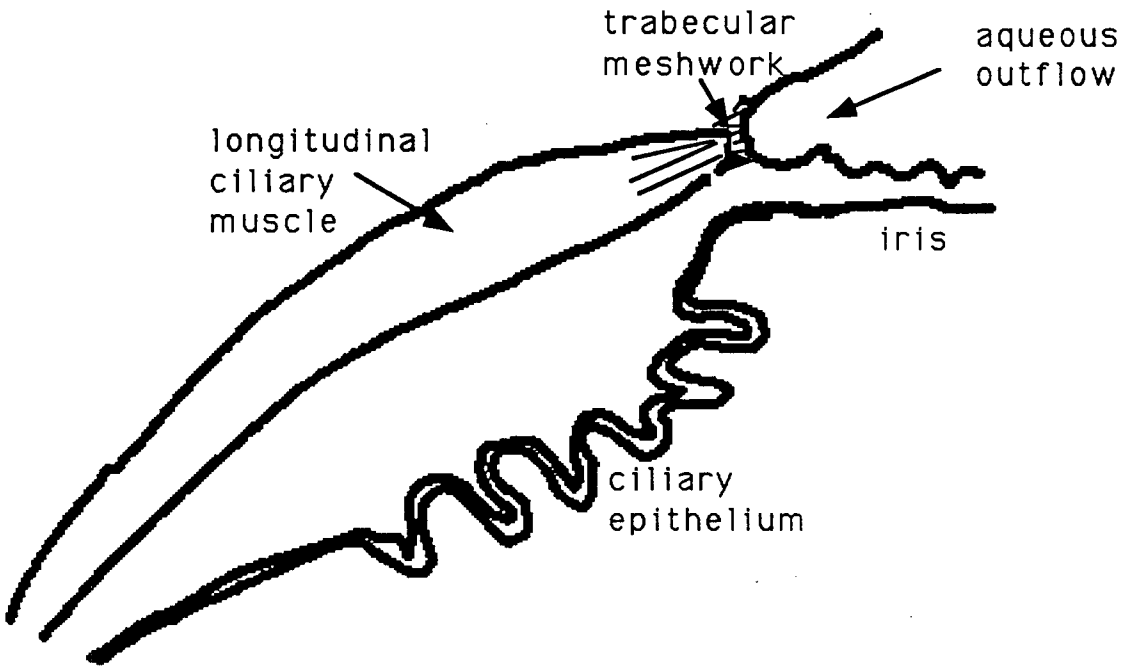
trabecular
meshwork
aqueous
outflow
longitudinal
ciliary
muscle
iris
ciliary
epithelium

consequence of long-term drug administration, not infrequently, the intensity of effect of a given dose is decreased. Although the mechanism by which subsensitivity occurs is not clear, it is thought that the target tissue may be adapting to changes in stimulation by decreasing its muscarinic receptor numbers (34), its second messenger coupling efficiency (35), or both.

Although the great utility of these cholinergic drugs is not to be denied, it would be an advantage to have a drug that accomplished the same therapeutic goal in a more selective way. In the last 10 to 15 years, considerable advances have been made in neuropharmacology and molecular biochemistry. Pharmacological refinements have facilitated more accurate recognition of receptor molecules allowing much greater ability to identify and discriminate between different receptor subtype populations. Advances in molecular biology, through the cloning of receptor molecules, have provided definitive evidence as to whether a single receptor subtype represents a distinct gene product. In addition, it has provides a way in which the genetic material (mRNA) encoding a receptor protein can be identified. These recent advances have already greatly increased our understanding of the role of muscarinic receptors in the physiological and pathophysiological settings of numerous organ systems, and may be of considerable value in understanding cholinergic-mediated processes in the eye.

Muscarinic Receptor Diversity: Pharmacological and Molecular Evidence

Until recently, all acetylcholine muscarinic receptors were thought to be alike. In the last decade however, it has been shown that these receptors form a heterogeneous population. Evidence for this was initially pharmacological in origin. Those receptors having high affinity for pirenzipine were classified as M1 muscarinic receptors (36, 37), and those with low affinity for Pirenzipine were called muscarinic M2 receptors. Evidence has been presented to suggest that the latter are not a homogeneous group (38) and more recently, muscarinic receptors classifications include an M3 subtype (39). The distinction between M1 and other muscarinic subtypes has been further strengthened by evidence for predominant associations of different muscarinic subtypes with differing effector systems. The dominant pattern that has emerged in signal transduction pathways, is one that supports M1 and M3 receptor coupling to inositol phosphate, and M2 coupling to adenylate cyclase (40). Progress in identifying the M1, M2, and M3 muscarinic receptor subtypes has been made by using receptor subtype-specific pharmacological ligands.

The most recent and definitive evidence for multiple muscarinic receptors has come from genetic cloning techniques delineating at least five different muscarinic subtypes (41, 42, 43). The nomenclature for the molecular forms has been denoted by the lowercase m's, m1 to m5 (41, 42), in contrast to the upper case M1, M2, and M3 muscarinic subtypes identified pharmacologically.

The muscarinic receptors belong to the growing family of seven-helix

receptors in which are included the rhodopsin and beta adrenergic receptors, with an extracellular amino terminus and an intracellular carboxy terminus (44-48). The features of signal transduction common to this group of receptors include binding the ligand extracellularly, and transduction of the signal through intermediary cytoplasmic guanosine triphosphate -binding proteins or G proteins (49). The shared structure of these receptor proteins by hydropathicity analysis (50) is a single chain of amino acids that are thought to span the membrane seven times, creating four extracellular and four intracellular loops (Figure 2). Thought to be important in the binding of Ach, the transmembrane domains are highly conserved among the five human muscarinic receptor subtypes (48, 51). Where these receptors diverge dramatically, is in the large third intracellular loop connecting the 5th and the 6th transmembrane domains (52). It is this region that is thought to confer the differential capacity of muscarinic subtypes to couple to distinct biochemical effectors or ion channels (53). Moreover, the most distal ends of the loop appear to be involved in the selective G-protein coupling of the receptor subtypes (54). Consistent with the primary G-protein specificity of the subtypes in this region (40, 42), the m1, m3, and m5 molecular species share the greatest amino acid homologies, as do the m2 and m4 species.

The relationship between the ligand binding site, and the molecular nature of the mRNA encoding the receptor has been examined, and although not unambiguously proven, from the testing of a number of selective antagonists on cell lines expressing individual cloned receptors

Figure 2

An illustration of the shared general amino acid structure of the muscarinic receptor subtypes, m1 to m5. (Peralta et al, The EMBO Journal. **6**(13): 3923-3929, 1987)

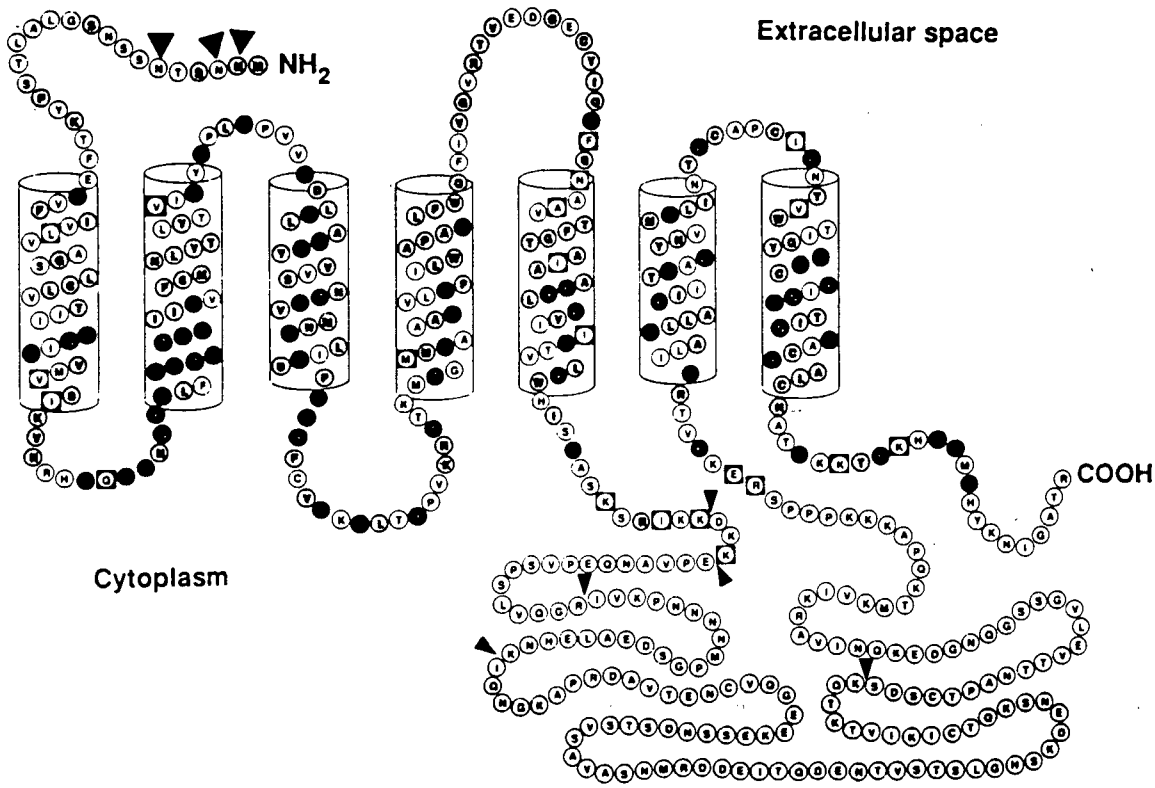
NH2
Extracellular space
COOH
Cytoplasm

(55), it appears that the m1 sequence corresponds to that of the M1 receptor, m2 to the M2 receptor and m3 to the M3 receptor. The pharmacology of the candidate M4 receptor as well as that of the expressed m4 and m5 species, while being different from M1, M2, and M3 receptors, have not been characterized well enough to allow a definite assignment of a pharmacological M4 (or M5) receptor subtype.

Second Messenger Systems

The examination of surface receptors in relation to the intracellular consequences of receptor activation is crucial to understanding the relationship between a given drug or neurotransmitter, the membrane receptor, and eventual cell response. The membrane receptor, once bound by the neurotransmitter or drug, must communicate the information intracellularly. It does this via two ubiquitous transmembrane signalling systems, also known as the adenylate cyclase and inositol triphosphate second messenger systems (Figure 3).

The adenylate cyclase system is well accepted as a major transmembrane signalling system, pioneered by the discovery of cyclic AMP in the 1950's by Earl Sutherland and Theodore Rall. Stimulation of the adenylate cyclase enzyme, leads to the formation of cAMP. Receptors that produce their actions via the adenylate cyclase pathway first interact with a guanyl nucleotide binding protein (G protein). The receptors linked or coupled to

Figure 3

An illustration of receptor-mediated signal transduction pathways following the activation of adenylate cyclase and phospholipase C.

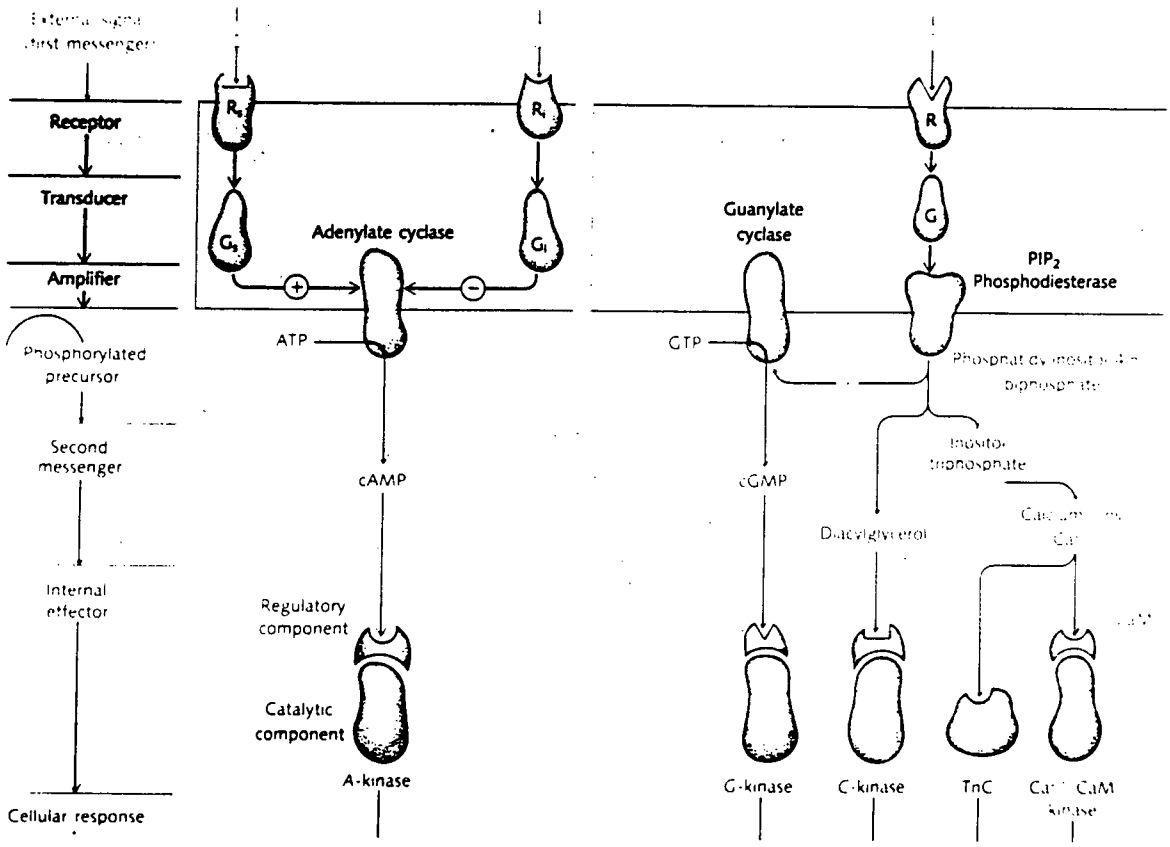
Receptor
Transducer
Amplifier
Phosphorylated precursor
Second messenger
Internal effector
Cellular response
Adenylate cyclase
ATP
cAMP
Regulatory component
Catalytic component
A-kinase
Guanylate cyclase
GTP
cGMP
G-kinase
PIP2 Phosphodiesterase
Diacylglycerol
C-kinase
TnC

the adenylate cyclase system may act in a stimulatory or inhibitory fashion, and do so via their interaction with different G proteins that either stimulate (Gs) or inhibit (Gi) the catalytic unit (C) of the enzyme. Although the exact mechanism by which this system operates is not known, the molecular properties of this system have become increasingly clear in the last decade. Both the Gs and Gi proteins have been purified to homogeneity (49, 56, 57) and more recently, have been sequenced and cloned (58).

In the past 5 years, the inositol triphosphate (IP3) molecule has received wide appreciation as another major second messenger, and is now believed to be an integral component of many signal transduction processes linked to intracellular calcium mobilization (59, 60). The stimulus for IP3 formation in a cell is the activation of a cell membrane receptor by a neurotransmitter or drug. This initiates activation of a membrane enzyme called phospholipase C (PLC), which triggers the breakdown of a phospholipid cell membrane component called phosphatidylinositol 4,5-biphosphate (PIP2), into IP3. Like the adenylate cyclase system, the interface between transmitter receptors and the phosphoinositide system is composed of G proteins. The accumulation of the IP3 molecule in the cell causes the release of intracellular calcium stores most likely from the endoplasmic reticulum (61). Intracellular calcium can regulate cell function in many ways.

In addition to IP3 formation, PLC activity leads to the fomation of another product called diacylglycerol (DAG). DAG is often referred to as the second limb of this PLC mediated pathway. DAG activates protein

kinase C (PKC), a phosphorylating enzyme of numerous proteins involved in signal transduction ultimately leading to cell response (62).

Second Messenger Coupling To Muscarinic Receptor Subtypes

Atempts to define differences in the functional properties of muscarinic receptor subtypes have led to the observation that muscarinic receptors do differ in their ability to regulate second messenger formation. On the basis of the functional responses of individual muscarinic subtypes, two categories have been established, one containing the odd numbered species (m1, m3, m5), with the even numbered in the other (m2, m4).

Measurements of agonist-induced responses in Xenopus oocytes and NG108-15 neuroblastoma-glioma hybrid cells expressing the individual mAChR species, demonstrate that the m1, m3, and m5 receptors, albeit not exclusively, couple to the same effector system. In general, these receptors stimulate the metabolism of inositol phosphates through a pertussis toxin-insensitive G protein and also stimulate the release of arachidonic acid, although via independent pathways (63, 64, 65, 66). This general pattern for the odd numbered species has also been shown for four human mAChR subtypes in transfected human kidney cell lines (40). Although these receptors have also been shown to stimulate an increase in cyclic AMP levels, it appears that this effect is secondary to inositol phosphate accumulation (64), as it is known that both IP3 and DG, products of PI

hydrolysis, increase intracellular calcium and protein kinase C, which then activates adenylate cyclase (62, 67, 68, 69). On the other hand, in the same cell lines, the m2 and m4 even numbered receptor subtype species cause a decrease of cAMP through a pertussis toxin-sensitive G protein. Occasionally however these even numbered species have also been shown to weakly stimulate the inositol phosphate response, and although the mechanism is unclear, it may be that these receptors do not have absolute selectivity for a single G protein.

The evidence for multiple muscarinic receptor subtypes which appear to be functionally different based on their coupling with distinct effector systems has tremendous implication in our further understanding of the muscarinic mediated physiological and pathophysiological processes in the eye. A knowledge of the differences between these receptor subtypes at the molecular level has already produced new and highly selective pharmacological tools with which to understand their functions. This, and a knowledge of the specific location of the muscarinic receptor subtypes, makes it possible to direct drug therapy toward the appropriate subtype, with potentially new therapeutic cholinergic strategies in clinical medicine.

As yet, the identification and localization of the muscarinic receptor subtypes is relatively unexplored in human ocular tissues. In the chapters succeeding General Methods (Chapter 2), the systematic localization of several muscarinic acetylcholine receptor subpopulations and second messenger molecules in donor human eyes will be described in the following manner: distributions of non-subtype specific muscarinic

receptors, and the M1, M2, M3 muscarinic receptor subtypes pharmacologically determined by in vitro autoradiography studies, distribution of the messenger RNA for the M3 muscarinic receptor subtype by the molecular biological approach of in situ hybridization, and localization of second messenger molecules PKC and IP3 receptor by in vitro autoradiography. I will conclude the thesis with a general discussion of the results of these studies and their implications.

CHAPTER 2: GENERAL METHODS

Specimens

The experiments reported in this thesis utilized the eyes of 35 human donors, obtained post-mortem from the Eye Bank of British Columbia as outlined in Table 1. We established several criteria for investigations performed on these specimens. Whole eye globes from patients having no documented history of acquired or hereditary ocular disease, of either sex, and between the ages of 24 years and 75 years., were accepted within a post-mortem interval not exceeding 12 hours, during which time the eyes were kept at $4^{o}C$ following enucleation. The 12 hour period limit was decided on the basis of receptor autoradiography experiments which indicated that eyes used beyond this time limit (included in Table 1), had significant artifactual binding.

General Processing of Whole Globes

Upon receipt, each pair of donor eyes was oriented using anatomical landmarks to identify the superior and inferior aspects of the left and right globes. Beginning with the superior aspect of the globe,

SEX/ AGE (yrs)	POST-MORTEM INTERVAL(hrs)	CAUSE OF DEATH	[3H] QNB	[3H] PIREN-ZIPINE	[3H] OXOTREM-ORINE	[3H] 4-DAMP	[3H] PDBU	[3H] IP3	[32P] m3 OLIGO	TOTAL RNA EXTRACTION
M/30	7	CARDIOVASCULAR ACCIDENT			*					
M/88	7	MYOCARDIAL INFARCTION	*	*	*					
M/61	8	MYOCARDIAL INFARCTION		*	*		*			
F/51	9.5	PULMONARY EMBOLUS	*	*	*		*	*		
M/61	9.5	DROWNING	*	*						
F/48	9.5	BREAST CANCER					*	*		
M/62	10	CARDIOMYOPATHY							*	
M/63	11.5	BREAST CANCER	*	*	*		*	*	*	
M/75	12	DIABETES	*						*	
M/59	13	LUNG CANCER	*	*		*	*	*	*	
M/66	14	CHRONIC RENAL FAILURE		*			*			
M/66	14	CHRONIC RENAL FAILURE	*							
M/57	17.5	MYOCARDIAL INFARCTION	*	*						
F/50	17.5	SUBARACHNOID HAEMORRHAGE	*							
M/60	19.5	SUBARACHNOID HAEMORRHAGE	*							
F/37	26	BRONCHOPNEUMONIA	*							
M/57	30	MYOCARDIAL INFARCTION	*							
M/64	44	CONGESTIVE HEART FAILURE	*							

SEX/ AGE (yrs)	POST-MORTEM INTERVAL(hrs)	CAUSE OF DEATH	[3H] QNB	[3H] PIREN-ZIPINE	[3H] OXOTREM-ORINE	[3H] 4-DAMP	[3H] PDBU	[3H] IP3	[32P] m3 OLIGO	TOTAL RNA EXTRACTION
M/62	1.5	CARDIOVASCULAR ACCIDENT								*
M/72	2.5	CARCINOMA OF OROPHARYNX				*	*	*	*	
M/72	2.5	MYOCARDIAL INFARCTION								*
M/75	3	BRAIN TUMOUR (GLIOBLASTOMA)	*	*		*	*	*		
M/40	3.5	MYOCARDIAL INFARCTION		*	*		*	*		
M/71	4.5	LUNG CANCER	*		*					
F/45	4.5	BREAST CANCER								*
M/58	5	LUNG CANCER				*				
F/42	5	CERVICAL CANCER	*	*	*		*	*	*	
M/41	5	MULTIPLE SCLEROSIS		*	*	*	*	*		
M/39	5	MYOCARDIAL INFARCTION		*			*	*		
F/41	5	MULTIPLE SCLEROSIS	*	*	*					
M/42	6	LUNG CANCER		*				*		
F/46	7	BREAST CANCER	*	*		*	*	*	*	
M/34	7	BRONCHOPNEUMONIA		*	*	*	*	*		

24 b

approximately 1.0 cm posterior to the limbus (Fig. 4), sterile microsurgical instruments were used to create an opening of approximately 1 cm length in the sclera, exposing the vitreous. This was frozen by apposition with a metallic spatula dipped in liquid isopentane cooled to -80°C, and an additional opening performed on the inferior aspect of the globe. The globe was gradually lowered (1 min.) into liquid isopentane cooled to -80°C on dry ice until fully immersed, while vitreous was seen to extrude through the opening. The hole made in the sclera was necessary to allow an escape route for the expanding vitreous, thereby removing the risk of breaking weak anatomical connections within the globe, maintaining its overall anatomical integrity. Each eye was individually wrapped in plastic wrap, then aluminum foil, labelled, and stored at -20°C until further use.

Tissue Preparation For In Vitro Autoradiography

The advantage of this technique was the ability to study the distributions of receptors in anatomically intact ocular tissue sections. This was performed in the absence of tissue fixation. The globes were mounted onto a cryostat chuck with Tissue Tek (O.C.T. Miles, Inc.) and positioned for sectioning in a Reichert-Jung cryostat set at between -18°C to -23°C. Using a sharpened Reichert microtome knife, frozen tissue sections were cut on a cryostat at a thickness of 20 μm and

Figure 4

Whole globe of a post-mortem human eye before freezing.

mounted onto subbed glass slides (1% gelatin, 0.001% chromium potassium oxide). To permit maximal inspection of most ocular structures, the antero-posterior horizontal plane was used in sectioning. Due to the lack of tissue fixation, there was considerable difficulty in maintaining anatomical intactness during sectioning. For each individual eye, this required the manipulation of parameters such as temperature of the cryostat, and the orientation of the tissue on the cryostat chuck. Sections were stored in slide boxes at -20°C for up to 4 weeks before use, with no apparent effect on receptor binding.

General Receptor Binding Methods

Investigations to define the pharmacokinetic nature of binding sites were performed by assessing the amount of tritiated ligand which had bound to an eye section under varying incubation times, wash times, and concentrations of radioligand employed.. Specific regions of slide mounted ocular sections were scraped with a single-edged razor blade, placed onto Whatman filter paper, and counted in a 1218 LKB Rackbeta scintillation counter, after suspension in Beckman EP scintillation fluid (4 mls). The resulting measurements of radioactivity were used as indicators of the amount of ligand which had bound to a section.

Where assessments of the quantity and affinity of a receptor in ocular tissues was desired, sections of tissue were incubated in the

appropriate buffer, containing increasing concentrations of tritiated ligand. To determine the total number of binding sites in the tissue (Bmax), and the equilibrium dissociation constant (Kd) which reflects the binding affinity of the ligand, Scatchard analysis (70) was performed using the curve fitting program LIGAND (71). To express the quantity of receptor protein in a tissue section as a portion of the total protein, the amount of protein in some tissue sections was determined by the method of Lowry et al (72).

In studies where equilibrium or steady state conditions were determined, tissue sections were incubated and washed for varying lengths of time, in buffer containing radioligand at a fixed concentration. As described above, the radioactivity bound to the tissue was then measured. By calculating the rate of formation (association rate constant or k+1) and the rate of dissociation (dissociation constant or k-1) of the radioligand-receptor complex, an independent estimate of the Kd, equal to k-1/k+1 could be calculated.

In Vitro Autoradiography

All of the radioligands used in the experiments were labelled with tritium (Hydrogen - 3 (^{3}H). The tritium half life is 12.43 $\pm$ 0.11 years, and therefore the labelled sections could be stored for repeated use. The type of decay is beta particle emission with a maximum emission energy

of 0.0186 MeV and mean of 0.0057 MeV. Film for high speed, high resolution direct autoradiography of tritium labelled compounds and other weak beta-emitting isotopes is used to detect the location of the radioligand remaining bound to the tissue sections. Beta particles emitted by tritium can penetrate only a few um of brain tissue. Therefore, the closer the film emulsion to the section, the less chance of overlapping trajectories of radioactive particles and a higher degree of resolution. Section thickness also influences the degree of resolution, the thicker sections having a higher probability of overlapping particle trajectories. Although sections for this technique are cut between 10 um to 20 um thick, all eye sections were cut at 20 um due to the difficulty in obtaining thinner sections in an acceptably intact form. The end result of the apposition of the labelled eye sections to LKB Ultrofilm-^{3}H is the visualization of reduced silver grains (1.8 ± 0.3 um) reflecting the location of the bound radioligand. Since the film response curve is not linear with exposure time (radioactivity X time), autoradiographs may have relatively different density patterns depending on the time of exposure. Maximum exposure time was not allowed to go beyond saturation as determined by tritium standards.

Receptor labelling procedures by in vitro autoradiography were performed in the following general way. After removal from the freezer, slide mounted sections included in the experiments were placed on a tray and allowed to thaw for 5 minutes. Two mls of solution containing the desired concentration of a radioligand in its appropriate

buffer were placed onto each slide, and the reaction allowed to proceed. As a control for non-specific binding, all studies included sections to which were added additional unlabelled competitor at a concentration 1000 fold the radioligand concentration used in the incubation medium. Slides were placed in slide racks, and separate washes were performed for slides with and without unlabelled ligand in dishes containing the appropriate buffer. Immediately after the wash, sections were dried under a stream of cool air and stored under a vacuum with dessicant for 12-16 hours. Slides were then mounted onto acid-free board, apposed to tritium-sensitive film (LKB Ultrofilm, Amersham) under dark room conditions (see Figure 8). Exposure times for all experiments varied from 2 weeks to 13 weeks. The films were developed for 5 minutes, fixed for 5 minutes (Kodak GBX), and then rinsed in running cold water for 20 minutes before being hung to dry.

Nissl Staining

On a routine basis, several eye sections used in each experiment were stained with cresyl-violet for detailed anatomical comparison with the autoradiogram following in vitro receptor autoradiography. In this way, the Nissl substance in cells is stained. Briefly, the sections were processed in the following way: several dips in distilled water, cresyl violet stain (0.5% cresyl-echt violet and 0.2% sodium acetate (Sigma

Chemical Co.), pH 3.4) 5 min., 70 % ethanol 30 seconds, 95% ethanol 30 seconds, 100 % ethanol 2 min. X 2, xylene 2 min. X 2. They were then coverslipped before examination under the microscope.

The anatomical integrity of 20 μm tissue sections, after having undergone autoradiography and cresyl violet staining, was relatively good. This is demonstrated in the histological sections shown in Figures 5a through 5e, in which major anatomical ocular structures and cell types are identifiable and intact, enabling reliable and adequate comparison with corresponding autoradiograms.

Computerized Densitometry

In order to calibrate receptor binding quantitatively by image analysis, a series of tritium tissue standards of similar thickness, prepared by Amersham, were apposed to LKB ultrafilm together with the sections of each eye, and exposed at the same time. All grey values of the autoradiograms were calibrated against the optical density readings of co-exposed density standards (Amersham) made from tritium-labelled brain grey matter tissue with intervening polymer layers (Fig.6). The 8 known values of tissue equivalent tritium concentrations ranged between 0.07 - 6.5 nCi/mg tissue. The autoradiograms were transilluminated with a fluorescent light source which was designed to provide a highly uniform field of illumination

Figure 5a and 5b

Human anterior segment histology (Nissl)

Abbreviations: a =anterior chamber angle, c = cornea, e = ciliary epithelium, i = iris, lm = longitudinal portion of ciliary muscle, m = ciliary muscle, t = trabecular meshwork, pe = pigmented epithelium, npe = non-pigmented epithelium.

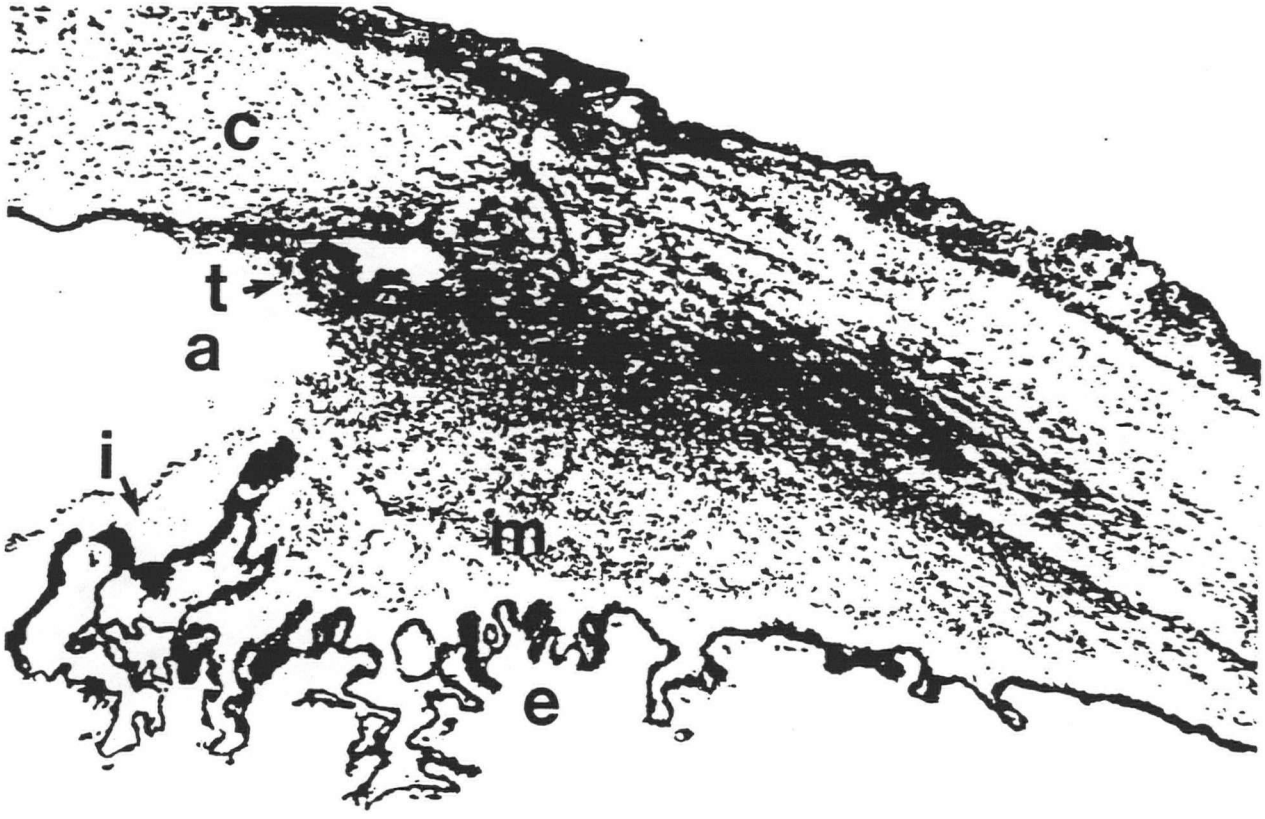
c
t
a
i
m
e

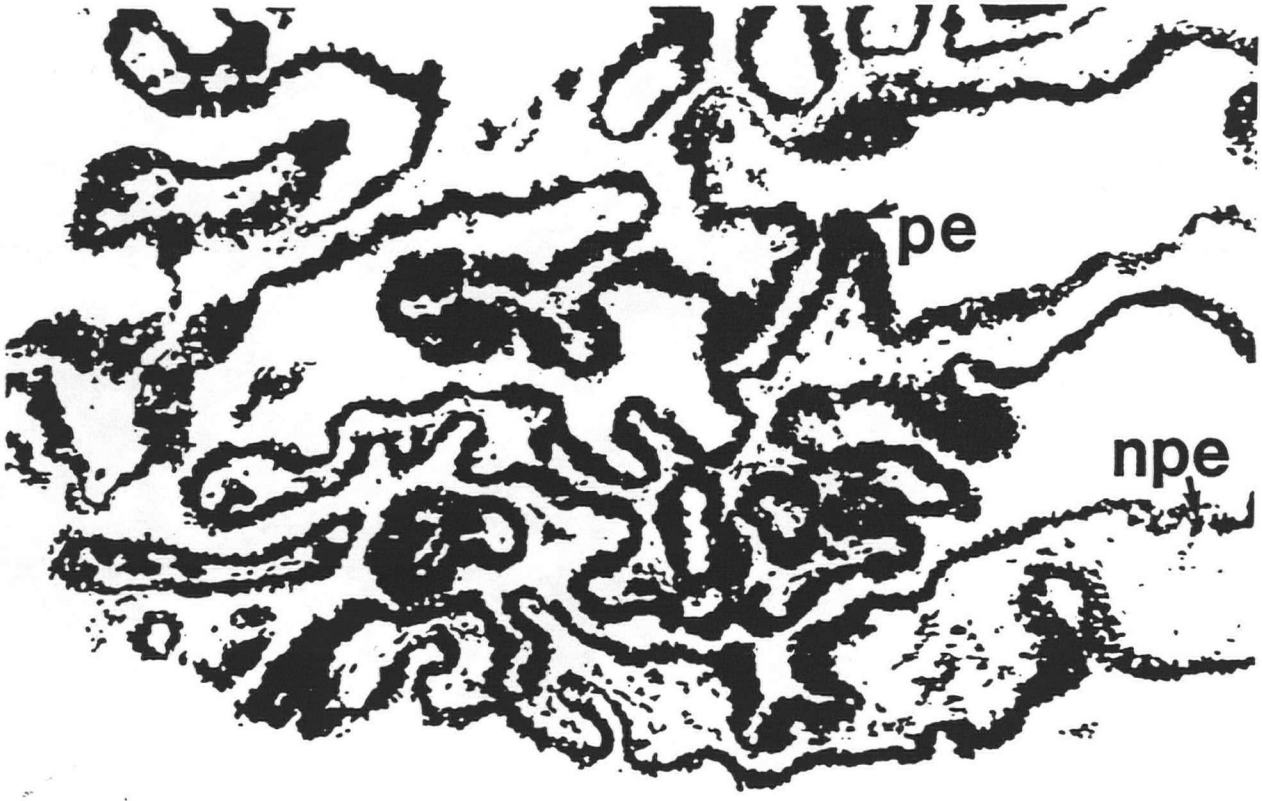
pe
npe

Figure 5c

Human iris histology (Nissl)

Abbreviations: a = anterior stromal border, p = posterior iris epithelium, s = stroma.


a
s
p

Figure 5d

Human cornea histology (Nissl)

Abbreviations: c = corneal epithelium, e = corneal endothelium


c
e

Figure 5e

Human posterior segment histology (Nissl)

Abbreviations: c = choroid, g = ganglion cell layer, ip = inner plexiform layer, in = inner nuclear layer, op = outer plexiform layer, p = photoreceptor layer, rpe = retinal pigment epithelium. Note: space beween rpe and c is artifactual separation of the layers.

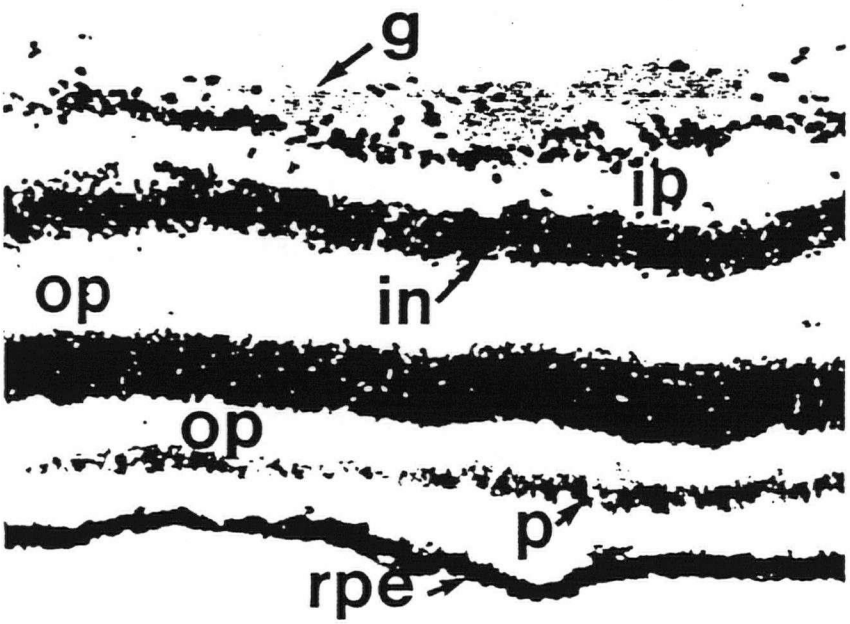
g
ip
op
in
op
p
rpe

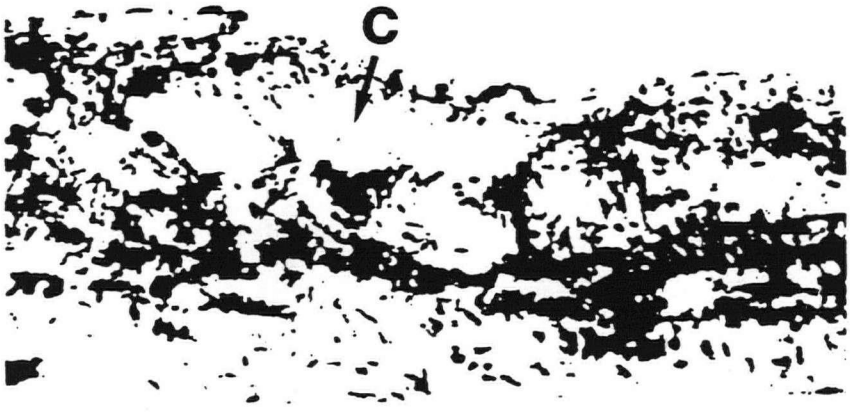
c

Figure 6

An example of an exposed density standard (Amersham) made from tritium-labelled brain grey matter tissue with intervening polymer layers. Each of the 8 bands varying in silver grain density represents a known value of tissue equivalent tritium concentrations ranging between 0.07 - 6.5 nCi/mg tissue from right to left. By image analysis, mean grey levels in autoradiograms are calibrated with the optical density readings of a co-exposed tritium standard, allowing the quantitation of mean grey levels in the region of interest.

TRITIUM STANDARDS

(Aristo Grid Products Inc.) and the images were captured and analyzed by the program IMAGE on a Macintosh II computer equipped with a video camera and frame grabber. Standard errors were calculated on the basis of optical density measurements made between a minimum of 5 adjacent sections on a single sheet of film, in addition to at least triplicate measurements of a single structure within an eye section.

Image Analysis System

The imaging system used to capture and quantify autoradiographic data was composed of the following equipment: Aristo Light Table, Nikon Micro-Nikkor 55 mm 1:28, Nikon F-C adaptor, Panasonic WV-BD400 CCD (charge coupled device) Camera, 0.002 uF Capacitor, Sony Trinitron PVM- 8200J Monitor, Data Translation Quick Capture Board, Macintosh IIfx computer, and the Image 1.23 computer program (written by Wayne Rasband at NIH).

The film containing the autoradiogram to be captured and analyzed densitometrically by the computer imaging system was first placed on an Aristo Light Table. This provided an even high intensity source of illumination. The lens, connected to the camera by a Nikon F-C adaptor, was used to focus the autoradiogram. The connected camera produced a linear response to light, such that although absolute quantities changed proportionately with varying degrees of light, relative quantitative

measurements on the autoradiogram were the same. The incoming light was digitized by the charge coupled device of the camera, converting it to an electrical signal. A coaxial cable transmitted the electrical signal to a Sony Trinitron PVM-8200J output monitor, where the image could be viewed. The same electrical signal was sent to a Data Translation Quick Capture Board inside a Macintosh IIfx computer. This board contained chips called analogue to digital converters (ADC chips) which converted the incoming electrical signal to digital information assigning it a value of between 0 and 255, thereby representing the optical density of a single pixel. These pixels were then assigned a colour reflecting a grey value. This information was then transferred to and processed by the main logic board of the computer. Once in the digital form and in its visible form on the computer screen, no further changes to the information occurred. The tritium standard with which the autoradiogram was to be calibrated, also on the same film, was used to obtain absolute measures provided that the same light level, the same aperture on the camera, and the same focal distance were maintained.

The use of a high intesity source of illumination avoided artifacts that are produced by low intensity light flickering. A good quality lens made the possible error introduced by dust or lens imperfections negligible. Because the camera that was used produced an artifial high-frequency signal which was added to the image signal, a 0.002 uF capacitor was added to the connecting cable as a simple high-frequency filter. This may have also filtered the image signal resulting in a lower quality of image resolution. Quantization noise normally introduced at the level of the ADC chip, resulting from a continuous analogue signal being sampled to a digital

signal was minimized by using high quality equipment.

MOLECULAR BIOLOGICAL TECHNIQUES

Eye Preparation for In Situ Hybridization

The detection of mRNA was carried out on entire sections of human eye specimens. Gloves were used for all steps to avoid RNAase contamination. With no prior treatment, donor human eyes were removed from the -20°C freezer, and 20 μm thick frozen sections were cut in an anterior-posterior horizontal plane on a cryostat set at temperatures varying between -20°C and -23°C. The cryostat sections were attached to subbed poly L-lysine-coated slides as they were cut, in order to prevent tissue detachment during the long hybridization and post-hybridization treatments, and high temperature washes. The slide mounted tissue was stored at -20°C for up to two weeks prior to further processing for the in situ hybridization procedure.

To process the slides, no proteinase K digestion was necessary to increase the penetration of our probes, as these studies were restricted to the use of oligonucleotide probes no longer than 50 nucleotides. Selected slides were removed from the freezer, placed in a slide rack, and allowed to warm to room temperature. The slides were then placed in a freshly prepared solution of 4% paraformaldehyde in PBS fixative for 30 minutes, and rinsed in PBS. Next, the slide mounted sections were incubated in a

fresh solution of 0.25% acetic anyhdride in 0.1 M triethanolamine and 0.9% saline, pH 8.0, for 10 minutes to block any positive charges on tissue. This was followed by a quick dehydration of the tissue in a series of ascending concentrations of fresh ethanol (50% EtOH, 70% EtOH, 95% EtOH, 100% EtOH, 100% EtOH) for 3 minutes each. The slides were drained (1 minute), followed by a defatting of the tissue by incubation twice in chloroform each time for 5 minutes. The slide mounted tissue sections were allowed to dry at room temperature for 1 -2 hours. These sections were then ready for the hybridization procedure and were either immediately processed, or stored for up to 2 weeks prior to use, at room temperature in a dust-free slide box reserved only for tissue processed for hybridization.

Synthetic Oligodeoxynucleotide Labelling

The method that was used to radioactively label these probes consisted of 3' end labelling using the DNA 3' End Labelling Kit (Molecular Biology, Boehringer Mannheim). All probes used were synthetic oligodeoxynucleotides prepared with free 5' and 3' hydroxyl groups (New England Nuclear , Dupont Canada). The principle of this labelling technique involves the addition of deoxynucleotide 5' triphosphates to the 3' end of nucleic acids in a template independent reaction. Using the nucleotide analogue deoxyadenosine 5' ([^{35}S]alpha thio) triphosphate , a

homopolymeric tail was produced. Terminal deoxynucleotidyl transferase from calf thymus, 25 units/ul, was used to add [α-^{35}S]dATP (Amersham) to the 3' end of the oligodeoxynucleotide probe.

To make up the labelling reaction, 10 pm (5 µl) of the probes, stored at -20°C, was added to 1ml eppindorf microfuge tubes. 5 µl of the reaction buffer provided by the kit: 5-times concentrated potassium cacodylate, 1 mol/l; Tris-HCl, 125 mmol/l; bovine serum albumin, 1.25 mg/ml; pH 6.6 at 25°C was added to this amount of probe, in addition to 3 µl of the cobalt chloride solution: 25 mmol/l provided 5 µl of [α-^{35}S]dATP which had been stored at -80°C and allowed to thaw for 15 minutes prior to use. Deionized distilled water, (Millipore), was added to make up a final reaction volume of 30 µl. Terminal transferase, 5 µl was added last, removing it from the -20°C freezer just prior to its addition to the reaction mixture. Quickly, centrifugation of the contents of the reaction mixture for under 5 seconds was carried out to bring the contents of the microfuge tube to the bottom. The labelling reaction mixture, now complete, was placed in an incubator pre-heated to 37°C and allowed to incubate for 1 hour. In this way, several probes were often labelled simultaneously. To terminate the reaction, the mixture was placed on ice and to it, 400 µl of 0.1M Tris-HCl, pH 7.7, 10 mM Triethylamine ammonium acetate (TEA), 1mM EDTA (Reagent A) was added. This reagent had been previously prepared and could be stored at 4°C for up to one month before use. The probes, now labelled, were either purified immediately, or stored at -80°C for extended periods of time, prior to purification.

Probe Purification

In order to separate the [^{35}S] labelled oligodeoxynucleotides from unincorporated radioisotope, protein, salt, and other low molecular weight materials, column purification was carried out. A Nensorb ^{TM} 20 Nucleic Acid Purification Cartridge (New England Nuclear) was attached to a stand up clamp as a secure support, and the sides tapped to settle the resin. Using an adapter and syringe used to form an air-tight seal, pressure was applied to induce a flow rate of less than 1 drop per 2 seconds for each step, without letting the bed go dry in between solution loading to the bed. After a methanol rinse (2 mls), a rinse with 0.1 M Tris-HCl, pH 7.7 at 25°C, 10 mM Triethylamine (TEA), 1mM EDTA solution (2 mls Reagent A) was performed. The radiolabelled oligonucleotide was then added (total volume 400 µls), and allowed to pass through the resin. A rinse with 2 mls of Reagent A was then performed twice. 1 ml of 20% ethanol was then applied as the final step in the purification process, during which the first 20 drops of the effluent was collected in an Eppendorf tube. This was counted in a 1218 LKB Rackbeta scintillation counter with 44.5% efficiency using Beckman scintillation fluid (4 mls), and stored at -80°C until needed for the hybridization procedure.

Hybridization

Hybridization buffer was prepared as a stock solution and stored at -20°C until used. Pure formamide was deionized with a resin and added at a concentration of 50% to the hybridization buffer. Dextran sulphate was made up with DEPC water volumetrically, and dissolved for 3-4 hours at 68°C in a water bath, stored at -20°C. This was added to the hybridization buffer at a concentration of 10%. Dextran sulphate is a large, non-reactive polymer that increases effective probe concentration at the tissue surface. To stabilize the probe and reduce background hybridization, 5 times Denhardt's solution, a mixture of proteins (100 mg Ficoll (Sigma), 100 mg polyvinylpuralidone (Gibco), and 100 mg BSA Fraction V(Sigma)), made up to a total of 100 ml with DEPC water, filtered, sterilized, aliquoted, and stored at -20°C) was also added to the hybridization solution. To aid in reducing background and non-specific binding of the probe to ribosomal RNA, and non-target mRNAs, very pure, RNAase free transfer RNA (tRNA, Boehringer Mannheim) was added at a concentration of 250 µg/ml. The hybridization solution was made up in 2 times saline sodium citrate (2 X SSC) buffer determined empirically. Once made up, the hybridization buffer was stored for up to 1 month at -20°C. Just before use, an appropriate aliquot was withdrawn from the stock solution and heated for 10 minutes in a 65°C water bath. Because S^{35} labelled probes were used in the detection procedure, to this, dithiothreitol (DTT, Sigma), an anti-oxidant was added to improve the stability of the radioactive sulfur to adenine bonds by maintaining the sulfur ions in a reduced state. This was

kept frozen at -20°C and added at a final concentration of 100 mM.

An illustration of the general in situ hybridization procedure is shown in Figure 7. To each eye section, 250 µl of buffer containing 5,000 cpm/µl of labelled probe was added, and covered with a glass coverslip. Incubation was performed in a humid chamber at 32°C for 18 hours. Following hybridization, sections were washed in 2 X SSC for 10 min., 1 X SSC for 20 min., at 45°C, and then 0.5 X SSC for 2 X 30 minutes at room temperature.

Controls were as follows: 1. Specificity of the receptor oligonucleotide was determined using Northern analysis (see Northern Blot Hybridization below). 2. Adjacent sections were treated with RNase (20 µg RNase A) for 60 minutes at 37°C prior to hybridization as per above. Sections from both experiments were placed against tritium sensitive film (Amersham) and exposure time, determined empirically, was 5-10 days.

Total RNA Isolation

Three pairs of eyes from different specimens were used for total RNA extraction (see Table 1). These eyes had been previously chosen, dissected, and stored for this purpose on the basis of post-mortem interval, using eyes that were received within as little time as possible after patients death (see Table 1 for details). This was done in order to ensure minimal RNA degradation.

Figure 7

The in situ hybridization techique is illustrated. A complementary strand of DNA can be used to probe highly specific gene sequences in cells of interest. The complement (cDNA) of a unique region of the transcript encoding a protein (mRNA) is radiolabelled. The cDNA probe anneals (hybridizes) to the mRNA, and its distribution in the slide mounted tissue sections is detected by autoradiographic methods. By this method, genetic sequences encoding specific proteins can be localized in ocular tissue sections.

IN SITU HYBRIDIZATION

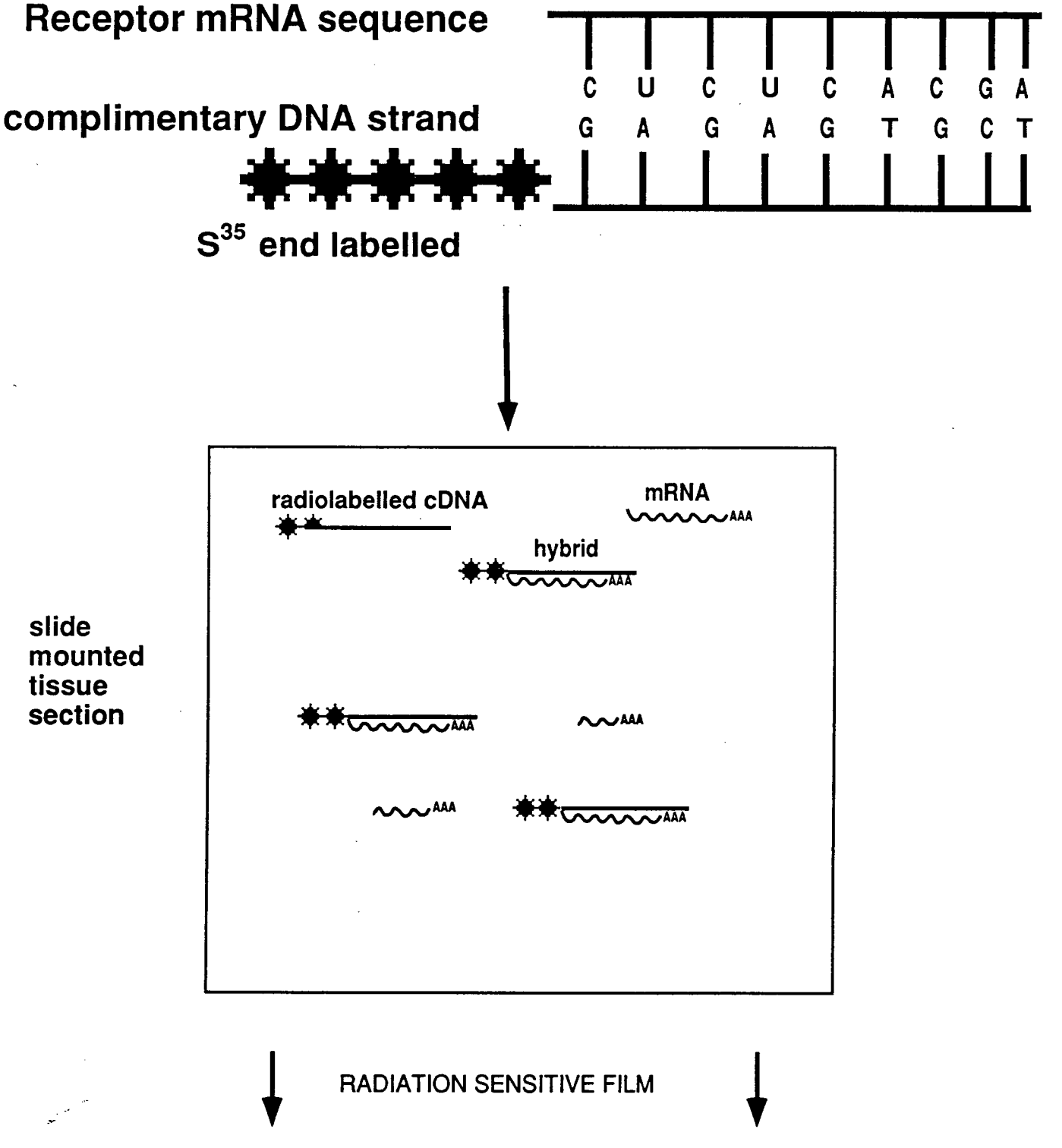

Upon receipt, sterile surgical instruments were used to quickly dissect out the anterior segment of the eye excluding the cornea and the sclera of the posterior segment. En bloc, the structures that were then frozen in liquid isopentane and stored at -80°C included the iris, the trabecular meshwork, the ciliary muscle, the ciliary epithelium, and the lens. The cornea was excluded due to difficulty in homogenizing this tissue adequately.

In preparation for the RNA extraction, care was taken to avoid inadvertently introducing RNAase activity into the tissue sample during or after the isolation procedure. Precautions included wearing gloves at all times, and for handling RNA, using wherever possible, sterile disposable plasticware. Non-disposable glass- and plasticware was treated before to ensure that it was RNase-free. Glassware was baked at 200°C overnight and plasticware was thoroughly rinsed before use with 0.1N NaOH, 1mM EDTA followed by RNase-free water. Solutions that were not supplied by the kit were treated with 0.05% diethylpyrocarbonate (DEPC) overnight at room temperature and then autoclaved for 30 minutes to remove any trace DEPC.

RNAgents ^{TM} Total RNA Isolation Kit was used for the total RNA extraction from the anterior segment of the human eye. Wherever possible, the following procedure was performed on ice.

Tissue was removed from the freezer, and the typical weight of both anterior segments from a pair of eyes approximated 1 to 1.4 grams. To adjust the initial weight of the tissue sample to the desired weight of 1 gram, part of the lens was removed.

1 gram of tissue was homogenized in 12 mls (1 volume) of denaturing solution (4 M Guanidine Thiocyanate, 25 mM Sodium Citrate pH 7.0, 0.5% sarcosyl, 0.1 M 2-mercaptoethanol) using a polytron homogenizer. 0.1 volume of 2M Sodium Acetate was added and mixed thoroughly by inversion. Following this, an equal volume of water-saturated phenol was added and again mixed by inversion. One fifth the original volume of chloroform: isoamyl alcohol mixture (49:1) was then added, vigorously shaken for 10 seconds, and then chilled on ice for 15 minutes. This was then transferred to a 50 mls polyproylene tube (DEPC- treated) and centrifuged at 10,000 X g for 20 minutes at 4°C. The top aqueous phase containing the RNA was carefully collected and transferred to a freshly DEPC-treated tube. To allow precipitation, an equal volume of isopropanol was added. This was stored in the freezer at -20°C for 30 minutes and followed by centrifugation for 15 minutes.

The pellet was completely dissolved in 0.4 volume of denaturing solution, and then re-precipitated by adding an equal volume of isopropanol as before. The supernatant was discarded, and the remaining pellet was washed with one volume of 80 % cold ethanol, and then centrifuged for 5 minutes. The pellet was dried in a speedvac for 15 minutes and resuspended in RNase-free, deionized water. The concentration of RNA was determined by measuring OD_{260} and the isolated RNA was stored at - 80°C.

Northern Blot Hybridization

Total RNA (10 μg) was denatured in 2.2 M formaldehyde, 50% formamide, 1 mM EDTA, 5mM sodium acetate, 20 mM morpholinopropane sulphonic acid (MOPS) pH 7.0, for 15 minutes at 55°C and electrophoresed though a 1.1 % agarose gel containing 20 mM MOPS, 1mM EDTA, 5mM sodium acetate, 0.66 M formaldehyde (pH 7.0). Electrophoresis was at performed at 50 V for 3 hours on 10 cm wide gels. The RNA samples for marker lanes contained 1 ug of ethidium bromide prior to loading on to the gels. Thus, staining of the lanes after electrophoresis was not necessary and ethidium bromide in the marker lanes did not interfere with subsequent transfer of RNA to membranes.

Electrophoresed RNAs were transferred to a nylon based membrane (Gene Screen, New England Nuclear). In this method, the gel was rinsed once in distilled water for 15 minutes and then rinsed twice (15 minutes each) in 0.025 M potassium phosphate buffer (PPB). Prior to tranfer, the nylon membrane was rinsed in distilled water and then soaked in 0.025 M PPB. In a buffer consisting of 0.025 PPB buffer, the RNAs were allowed to transfer overnight using the following apparatus. As a solid support, an upside down glass buffer dish larger than the size of the gel was used, onto which a piece of Whatmann 3MM filter was placed. Onto this, the gel was placed in an inverted and centered position. This was placed inside a large baking dish, which was filled with 0.025 PPB until the level of the liquid almost reached the top of the solid support. A nylon membrane 1mm

larger than the gel in both dimensions was cut, wet with deionized water, and then immersed in buffer for 5 min.and placed on top of the gel. Two pieces of 3MM paper cut to the same dimensions as the gel were placed on top of the nylon membrane. A stack of paper towels of 10 cm was placed on top of this. The transfer of RNA molecules eluted from the gel and deposited on the membrane was allowed to proceed overnight for approximately 16 hours.

Following the transfer, the filters were rinsed in 0.025 PB with the RNA side up for 5 minutes.After wrapping them in saran wrap, they were UV cross-linked with a transilluminator for 2 minutes. The nylon membranes were dried by baking at 80°C.

Filters containing total RNA were pre-hybridized and hybridized in 900 mM NaCl, 6 mM EDTA, 1% Triton-X 100, 10% dextran sulphate, and 5 X Denhart's solution. DNA probes were labelled as described in the Oligonucleotide Labelling section, using P^{32} dCTP instead of S^{35} labelled αdATP to a specific activity of approximately 5 X 10^8 cpm/μg. After hybridization the filters were washed twice for 30 minutes at 40°C in 1 X SSC, 0.02 % Triton X -100, and then for 1 hour at 40°C in 0.5 X SSC, 0.2 % Triton X -100. Filters were autoradiographed using XAR -5 films in the presence of an intensifier screen for 1-3 days.

CHAPTER 3: THE DISTRIBUTION AND QUANTIFICATION OF MUSCARINIC RECEPTORS IN THE HUMAN EYE

Through the development of homogenate binding techniques which identify drug and neurotransmitter receptors directly (1, 2), muscarinic receptors in the eyes of many non-human species have been extensively characterized by binding assays. A major limitation of the homogenate binding technique is that it provides no information on the anatomical distribution of receptors, and to date, no detailed examination of the distribution of muscarinic acetylcholine receptors in the eye of any species has been performed.

In the last decade, the introduction of the method of in vitro autoradiography (73) (see General Methods, Chapter 2) has essentially solved this problem. This approach has been used most extensively in the brain to map receptors under both in vivo (2) and in vitro conditions (73). Under in vitro conditions that optimize the ability of a drug to remain bound to the receptor in situ, a radioactively labelled drug is allowed to interact with intact tissue sections. These thin frozen sections of tissue have been mounted onto emulsion coated slides (2, 74), apposed to emulsion coated cover slips (73), and more recently, have been placed against tritium sensitive sheet film (75) which after development, produces silver grains wherever the radioactive probe is bound to the receptor. Thus, the autoradiographic signal produced allows visualization of where the drug has bound, or the location of the receptor target in the tissue (Figure 8). In this way, numerous studies have been performed to localize muscarinic

Figure 8

The technique of in vitro autoradiography is outlined, in this case using the radioactively labelled drug [^{3}H]QNB. The radioligand is added to slide mounted intact eye tissue sections, and allowed to interact under conditions which favour its binding to the receptor of interest. The binding sites are detected by apposing radiation-sensitive film to the tissue, and after development, the distribution of the binding sites is determined by visualization of the signal on the film. In the control condition, binding is performed in the presence of an excess of unlabelled competitive agent (atropine). This controls for the specificity of the the drug-receptor interaction.

METHODS

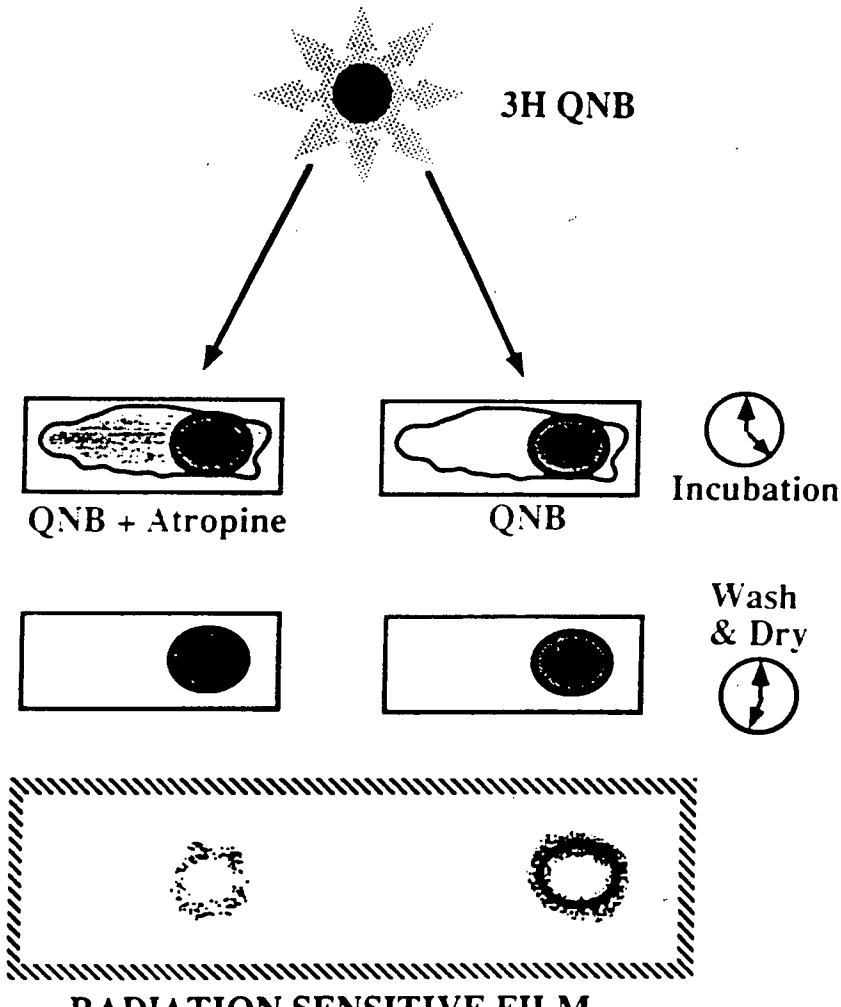
3H QNB
QNB + Atropine
QNB
Incubation
Wash
& Dry
RADIATION SENSITIVE FILM

acetylcholine receptors in the brain. The latter technique has been advantageous for the measurement of receptor densities, particularly with the introduction of computer programs capable of quantifying densities in an image.

In vitro autoradiography was used to localize muscarinic receptors in this study because it has the added advantage of being applicable to the study of post-mortem human tissue, and this has been combined with quantitative densitometric analysis. In addition, several binding characteristics of the receptor-ligand interaction were determined. Using [^{3}H] Quinuclidinyl benzilate ([^{3}H]QNB), the best high affinity, reversible, and general muscarinic receptor antagonist available, this chapter presents the results of our investigations into the pharmacological characteristics, the anatomical distributions, and densities of muscarinic acetylcholine receptors in different human eye structures.

Procedure

Whole globes from adult patients with no documented history of acquired or hereditary ocular disease (see Table 1 for details of tissue specimens used), were processed in preparation for autoradiography as detailed in General Methods (Chapter 2).

Muscarinic receptors were labelled by incubating sections with 1 nM concentrations of [^{3}H]QNB ([^{3}H]QNB: 32.9 Ci/mmol, Amersham). Experiments were conducted in the presence and absence of 5 μm atropine

sulphate (New England Nuclear Corp.) a muscarinic antagonist, representing a control for non-specific activity. Early studies included unlabelled QNB as controls, and gave similar results. Autoradiography was performed using the optimum binding conditions delimited by preliminary characterization experiments. In brief, sections were incubated for 45 min. in sodium phosphate buffer, pH 7.4, at room temperature, followed by two 5 minute washes in ice cold buffer. All sections were dried and subsequently apposed to tritium sensitive film, (LKB Ultrofilm, Amersham) for 3 weeks in the dark.

The procedure for the characterization experiments of the iris/ciliary body, was carried out under the same conditions as described above for autoradiography. Instead of apposing the sections to film, the iris/ciliary body from each eye section was scraped with sterile razor blades from the slide into liquid scintillation vials, for measurement of radiation levels. Quantitative densitometry was performed as described in Chapter 2.

Results

Characterization of [^{3}H] QNB binding sites in human iris/ciliary muscle

The association time course of (3H)QNB binding was determined (Fig.9 *a*) by incubating sections with 5 nM of (3H)QNB for various times at room temperature. Equilibrium binding was achieved within 25 minutes, and remained stable for another 40 minutes.The association rate (k_{+1}) was calculated to be 2.6 x min^{-1} nM^{-1}. In subsequent experiments,

Figure 9

Panel A: Time course of association of [^{3}H]QNB binding to human iris/ciliary body tissue. Tissue scrapes were incubated with 1nM [^{3}H] QNB for various time intervals as described in Materials and Methods. The difference between the values obtained in the absence and presence of 10 uM atropine measured simultaneously, represents specific binding. Each value is the mean of six determinations.

Panel B: Time course of dissociation of [^{3}H]QNB binding to human iris/ciliary body tissue. Iris/ciliary body tissue was incubated at room temperature in the presence of 1 nM [^{3}H]QNB for 45 min. Dissociation was initiated by washing the slides in buffer, and the decline in bound [^{3}H]QNB was then determined at various times thereafter. Each value is the mean of six determinations.

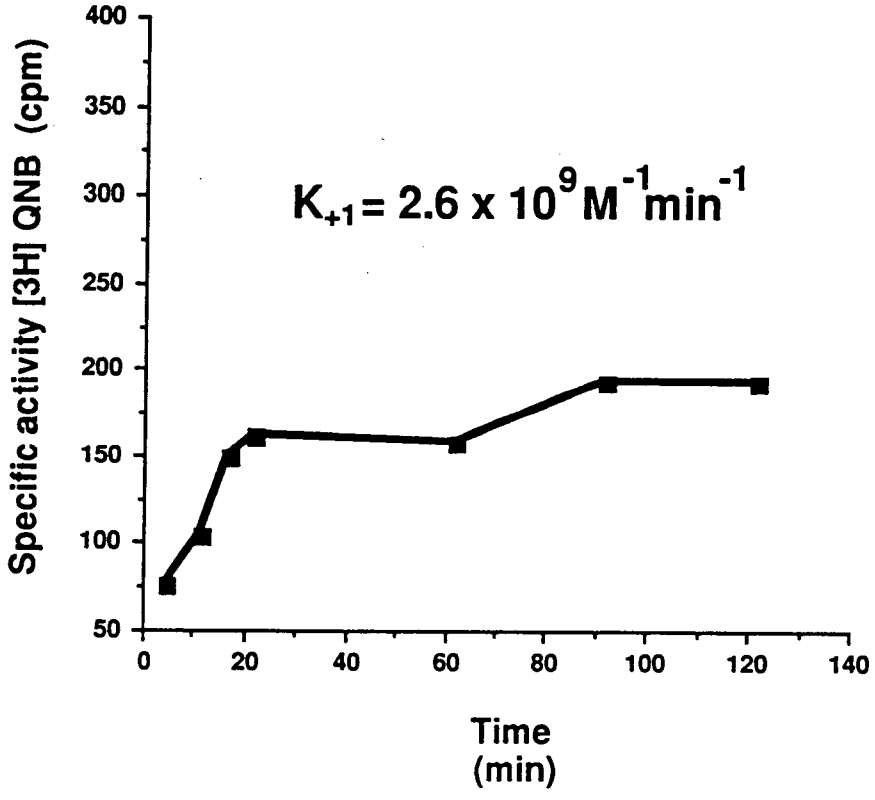
Specific activity [3H] QNB (cpm)
400
350
300
250
200
150
100
50
0
20
40
60
80
100
120
140
Time
(min)
$K_{+1} = 2.6 \times 10^{9} M^{-1} min^{-1}$

A

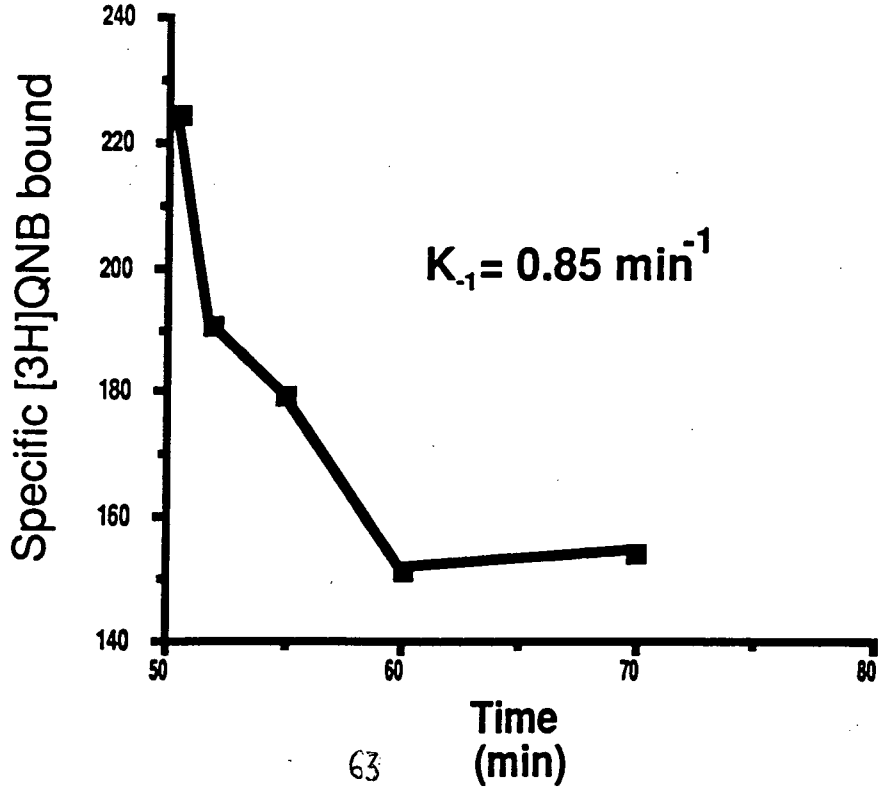
Specific [3H]QNB bound
240
220
200
180
160
140
50
60
70
80
Time
(min)
$K_{-1} = 0.85\ min^{-1}$

B

tissue was incubated for 45 minutes.

This reaction was reversible as shown in Figure 9 *b*. Sections were washed in 4^0 C sodium phosphate buffer, pH 7.4 in the absence of [^{3}H]QNB for various times to determine the dissociation rate constant and to remove unbound ligand. A rapid decline in specific binding over 10 minutes was observed. The dissociation rate constant (k_{-1}) was calculated to be 0.85 min^{-1}. The equilibrium dissociation constant (K_D) calculated from Kd = k_{-1}/k_{+1} was 0.33 nM (76, 77).

Using the above incubation conditions, increasing the concentrations of [^{3}H]QNB, saturability of [^{3}H]QNB binding sites was demonstrated (Figure 10). Scatchard analysis of the saturation binding data revealed a single class of binding sites with a K_D of 0.51nM, and the total number of bound sites (B_{max}) of 318 fmol/ mg protein. The value of K_D (0.33 nM) calculated from the association and dissociation kinetic data ($K_D = k_{-1}/k_{+1}$) corresponds well with that obtained from equilibrium saturation data.

[^{3}H]QNB Autoradiography

The binding site pattern for [^{3}H]QNB is shown in Figure 11 *b*. The silver grain densities that are produced by the radioactive emission of the [^{3}H] QNB (seen in white) reflect the spatial distribution of the drug bound to the eye section *in situ*. The control section as shown in Figure 11 *c*, shows virtually no non-specific binding of [^{3}H] QNB, the binding being

Figure 10

Specific binding of [^{3}H]QNB to human iris/ciliary body tissue as a function of ligand concentration. Incubations were carried out for 45 min. at 25^0 C in the presence of increasing concentrations of [^{3}H]QNB. Non-specific binding was measured by addition of micromolar concentrations of atropine. Specific binding was determined as the difference between total and non-specific binding at each concentration. Experiments were run in triplicate, and each value is the mean of six to nine determinations. Inset: Scatchard plot of the specific binding data.

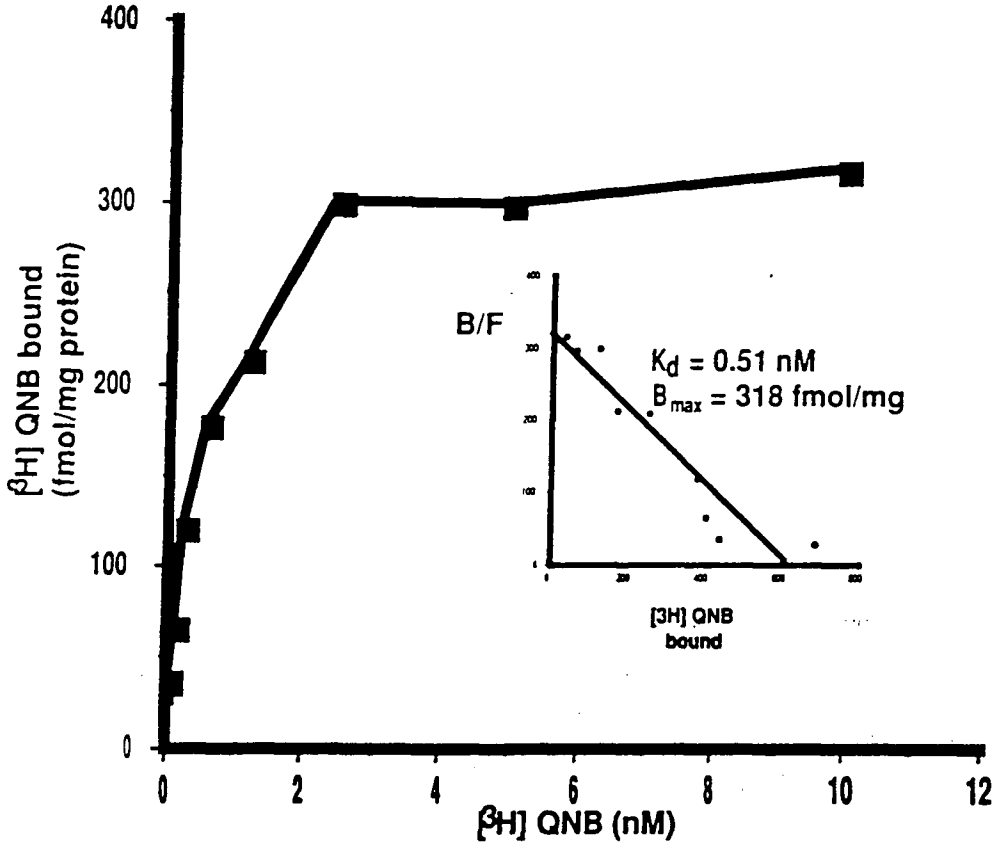
400
300
200
100
0
[3H] QNB bound
(fmol/mg protein)
0
2
4
6
8
10
12
[3H] QNB (nM)
B/F
Kd = 0.51 nM
Bmax = 318 fmol/mg
[3H] QNB
bound

Figure 11

A: An example of a slide mounted frozen section of a human eye after staining with Nissl. This section was used to generate the autoradiogram in B. (Darkfield)

B: Autoradiogram of [^{3}H]QNB binding in a human eye section. Incubations were carried out at 1nM [^{3}H]QNB as described in Materials and Methods. Areas seen in white reflect greater [^{3}H]QNB binding. Experiments were done in triplicate and in five different specimens all giving similar binding patterns of [^{3}H]QNB. Note the absence of binding in the optic nerve. Abbreviations: ON= optic nerve.(inverted grey scale).

C: Control autoradiogram of [^{3}H]QNB binding in a human eye. Incubations with 1nM QNB were carried out in the presence of 10 uM atropine, effectively competing for virtually all of the binding sites seen in Panel B. Control sections were included in every experiment, in each case giving similar results.

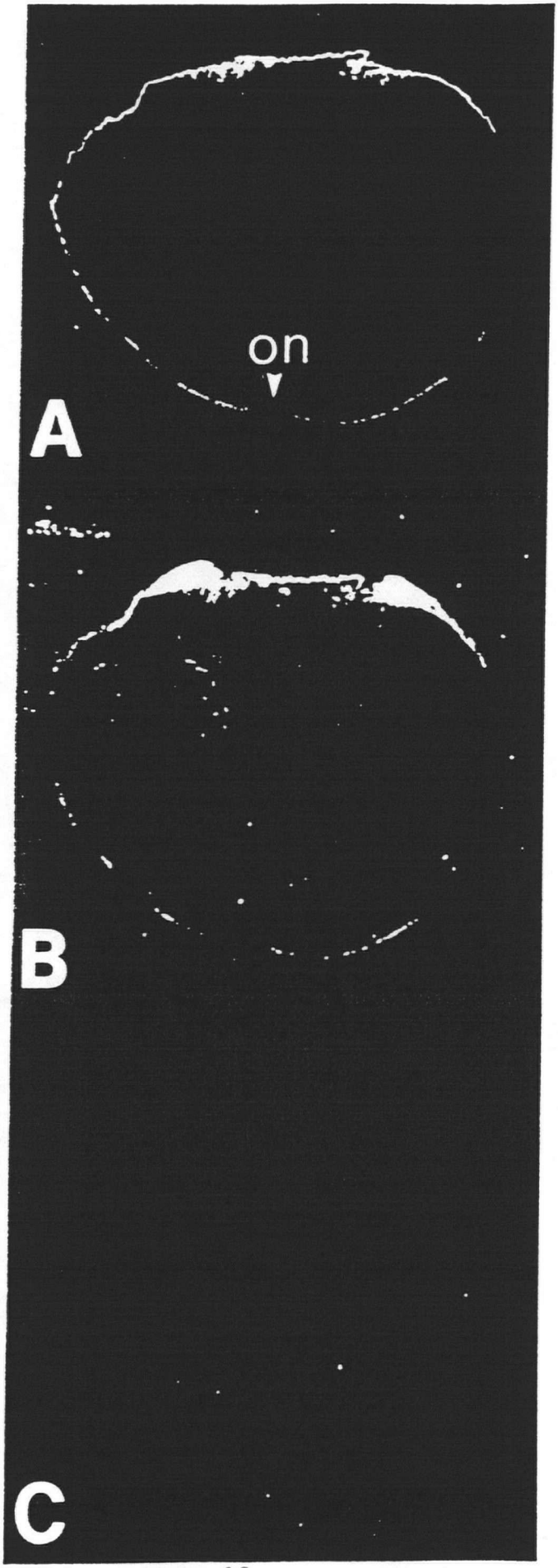
on
A
B
C

effectively blocked by competition with unlabelled atropine. The original anatomically intact whole adult eye section containing optic nerve and lens from which the autoradiogram was generated was stained for Nissl substance with Cresyl Violet, and is shown in darkfield view in Fig. 11 *a*. The autoradiographs and Nissl photographs were processed at the same magnification to facilitate anatomical comparison.

Comparing the anterior segment of the histologically stained section in Figure 12 *a* with the corresponding region of the inverted autoradiogram (Figure 12 *b*), the ciliary muscle, iris, and ciliary epithelium contain high densities of binding sites, with virtually no detectable concentration of binding sites in the cornea or lens. Visual inspection clearly reveals the highest density of receptors in the ciliary muscle.

In the posterior segment of the same section (Figure 13 *a*), three distinct bands of labelling can be discriminated (Figure 13 *b*). They correspond specifically to the retina, retinal pigment epithelium and the choroid.

Quantitation by Computerized Densitometry

Quantitative binding site analysis was performed for each of the five specimens studied. For each eye, computerized densitometric measurements of the following structures found to contain muscarinic binding sites by autoradiography were performed: ciliary muscle, iris, ciliary epithelium, retina, retinal pigment epithelium. The absolute values obtained are shown in Figure 14 *a*. What is most obvious from the figure is that in each

Figure 12

Panel A: Darkfield higher power of anterior segment of the human eye section shown in Figure 11.

Panel B: Autoradiogram of [^{3}H]QNB binding in human anterior segment corresponding to Panel A shows intense binding in ciliary muscle, iris, and ciliary epithelium. Note absence of binding in the cornea and the lens (inverted grey scale). Abbreviations: i= iris, cm = ciliary muscle, ce = ciliary epithelium, c = cornea, l = lens.

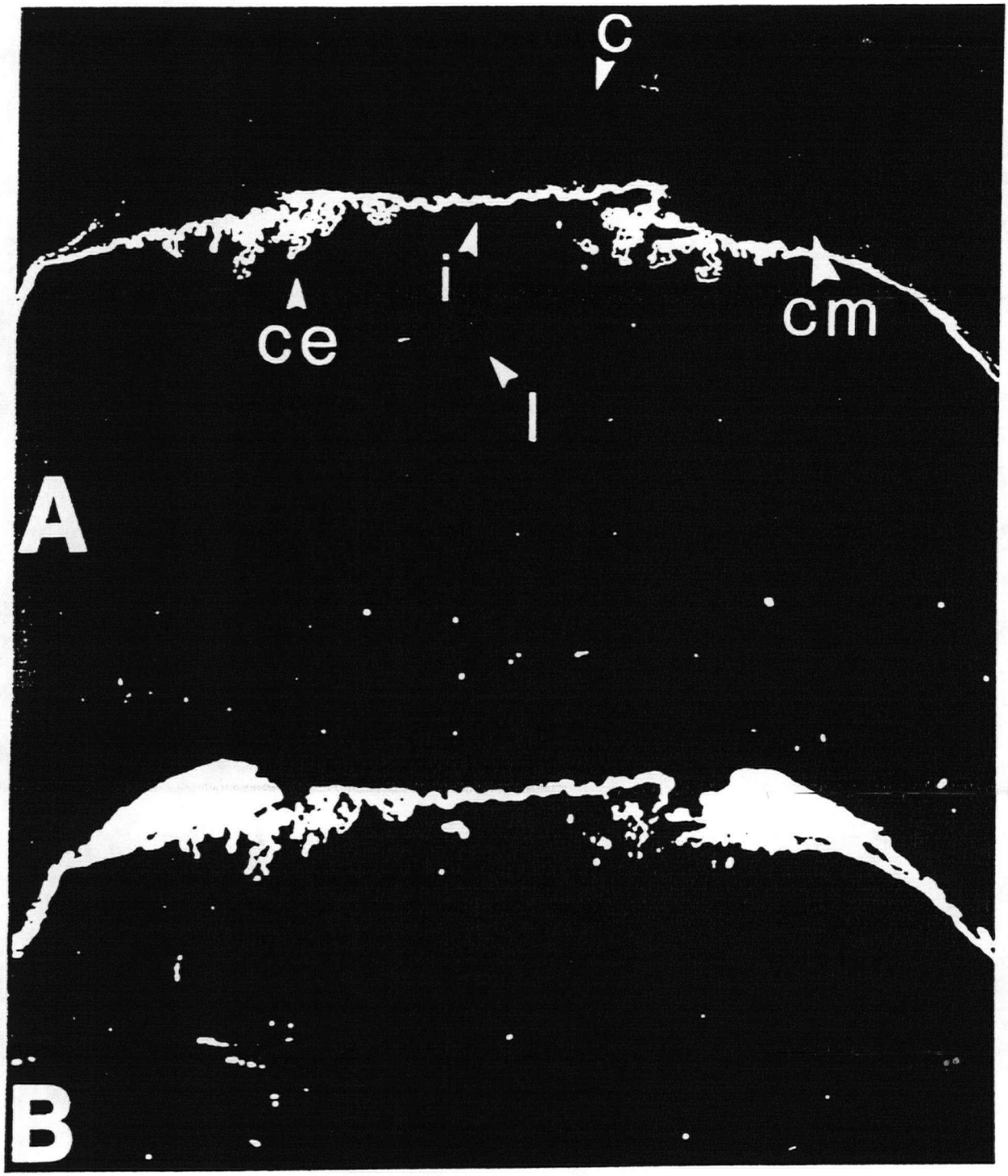
c
ce
i
cm
l
A
B

Figure 13

Panel A: Darkfield higher power of human posterior segment seen in Figure A.
Panel B: Autoradiogram corresponding to Panel A (inverted grey scale). In human posterior segment [^{3}H]QNB binding is detected in three distinct layers; the retina, the retinal pigment epithelium, and the choroid. Abbreviations; r = retina, rpe = retinal pigment epithelium, ch = choroid.

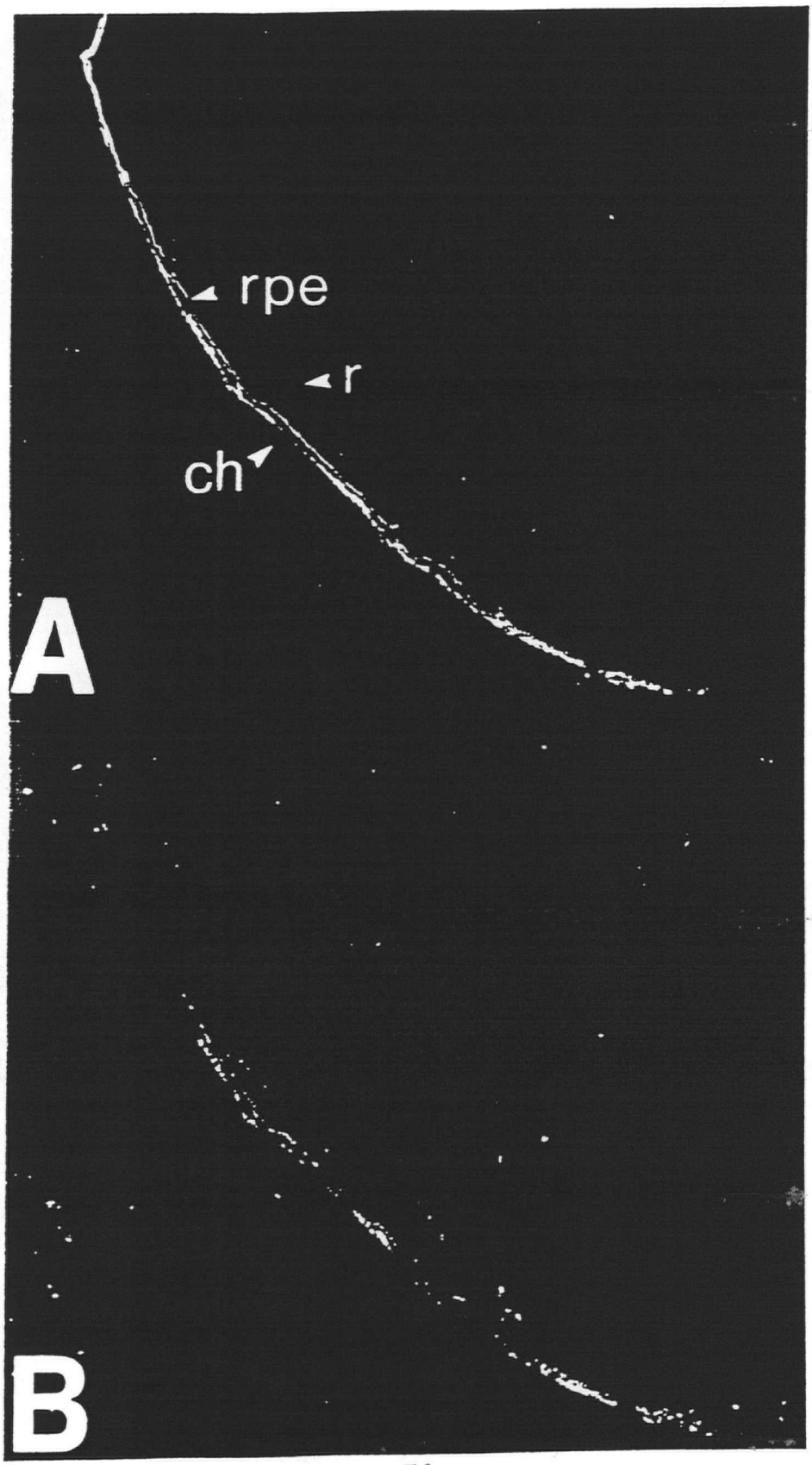
rpe
r
ch
A
B

Figure 14

Panel A: Quantitation (nCi/mg) of mean grey levels in ocular structures by image analysis of autoradiograms showing [^{3}H]QNB binding from five human eye specimens. Following the calibration of autoradiograms with tritium standards containing known quantities of radiation, optical density readings of each of the structures shown were determined for each eye. Ciliary muscle and retinal pigment epithelium have highest and lowest densities of muscarinic binding sites. Each value represents the mean of three independent measurements with standard errors ranging from 0.03 to 0.09.

Panel B: Specific activity in the structures in 5 specimens is expressed as a percentage of ciliary muscle activity. Note the consistent proportions, with ratios of iris and ciliary epithelium binding to ciliary muscle binding almost equal. Inset: Average proportions of specific activity across the examined structures in the 5 eyes examined. Standard error bars are shown.

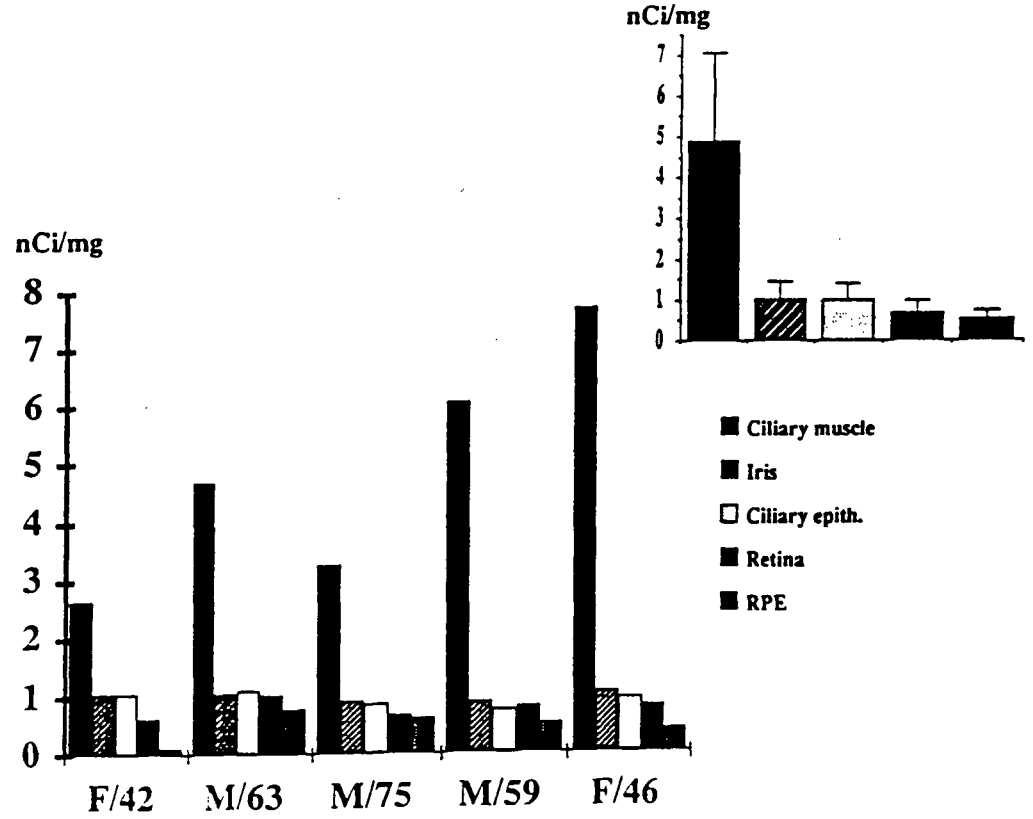
nCi/mg
8
7
6
5
4
3
2
1
0
F/42
M/63
M/75
M/59
F/46
nCi/mg
7
6
5
4
3
2
1
0
Ciliary muscle
Iris
Ciliary epith.
Retina
RPE

A

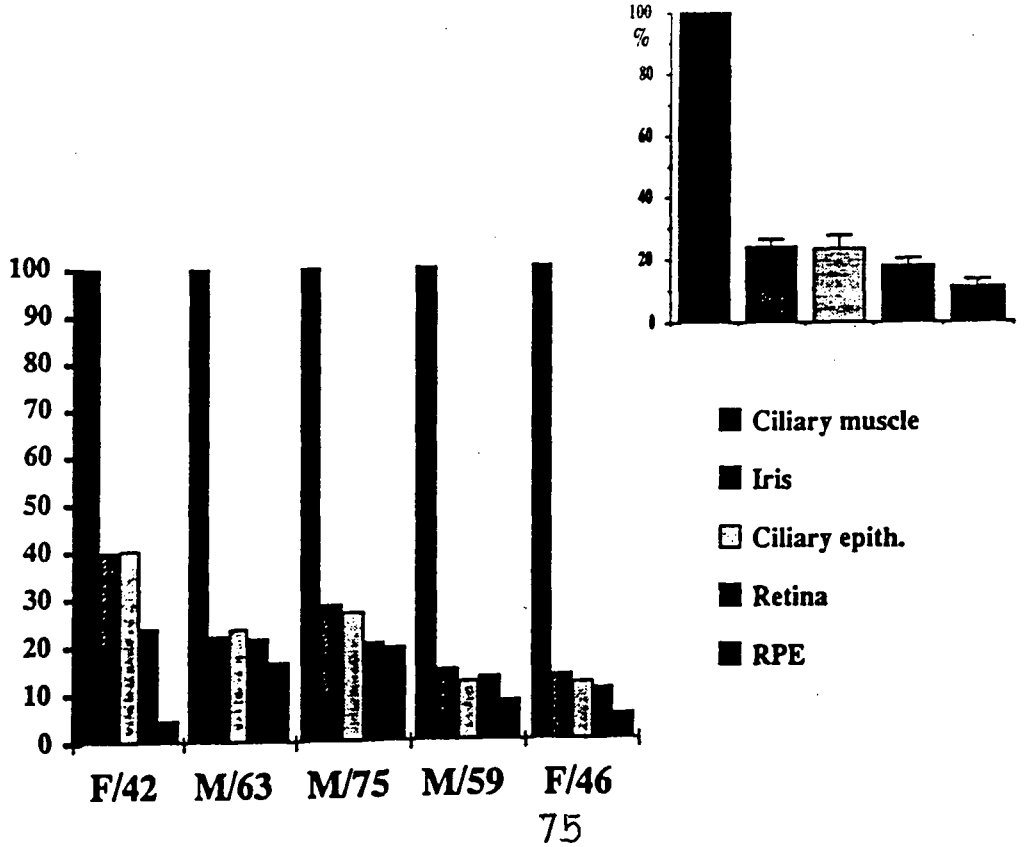
100
90
80
70
60
50
40
30
20
10
0
F/42
M/63
M/75
M/59
F/46
100
%
80
60
40
20
0
Ciliary muscle
Iris
Ciliary epith.
Retina
RPE

B

specimen, the ciliary muscle contains the highest density of binding sites, and the retinal pigment epithelium consistently shows the lowest density of binding sites. The standardized graph shown in figure 14 *b* facilitates examination of the binding site densities in structures relative to the ciliary muscle. The ratios of the bound activity in the ciliary muscle to that found in other structures consistently increases in the following order: iris and ciliary epithelium, retina, retinal pigment epithelium. The most consistent feature across all specimens is the nearly equal relative densities of the iris and ciliary epithelium seen easily once standardized against the ciliary muscle, their difference varying between 0.4 % - 3.6% (S.D.= 2.3). Although in figure 14 *b* the ciliary muscle is shown to have an average of 5 times the specific activity of the iris and ciliary epithelium, 6 times the activity of the retina, and an average of 11.8 times the activity of the retinal pigment epithelium, these ratios are seen to vary by a factor of 2, 1.5, and 2.3 respectively. Each optical density value was calculated by averaging three independent measurements, each measurement made in adjacent sections of the same specimen. The standard errors of measurements made from adjacent sections of an eye specimen ranged from 0.03 to 0.09 in the eyes examined.

Summary

This is the first report of an in vitro autoradiographic and quantitative densitometric analysis of muscarinic receptors in complete sections of the

human eye. The biochemical characterization of [^{3}H]QNB binding sites in human iris/ciliary body as described in Figures 9 and 10, is consistent with a previous study in which [^{3}H]QNB binding sites in the human iris and ciliary muscle were characterized by homogenate binding methods (78). Other studies in primates have also been done (165), and their higher values of Bmax obtained may be due to the inclusion of ciliary processes in our preparation.

The results of autoradiographic experiments to map the normal distributions of [^{3}H]QNB binding sites in the adult human eye are consistent with previous work, predominantly determined by the homogenate ligand binding method. Not surprisingly, both the iris and the ciliary muscle showed high concentrations of muscarinic binding sites. Muscarinic receptors in the iris have been reported in numerous species using homogenate binding techniques and in human iris sphincter and dilator muscles, they have been shown autoradiographically with the irreversible ligand (3H)-propylbenzilylcholine mustard (PrBCM) (79). Homogenate studies have also demonstrated muscarinic receptors in primate ciliary non-pigmented epithelium (80). Our finding that the ciliary muscle revealed the highest density of muscarinic acetylcholine receptor binding sites is consistent with the high concentration of muscarinic receptor binding sites found to exist in the ciliary muscle of the cynomologus monkey (34). The distinct band of muscarinic receptors we have identified in the human retina is consistent with previous autoradiographic determinations of [^{3}H]QNB muscarinic binding sites in the human retina (81). Pharmacological studies support the presence of muscarinic receptors in the retinal pigment epithelium (82), and their

presence in the choroid is consistent with the vasodilating effects of parasympathetic stimulation on choroidal microcirculation.

Interestingly, the epithelium of the cornea, containing some of the largest amounts of acetylcholine known to exist in mammalian tissue (19), does not appear to display any significant concentration of muscarinic binding sites. Rabbit, bovine, and human corneas have been searched using homogenate binding techniques with similar results (83, 84). More recently however, using whole corneas, they have been identified by ligand binding, although in sparing quantities(85)]. This may be due to the evaluation of a large number of selective corneal cell populations in that study, compared to the examination of a limited number of corneal epithelial cells, and thus receptor paucity per eye section in our own studies. The use of an as yet unavailable iodinated ligand with high affinity for muscarinic receptors, and having much higher specific activity, could clarify this point.

The intricacy of the small anatomical structures of the eye makes this tissue particularly well suited to quantitative analysis by microdensitometry. Densities of [^{3}H]QNB-labelled autoradiograms were measured within highly circumscribed regions and readily compared to other ocular structures. We were fortunate enough to be able to validate our own work against a previous study in which muscarinic receptors in the human eye were studied by homogenate binding methods (78). In this study, the number of receptors was measured in the ciliary muscle, the iris and the retina, and quantitative comparison showed the ciliary muscle to possess a specific activity 10 times and 50 times the amount found in these structures respectively. The somewhat lower ratios that we obtained can be

explained by the higher sensitivity of densitometry over the homogenate technique particularly for tissues of small anatomical regions for which accurate dissection is difficult. In spite of the variations in the densities of binding sites between the different adult specimens used (Table 1), several consistent features were noted when comparing the overall *relative* concentrations of receptors in the ocular structures measured. The ciliary muscle and retinal pigment epithelium consistently showed the highest and lowest specific binding respectively. The ratios of ciliary muscle activity to those of the other structures consistently increased in the order of the iris and ciliary epithelium, retina and retinal pigment epithelium. In addition, the specific activities of the iris and of the ciliary epithelium were very close. The stability of this parallelism was seen in each donor specimen examined.

This adapted quantitative autoradiographic study of muscarinic receptors in the human eye may help to clarify the neuropharmacological basis for many cholinergic drug effects in ocular structures, and should prove to be a useful adjunct to more directed receptor-related investigations at the biochemical and physiological level.

CHAPTER 4: THE DISTRIBUTION OF M1 AND M2 MUSCARINIC RECEPTOR SUBTYPES IN THE HUMAN EYE

In the previous chapter, [^{3}H]QNB was used to define the normal distributions of muscarinic binding sites in the adult human eye. In spite of it being a highly specific muscarinic ligand, it does not however, distinguish between muscarinic acetylcholine receptor subtypes (86). In the present chapter, we extend the autoradiographic approach previously used to localize muscarinic binding sites in the human eye, to the study of the anatomical distributions of M1 and M2 muscarinic receptor subtype binding sites using [^{3}H]pirenzipine and [^{3}H]oxotremorine respectively.

The initial classification of muscarinic receptors into M1 and M2 subtypes (87) was supported by several independent pharmacological observations; the finding of two different muscarinic acetylcholine responses in the opposum esophageal sphincter (88), high and low affinity binding profiles for tritiated ACh (89), and the selective affinity of the high affinity binding site (M1) for pirenzipine (36, 37). Those receptors having low affinity for Pirenzipine were called M2 sites. Since then, this distinction has been further supported by well characterized and described direct autoradiographic distribution studies of the M1 and M2 muscarinic subtypes in the brain using [^{3}H]pirenzipine and [^{3}H]oxotremorine repectively, with noted regional preference for each of these subtypes (90, 91).

In this chapter, by the autoradiographic method previously employed to localize non-subtype specific muscarinic receptors, the anatomical

distributions of the M1 and M2 muscarinic receptor subtypes in the human eye are described by using [^{3}H]pirenzipine and [^{3}H]oxotremorine respectively.

PROCEDURE

Experiments for each ligand were conducted independently on eyes considered to be normal adult specimens with no documented history of acquired or hereditary ocular disease. Experiments with each of the ligands employed were performed on all of the specimens indicated in Table 1.

Sections were prepared as previously described (Chapter 2). Using established procedures (90, 91), autoradiography using [^{3}H]oxotremorine (87 Ci/mmol, New England Nuclear, Missassauga, Ontario) and [^{3}H]pirenzipine (82 Ci/mmol,New England Nuclear, Missassauga, Ontario) was carried out using a buffer of 20 nM HEPES-Tris pH 7.5, 25°C containing 10 mM Mg^{+2}. Incubation at 25°C was carried out at radioligand concentrations of 1nM for 30 min. and 60 min. for [^{3}H]oxotremorine and [^{3}H]pirenzipine respectively. In each case, washes consisted of three successive 2 min. changes in ice cold buffer with a final rinse in deionized water.

Distributions Of [^{3}H]Pirenzipine And [^{3}H] Oxotremorine Binding Sites

The distribution of high affinity sites for [^{3}H]pirenzipine (M1 sites) is

shown in figure 15. The [^{3}H]pirenzipine binding sites reveal a distribution confined predominantly to the anterior segment structures: the ciliary muscle, iris, and ciliary epithelium specifically (16 *a*). Close scrutiny of the ciliary muscle reveals a pattern of most concentrated binding in its longitudinal muscle. No binding in the cornea or lens is detectable. Non-specific binding in these structures is virtually absent as seen by the control section (fig.16 *b*). The posterior chamber shows some labelling of distinctly lower density, in the retinal layer (Fig. 15).

Figure 17 shows the pattern of distribution of the [^{3}H]oxotremorine labelled receptor binding sites. The original eye section is stained for Nissl substance and is shown as a darkfield photomicrograph (Fig. 17 *a*). Most notable is the prominent dense band in the posterior segment, corresponding anatomically to the retina (Fig. 17 *b*), the layers of which are not identifiable with this method. Labelling can also be seen to extend into the anterior segment (Fig. 17 *b*). No detectable binding sites are noted in the cornea or lens. In the control section (Fig. 17 *c*), excess unlabelled atropine effectively blocks all binding as shown in the autoradiogram.

Comparison of a high power view of the anterior segment of the autoradiogram and its complementary Nissl stained section (Fig.18) reveals a zone of dense labelling that corresponds to only a single circumscribed region of the ciliary muscle, specifically, the longitudinal muscle portion of the ciliary muscle (Fig. 18 *a*). No detectable binding is seen in the cornea or lens. These findings were consistent in all the specimens examined.

Figure 15

Autoradiogram of [^{3}H]pirenzipine binding sites in a human eye section showing pronounced binding in the anterior segment.

Figure 16

Panel A: Higher power view of the angle of the anterior segment of autoradiogram seen in Figure 12. Abbreviations: a = ciliary muscle, b = iris, c = ciliary epithelium.
Panel B: Control autoradiogram in the same region of an adjacent section generated by [^{3}H]pirenzipine competition with atropine sulphate.

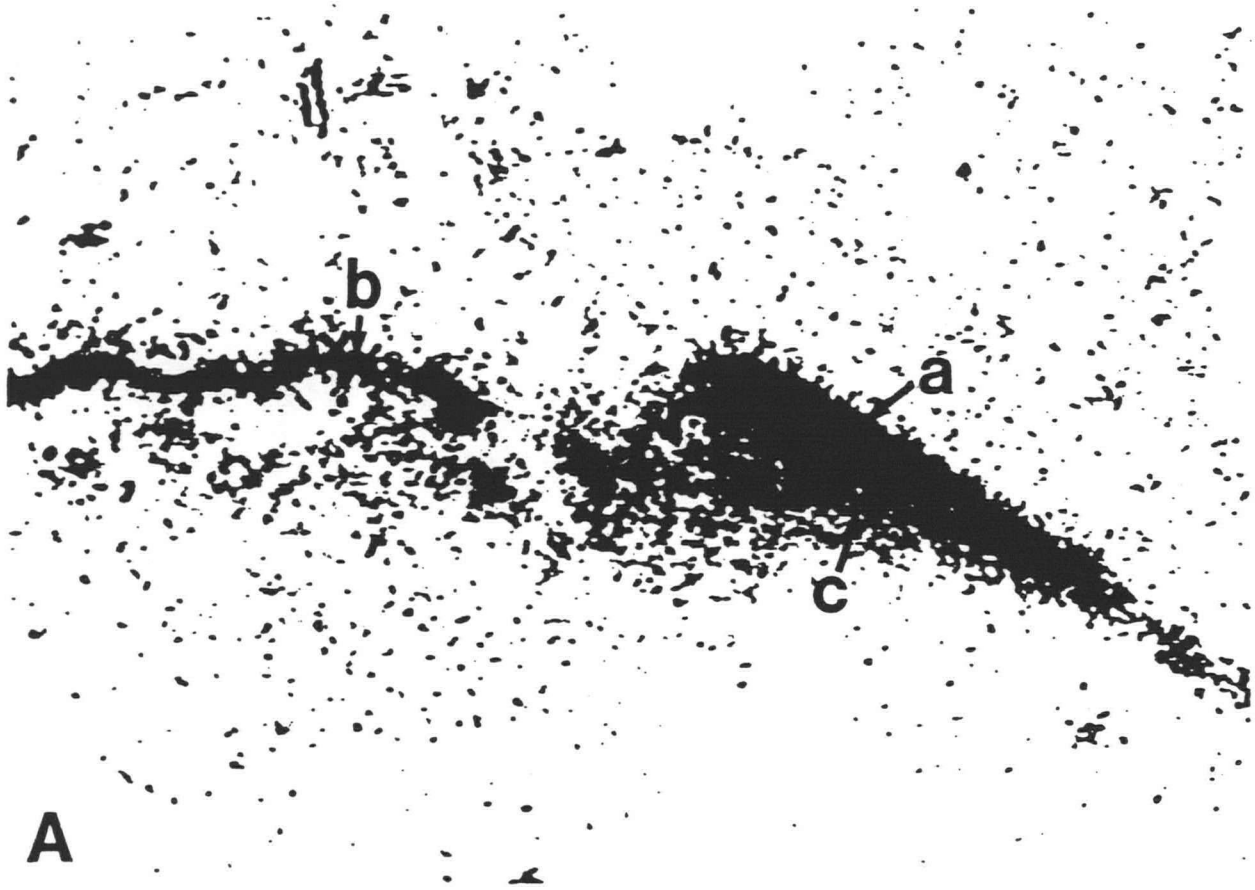
b
a
c
A


B

Figure 17

Panel A: (Darkfield) Human eye section used to generate autoradiogram, stained for Nissl substance. Human eyes frozen 3.5 to 11 hours post-mortem were sectioned and slide mounted. Abbreviations: c = cornea, cm = ciliary muscle, r = retina.

Panel B: Example of an autoradiogram (inverted grey scale) of [^{3}H]oxotremorine binding in the same human eye section. Incubations were carried out at 1nM and 5nM[^{3}H]oxotremorine as described in Procedure with equivalent results. [^{3}H]oxotremorine binding seen in white. Experiments were performed on eight eye specimens all giving the same distributions. Note the presence of binding in both the ciliary muscle and retina.

Panel C: Control autoradiogram of [^{3}H]oxotremorine binding in a human eye. Incubations with 1nM and 5nM [^{3}H]oxotremorine were carried out in the presence of 1 uM concentrations of atropine, effectively competing for virtually all of the binding sites seen in Panel B. Control sections were included in every experiment, in each case giving similar results.

c
cm
r
a
cm
r
b
c

Figure 18

Panel A: High power darkfield view of anterior segment of a human eye section stained for Nissl substance. Abbreviations: cm = ciliary muscle, c = cornea, lcm = longitudinal ciliary muscle, l = lens, i = iris.

Panel B: High power view of inverted autoradiogram corresponding to the same anterior segment region as seen in Panel A. Using 1nM [^{3}H]oxotremorine, dense labelling is confined to the longitudinal portion of the ciliary muscle only. Abbreviations: lcm = longitudinal ciliary muscle.

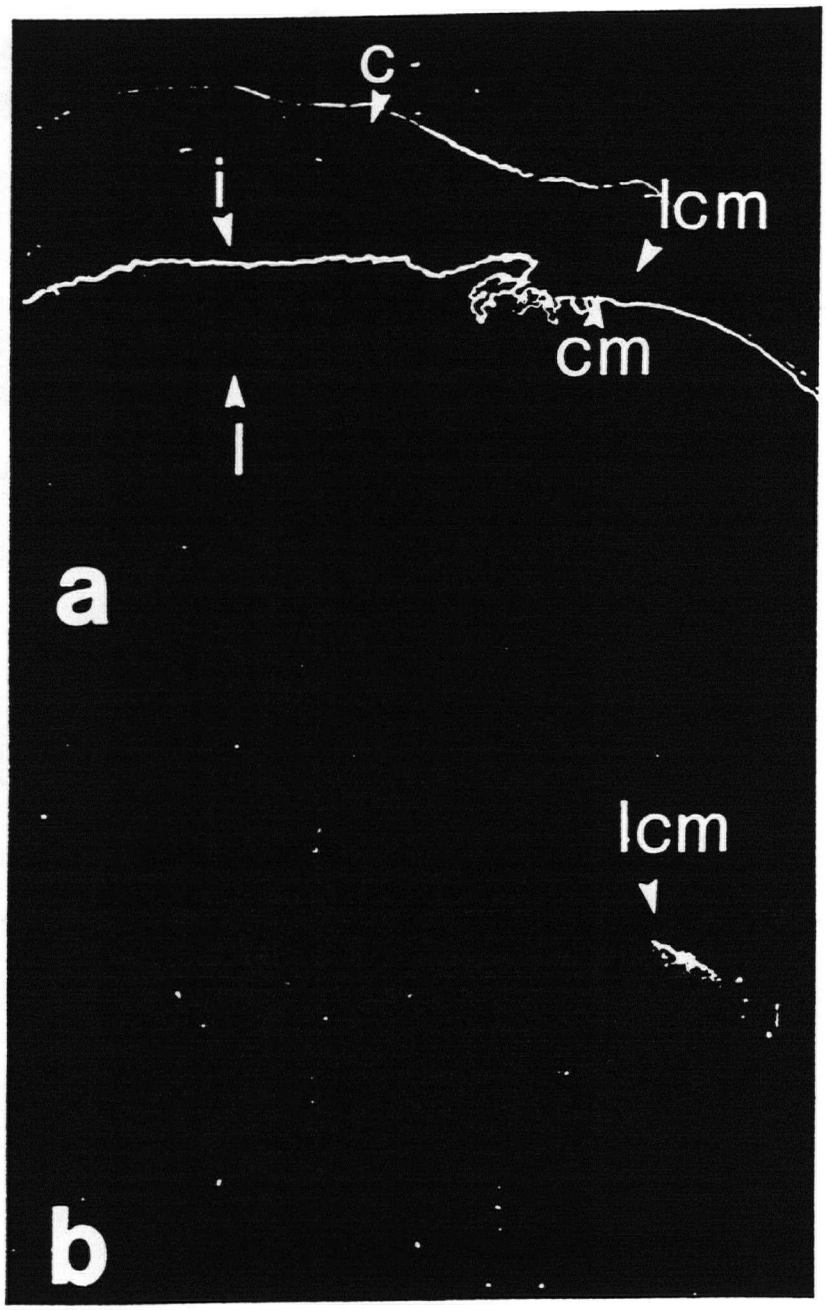
c
i
lcm
cm
l
a
lcm
b

SUMMARY

These studies demonstrate direct anatomical evidence for the presence of muscarinic receptor subtypes in the human eye, with the most striking feature being the differential distribution patterns of [^{3}H]pirenzipine and [^{3}H]oxotremorine binding used to identify M1 and M2 muscarinic receptor subtypes respectively.

[^{3}H]pirenzipine binding sites reveal a higher density of binding in the anterior segment of the eye, and in contrast to this, the [^{3}H]oxotremorine binding sites are almost exclusively retinal, with some density seen in the ciliary muscle. There are few studies in which muscarinic subtypes have been studied pharmacologically in ocular tissues. However, consistent with our finding of [^{3}H]oxotremorine binding sites in the human retina, membrane binding techniques to classify muscarinic receptors in calf retina (92) and in the chick embryo retina (93) demonstrate the predominance of the M2 muscarinic receptor subtypes. Interestingly, our recent studies in adult cat eyes (unpublished observations) demonstrate a complete absence of the M2 retinal receptors in the retina, suggesting interspecies variation, and the need to consider carefully ones choice of animal model for investigations of a physiological nature.

There have been no previous reports to localize muscarinic receptor subtypes in the ciliary muscle of man. Evidence for the presence of at least two subtypes in the human ciliary muscle is presented by [^{3}H]pirenzipine binding sites throughout the ciliary muscle, in addition to a different population of muscarinic receptors detected by [^{3}H]oxotremorine, unique

to only the longitudinal portion of the ciliary muscle. By homogenate binding assays, two muscarinic populations suggestive of M1 and M2 subtypes, have also been identified in the rabbit iris/ciliary body (94).

Although contraction of the ciliary muscle controls accomodative mechanisms in the eye, it is the specific contraction of the longitudinal muscle portion of the ciliary muscle, the tendons of which insert into the trabecular meshwork, that is believed to contribute to outflow facility of aqueous humour (Chapter 1). The data presented provides anatomical-pharmacological evidence supporting a potentially unique function for the longitudinal ciliary muscle, and may be of value to pharmacological strategies in which a more selective increase in outflow without accomodative side effects is desired as in glaucoma therapy. In vivo pharmacological and accomodative studies in an appropriate animal model will be an important step in clarifying the contributions to cholinergic mediated changes in accomodation and aqueous outflow.

Pharmacological agents used to identify muscarinic receptor subtypes do not necessarily identify the same cloned receptor subtypes as do molecular biological approaches (41). While [3H]oxotremorine is a selective M2 agonist, it has been shown to bind to heterogeneous M2 sites (95). The genomic classification for the population of muscarinic receptors labelled by this ligand that we have identified in the longitudinal ciliary muscle is still awaiting clarification. The localization of these putative M1 and M2 muscarinic receptor subtypes and other muscarinic subtypes in the eye, is crucial to hypotheses regarding cholinergic receptor function, and to the interpretation of highly specific drug effects in the eye. Further clarifications by immunocytochemical localization studies as subtype-

specific monoclonal antibodies become available, and by in situ hybridization, in which the mRNA encoding the receptor is probed by cDNA's of the cloned muscarinic receptor subtypes, will be useful contributions to a better understanding of these specific localizations.

CHAPTER 5: THE DISTRIBUTIONS OF THE M3 MUSCARINIC RECEPTOR SUBTYPE AND THE m3 TRANSCRIPT IN THE HUMAN EYE

In chapter 4, 2 muscarinic receptor subtypes were localized by in vitro autoradiographic methods in the human eye. In recent years however, ligand binding studies indicate that at least 3 muscarinic subtypes can be pharmacologically defined (96, 97). On the basis of functional studies, 4-diphenylacetoxy-N-methyl-piperidine methiodide (4-DAMP) has been described as possessing selectivity for the M3 receptor (39). Investigations to evaluate [^{3}H]4DAMP as a probe to directly label muscarinic receptors, indicate that [^{3}H]4DAMP is a useful ligand for selectively labelling both the M1 and M3 muscarinic subtypes (98). This information provided the opportunity to localize the M3 receptor muscarinic receptor subtype in our eye specimens indirectly by competition with the M1 antagonist, pirenzipine.

Important contributions to muscarinic receptor subtype identification have come from studies combining information from both pharmacological and molecular perpectives. Advances in molecular techniques have recently provided ways in which the messenger RNA encoding a receptor protein, can be identified and localized. Thus, *in situ* hybridization provides a map of mRNA, in contrast to a map of the receptor as shown with in vitro autoradiography. Recent information by Northern Blot analysis suggests that in the bovine eye, the m3 transcript predominates in the iris and the

ciliary epithelium over the m1, m2 and m4 transcripts examined (99). Because we were interested in investigating the M3 subtype in the human eye, in this chapter, the autoradiographic approach previously used to define the distributions of general muscarinic receptor binding sites, and M1 and M2 muscarinic receptor subtype binding sites (Chapters 3 and 4) is extended in this chapter to the study of the anatomical distribution of M3 muscarinic receptor subtype. This approach is further compared to the localization of m3 transcripts using in situ hybridization techniques.

PROCEDURE

Sections were prepared as described in Chapter 2 and the specimens used are shown in Table 1. Autoradiography using 0.5 nM [^{3}H]4DAMP ([^{3}H]4DAMP: 82.6 Ci/mmol, New England Nuclear, Missassauga, Ontario) was performed by incubating the sections for 45 min. at room temperature in a buffer consisting of Tris 50 mM, EDTA 1 mM, PMSF (phenylmethyl-sulfonylfluoride) 0.1 mM at pH 7.4 in the presence of 0.5µm unlabelled pirenzipine. Preliminary experiments showed that at this concentration, over 85% of M1 sites were blocked, determined by characterization experiments in which sections were incubated with [^{3}H]4DAMP in the presence of increasing concentrations of unlabelled pirenzipine under the same conditions as described for autoradiography (Fig.19). This was followed by three washes in ice cold buffer at 5 minute intervals. Instead

Figure 19

Competition curve of [^{3}H]4DAMP binding to human iris/ciliary body tissue in the presence of unlabelled pirenzipine. Tissue scrapes (see General Methods) were incubated with 0.5 nM [^{3}H]4DAMP for 20 min. in the presence of increasing concentrations of pirenzipine. Greater than 85% inhibition of [3H]4DAMP at micromolar concentrations of pirenzipine is noted.

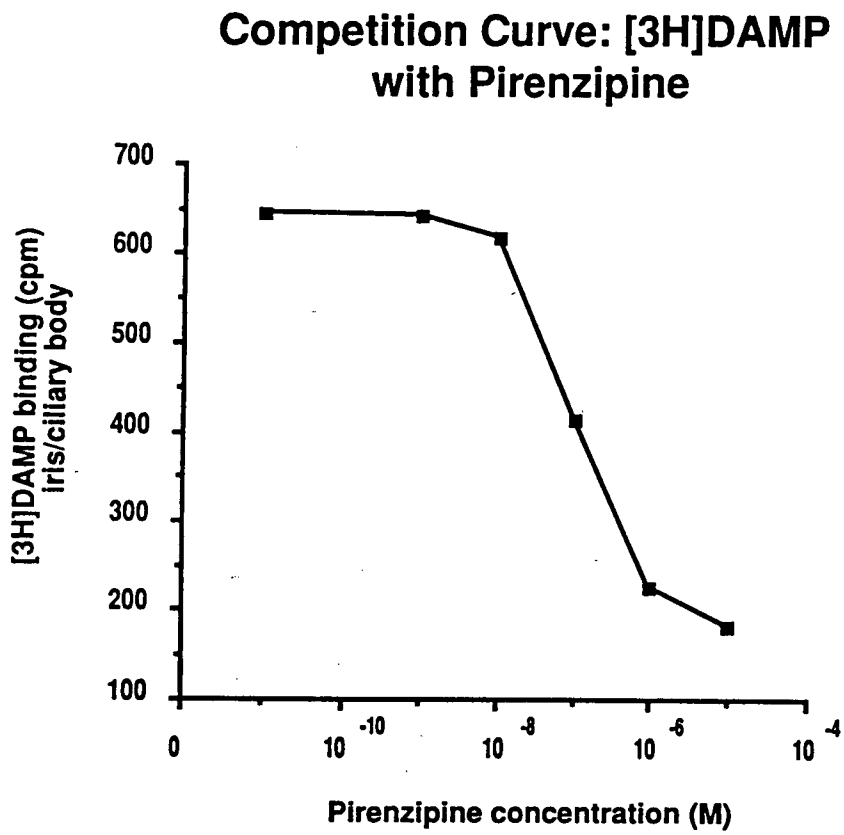
Competition Curve: [3H]DAMP with Pirenzipine
[3H]DAMP binding (cpm) iris/ciliary body
700
600
500
400
300
200
100
0
10 -10
10 -8
10 -6
10 -4
Pirenzipine concentration (M)

of apposing the sections to film, the iris/ciliary body from each eye section was scraped from the slide into liquid scintillation vials, for measurement of radiation levels. For autoradiography, other sections were dried, and autoradiograms were developed after 3 weeks of exposure to isotope sensitive film (LKB ultrafilm, Amersham).

Northern blot hybridization and in situ hybridization procedures with [^{32}P]m3 oligonucleotide and [^{35}S]m3 oligonucleotide probes have been previously described (Chapter 2). A mixture of three probes each of 48 nucleotides were used. Their sequences were as follows:

5'GCGCACGGACTGAGGGCCCGAGCTGCCATTGACAGGTGTGAAGTTGC

5'CTTCTTGACGCTCTGCTTCATTAGTGGGCTCTTGAGGAAGGCCAGCGT

5'GCGCTGGCGGGGGGGCCTCCTCCAGCTTGCCATTGCGCAGCTCCTCCC

RESULTS

In Vitro Autoradiography

The visualization of loci specific for the M3 subtype was performed using unlabelled Pirenzipine at um concentrations, determined by competitive binding studies using 0.5 nM [^{3}H]4DAMP in the presence of increasing concentrations of Pirenzipine to block M1 muscarinic receptor subtype binding sites(Fig. 19). Figure 20 *a* shows a whole eye section labelled with [^{3}H]DAMP in the presence of a 1 μM concentration of unlabelled Pirenzipine. Non-specific binding in the presence of Atropine

Figure 20

Panel A: Autoradiogram of M3 binding sites in a human eye section. Incubations were carried out at 0.5 nM [^{3}H]4DAMP in the presence of unlabelled pirenzipine as described in Chapter 5 procedures. Increased optical densities reflect greater binding. Experiments were done at least in triplicate and in five different specimens all giving similar binding patterns of [^{3}H]4DAMP. Note the presence of binding in the corneal epithelium. Abbreviations:
C = corneal epithelium.

Panel B: Control autoradiogram of M3 binding sites in an adjacent human eye section. Incubations were carried out in the presence of 10 uM atropine, effectively competing for virtually all of the binding sites seen in Panel A. Control sections were included in every experiment, in each case giving similar results.

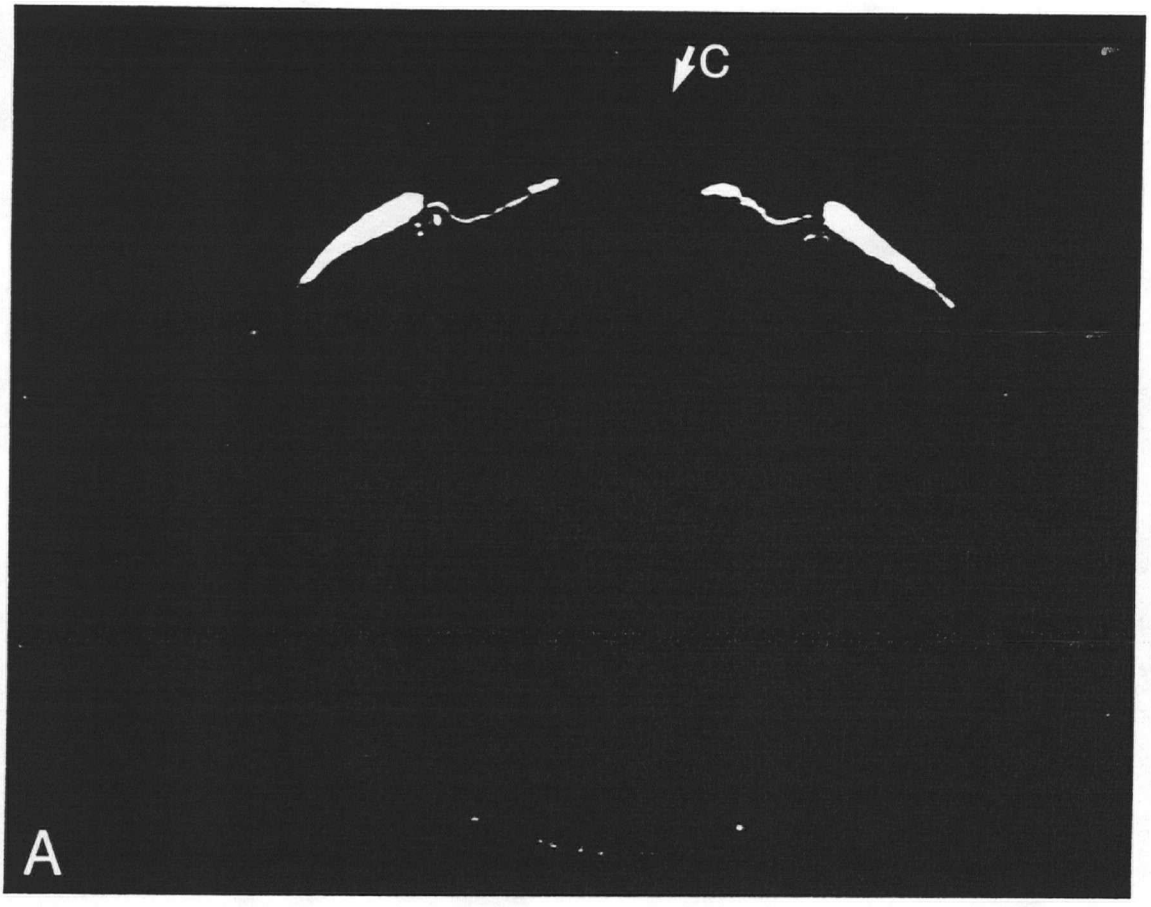
C
A

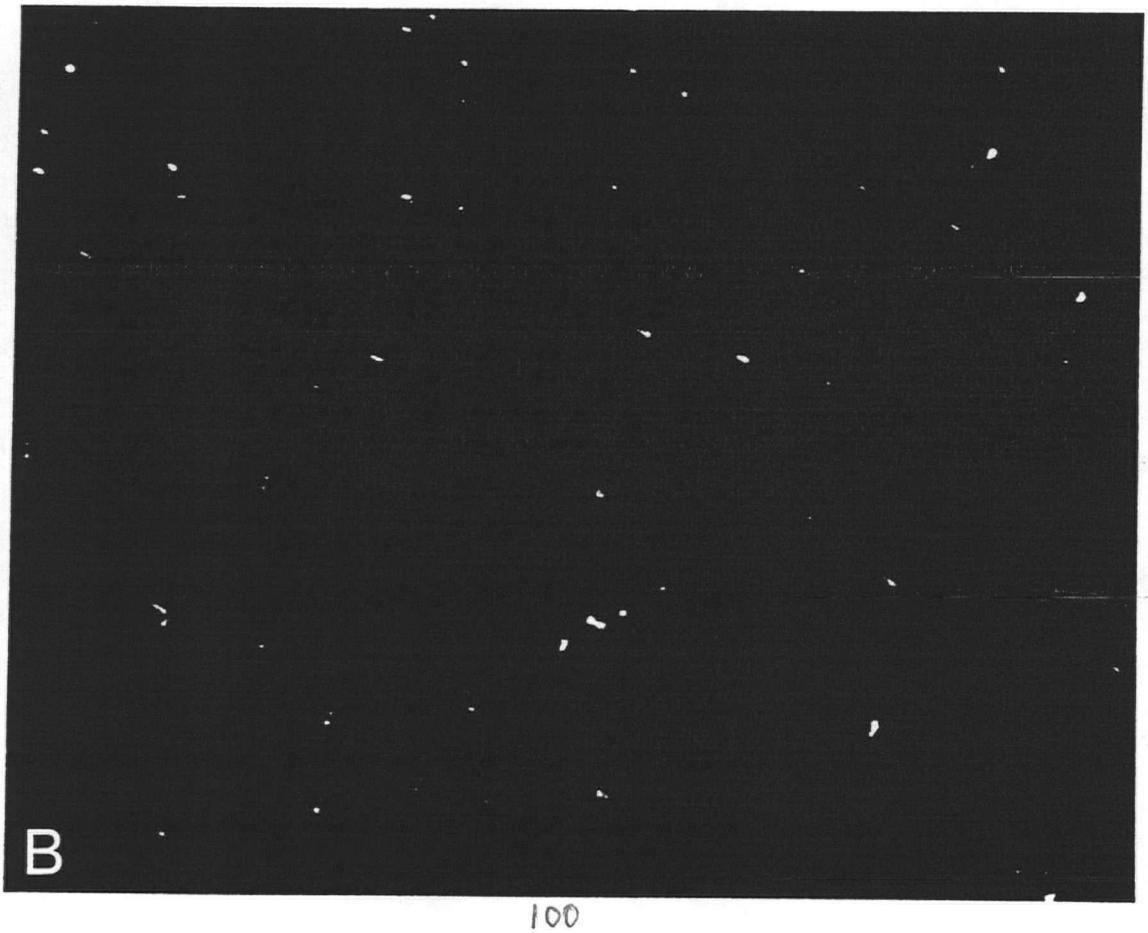
B

sulphate was virtually absent as seen by the control section (Fig. 20 *b*). In the anterior segment of the eye (Fig. 21 *a*), the binding sites specific for the M3 muscarinic receptor subtype were most highly concentrated in the ciliary muscle and were also noted in the corneal epithelium, the iris, the ciliary epithelium, and the active lens epithelial cells situated anteriorly and at the equator. In the posterior segment (Fig. 21 *b*), the M3 muscarinic receptor binding site was localized to the retinal, retinal pigment epithelial, and choroidal layers.

In Situ Hybridization

Total RNA from the anterior segment of the human eye as described in Chapter 2 was extracted and gel electrophoresed. Both 28S and 18S ribosomal bands were clearly visualized (Fig. 22).

Specific hybridization to M3 muscarinic receptor subtype mRNA was demonstrated by the Northern blot which revealed a single band of 3.7 kb (Fig. 23).

Structures which exhibited hybridization to the radiolabelled cDNA probe (Dupont) complementary to a sequence specific for the human m3 transcript were distributed throughout the anterior segment (Fig. 24 *a*). As seen from tissue autoradiograms, moderate to heavy labelling was seen in the iris, with the silver grains most numerous in the anterior stromal border and posterior layers reflecting the distribution of cells in the iris.

Figure 21

Panel A: Higher power view of the anterior segment angle of the [^{3}H]4DAMP labelled autoradiogram seen in Figure 16 A. Binding sites for the M3 muscarinic receptor subtype are most highly concentrated in the ciliary muscle, and are also noted in the corneal epithelium, the iris, the ciliary processes, and the anterior lens epithelium. Abbreviations: a = ciliary muscle, b = corneal processes, c = iris, d = ciliary epithelium, e = anterior lens epithelium.

Panel B: Higher power view of the posterior segment of the [^{3}H]4DAMP labelled autoradiogram seen in Figure 16A. Binding sites are present in the retina and retinal pigment epithelium. Abbreviations: r = retina, RPE = retinal pigment epithelium.


A
b
a
e
c
d


B
r
rpe
ch

Figure 22

An ethidium bromide stained gel is shown before transfer to nylon membrane. 10 ug samples of total RNA from the anterior segment of a human eye (45 yr., 4 hr. post-mortem) was electrophoresed through a 1.1% agarose gel containing 0.66 M formaldehyde (see Chapter 2). Ribosomal 28S and 18S heavy white bands are seen. Extreme right and left lanes represent marker bands.

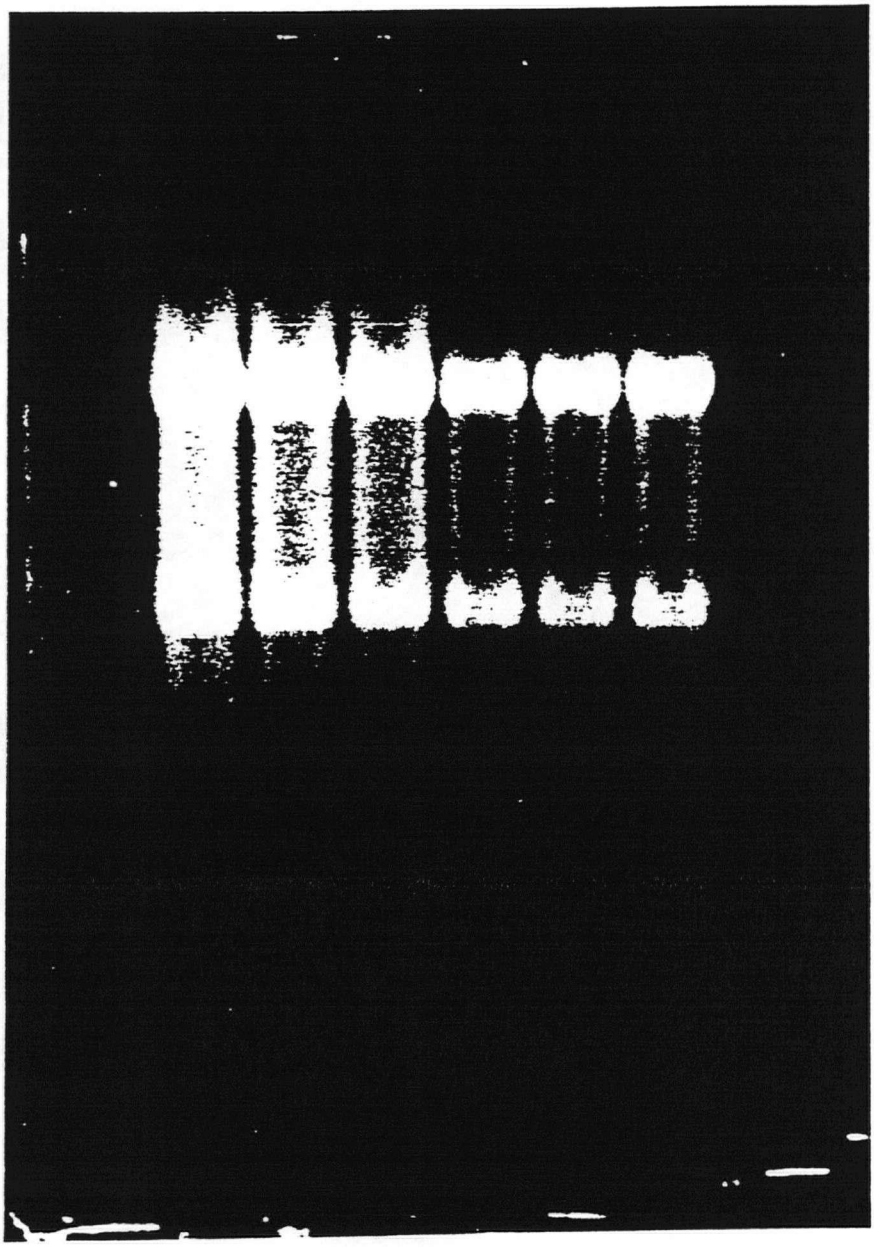

Figure 23

Results of hybridization of the ^{32}P labelled m3 receptor oligonucleotide to a blot of 10 ug total RNA from the anterior segment of a human eye (F 45 yr., 4 hr. post-mortem) showing a single band.

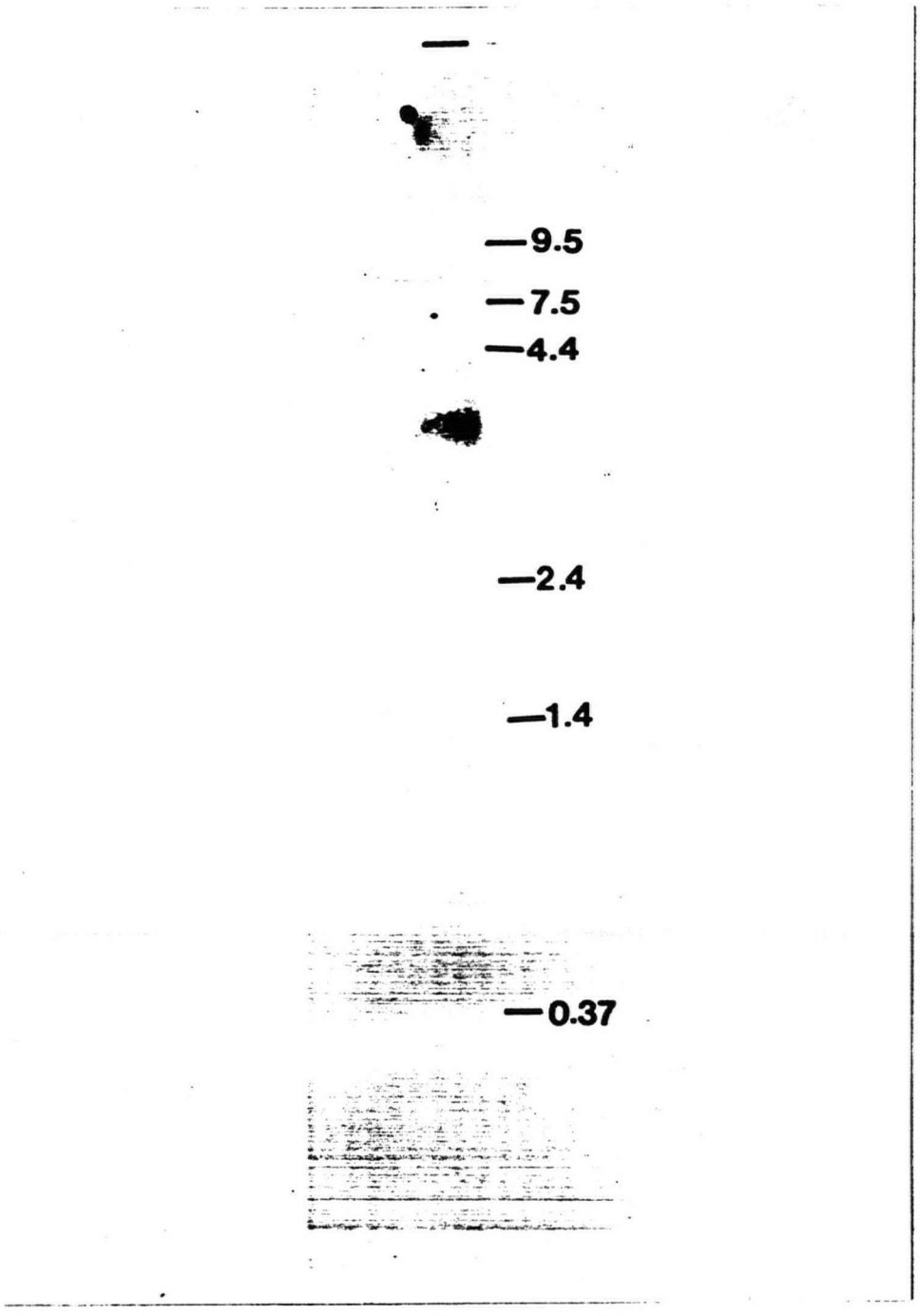
9.5
7.5
4.4
2.4
1.4
0.37

Figure 24

Panel A: Autoradiogram of the anterior chamber angle visualized by in situ hybridization with an cDNA oligonucleotide probe for the M3 muscarinic receptor subtype. The corneal epithelium is heavily labelled and of higher density than the corneal endothelium. The ciliary muscle and the ciliary epithelium are also labelled. Dense silver grains are noted in both the iris anterior stromal border and posterior epithlelial layers. The anterior lens epithelium is distinctly demarcated. The region of the trabecular meshwork is also labelled. Abbreviations:, a = corneal epithelium, b = corneal endothelium, c = iris anterior stromal border, d = iris posterior epithelial layer, e = ciliary epithelium, f = anterior lens epithelium, g = ciliary muscle, h = trabecular meshwork.

Panel B: Control autoradiogram of the anterior segment of an adjacent section to that seen in Panel A. RNase pretreatment (see Chapter 2) abolished hybridization as seen by the low and uniform level of signal compared to the cDNA derived autoradiogram.

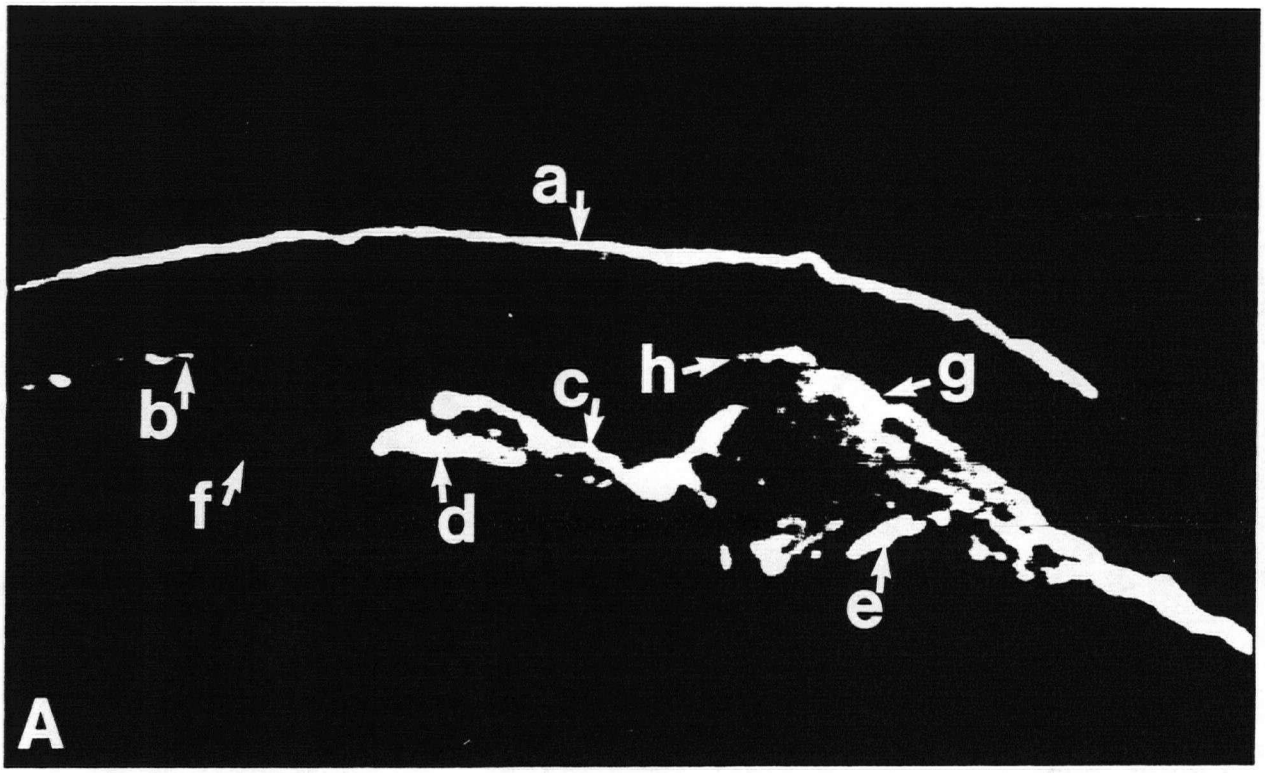
a
b
c
d
e
f
g
h
A


M3 control
B

Corneal epithelium showed heavy uniform labelling relative to the thinner corneal endothelium. The m3 transcript was also noted in both the ciliary muscle and ciliary epithelium. In the angle of the anterior segment, the region corresponding to the trabecular meshwork was distinctly demarcated by an increase in the silver grains.

Additionally, RNase pretreatment abolished hybridization, producing a very low and uniform level of signal compared to the cDNA derived autoradiogram (Fig. 24 *b*) .

SUMMARY

In vitro autoradiographic and in situ hybridization approaches were used to determine the distributions of M3 receptor and m3 transcript in human ocular structures. To date, there have been no previous reports to localize either of these molecules in eyes of any species by direct anatomical methods.

The main findings were the wide distribution of the M3 muscarinic receptor subtype binding site and m3 transcript in the anterior segment of the human eye. The M3 binding site and m3 mRNA co-localized in the corneal epithelium, anterior lens epithelium, ciliary muscle, iris, and ciliary epithelium. In situ hybridization in addition, detected transcript in both the corneal endothelium and trabecular meshwork, although these areas were not seen with receptor autoradiogaphy. Probe specificity for m3 mRNA was ascertained by Northern Blot Hybridization.

The bovine eye has been studied by Northern Blot analysis of the m1 to

m5 species, and the m3 transcript has been shown to predominate (99). Of the muscarinic subtypes that have been examined in ocular tissues, several lines of evidence suggest the presence of M3 receptors in ocular tissues. In the cat and human iris sphincter, 4-DAMP is a more potent inhibitor of [^{3}H]QNB binding and carbachol -induced PI hydrolysis than pirenzipine or AF-DX 116 (11-2((2-((diethylamino)methyl)-1-piperidinyl) acetyl)-5,11-dihydro-6H-pyrido(2,3-b)(1,4)benzodiazepin-6-one), a potent M2 antagonist (100,101). Further-more, 4-DAMP has been shown to inhibit carbachol stimulated Ca++ mobilization in cultured human trabecular meshwork cells (102), and the carbachol induced phosphoinositide response in SV40 transfected human non-pigmented ciliary epithelial cells respectively (103). These studies are consistent with the results presented in this chapter.

Direct anatomical evidence for the M3 muscarinic receptor subtype ligand binding site and its associated mRNA in the corneal epithelium and the anterior lens epithelium has been presented. Its role and possible association with the large quantities of acetylcholine known to exist in the corneal epithelium (19) require further investigations.

The clear mapping of M3 receptors in the front of the eye, is an observation of clinical and therapeutic relevance. Considering that miotic therapy and the medical mangement of raised intraocular pressure depend heavily on directing low specificity cholinergic agents to the anterior chamber, these results may be contributory to the rational design of subtype- specific drugs. The further study of the intracellular consequences

of muscarinic receptor subtype activation may provide insights into the mechanisms by which these subtypes are differentially regulated, providing the means to target and control independent receptor populations in the human eye.

CHAPTER 6: DISTRIBUTIONS OF INOSITOL TRIPHOSPHATE (IP3) RECEPTORS AND PROTEIN KINASE C (PKC) IN THE HUMAN EYE

The previous chapters examined the heterogeneous distributions of muscarinic receptor subtypes in human eyes. Recently, the examination of cell surface receptors for hormones and neurotransmitters, in relation to the intracellular consequences of receptor activation has been a subject of intense investigation. Muscarinic receptors have been shown to mediate the activation of a membrane enzyme called phospholipase C (104, 105, 106), which specifically breaks down a phopholipid cell membrane component called phosphatidylinositol 4,5-biphosphate (PIP2) into IP3 (see Figure 3). The accumulation of the IP3 molecule in the cell causes the release of calcium from intracellular stores, activating calcium dependent processes in the cell. PLC activation also leads to the simultaneous production of diacylglycerol, the "second limb" of the bifurcating pathway. It is this messenger which then activates protein kinase C (PKC) in the presence of calcium and phopholipid. This phosphorylation of proteins by the enzyme PKC is a major means for mediating cell responses (107). PKC is now known to act as the major phorbol-ester receptive protein, and can also be regulated by cAMP and the arachidonic acid cascade (108, 62).

Using ligand binding with tritiated Ins(1,4,5) P_3 and phorbol-12, 13-dibutyrate ([^{3}H]PDBu), the cerebral cortex, and other brain structures

such as cerebellum have been shown to contain large concentrations of IP3 receptors and phorbol ester binding sites (109, 110, 111)]. To date, no binding studies to localize IP3 and phorbol ester binding sites have been performed in human ocular tissues. This chapter localizes the two branches of the phospholipase C activated bifurcating pathway identifiable by examining the distributions of the IP3 receptor and protein kinase C using [^{3}H]Ins (1,4,5) triphosphate ([^{3}H]IP3) and [^{3}H]phorbol-12, 13-dibutyrate ([^{3}H]PDBu) respectively. In addition, computerized densitometry for each of these ligands is described.

PROCEDURE

Eye specimens (see Table 1) were obtained and processed according to previously described methods (Chapter 2). IP3 receptors were labelled by incubating sections with 20 nM concentrations of [^{3}H]IP3 : (Inositol 1,4,5 triphosphate, D-[inositol-1-^{3}H(N)]-: S.A. 17.0 Ci/mmol, NEN, Dupont Canada Inc., Lachine, Quebec). This concentration was used based on generally accepted protocols in the literature for the brain, and in addition the K_D from binding studies in bovine iris fractions (112). Experiments were conducted in the presence and absence of 20 µM unlabelled IP3 (D-myo-inositol 1,4,5-triphosphate hexasodium salt triphosphate: Research Biomedical Inc., Natick , Massachusetts) representing a control for non-specific binding. In brief, sections were incubated for 20 minutes in 20 mM Tris-HCl, 20 mM NaCl, 1mM EDTA, 100 mM KCl, 1 mg/ml BSA at pH 8.5, at 4°C, followed by a 20 second rinse in ice cold buffer. All

sections were dried and subsequently apposed to tritium sensitive film, (LKB Ultrofilm, Amersham) for approximately 6 weeks in the dark.

Autoradiography with [^{3}H]PDBU (Phorbol-12,13-dibutyrate, [20- ^{3}H (N)]: S.A. 20.0 Ci/mmol, NEN, Dupont Canada Inc., Lachine, Quebec) was carried out in Tris-HCl 0.05 M, pH 7.4 at 25°C, at a concentration of 20 nM for incubation period of 3 hours at room temperature. The concentration of 20 nM was determined by a saturation study in which increasing concentrations of [^{3}H]PDBU were incubated with the sections, the radioactivity measured and saturation concentraton determined (Figure 25). Three 5 min. washes in the same buffer were carried out at 4°C. Non-specific binding was defined as the binding seen in the presence of micromolar concentrations of unlabelled PDBU (Phorbol-12 myristate 13-acetate, Sigma, St. Louis, Missouri). Sections were apposed to film for 4 weeks. After autoradiograms were generated, the original eye sections were then stained with cresyl violet for Nissl substance for comparative anatomical reference. Quantitative densitometry by image analysis was performed as described in Chapter 2.

Localization Of [^{3}H]Inositol Triphosphate Binding Sites

In vitro autoradiographic procedures were performed using [^{3}H]IP3 as a high affinity ligand for its binding site. Figure 26 *a* is an autoradiogram demonstrating [^{3}H]IP3 labelled sites in an anatomically intact adult eye section. The silver grain densities produced by the radioactive emission of

Figure 25

Specific binding of [^{3}H]PDBu to human iris/ciliary body tissue as a function of ligand concentration. Incubations were carried out for 3 hours at 25^0 C in the presence of increasing concentrations of [^{3}H]PDBu (see Chapter 6). Non-specific binding was measured by addition of micromolar concentrations of unlabelled PDBu. Specific binding was determined as the difference between total and non-specific binding at each concentration. Experiments were run in triplicate, and each value is the mean of six to nine determinations. Saturation of [3H]PDBu binding sites is noted at 20 nM.

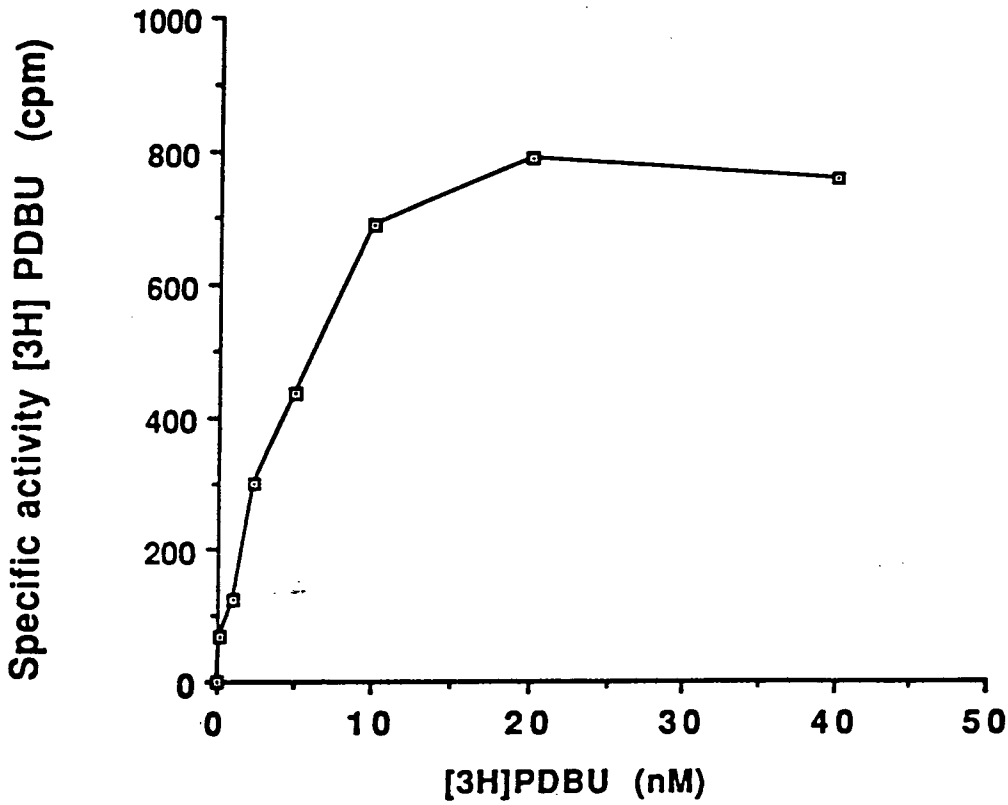
Specific activity [3H] PDBU (cpm)
1000
800
600
400
200
0
0
10
20
30
40
50
[3H]PDBU (nM)

Figure 26

Panel A: Autoradiogram of [^{3}H]IP3 binding in a human eye section. Incubations were carried out at 20 nM [^{3}H]IP3 as described in Procedures of Chapter 6. Increased optical densities reflect greater [^{3}H]IP3 binding. Experiments were done in triplicate and in at least five different specimens all giving similar binding patterns of [^{3}H]IP3. Note the high concentration of binding in the ciliary muscle. Abbrev.: cm = ciliary muscle.

Panel B: Control sections were present in every [3H]IP3 in vitro autoradiography experiment by including 20 μm unlabelled IP3, effectively competing for virtually all of the binding sites seen in Panel A.

A

B

the [^{3}H]IP3 reflected the anatomical distribution of the drug bound to the eye section *in situ.* The control section as shown in Figure 26 *b* showed virtually no non-specific binding of [^{3}H]IP3, the binding being effectively blocked by competition with unlabelled inositol triphosphate.

In the anterior segment (Fig. 28 *a*), the highest density of silver grains was found in the ciliary muscle. The ciliary epithelium was also labelled. In the cornea, binding sites were of higher density in the epithelial than the endothelial layer. Relative to the central area of the endothelial layer, the peripheral margins corresponding to the trabecular endothelium had higher silver grain densities. Although in the iris, the most notable binding was seen in the posterior layer, the anterior stromal border was also distinctly labelled.

In the posterior segment (Fig. 29 *a*), three distinct bands of labelling can be discriminated, corresponding specifically to the retina, retinal pigment epithelium and the choroid.

Localization Of [^{3}H] PDBu Binding Sites

Human eye sections adjacent to the sections used to determine the loci of [^{3}H]IP3 binding sites, were used to visualize [^{3}H]PDBU binding sites as seen in the autoradiogram (Fig. 27 *a*). Effective competition by unlabelled PDBU is shown in the control panel (Fig. 27 *b*).

In contrast to the density distribution seen using [^{3}H]IP3, [^{3}H]PDBU clearly showed the highest concentration of silver grain densities in the retina (Fig. 29 *b*). In the anterior segment (Fig. 28 *b*), the most

Figure 27

Panel A: Autoradiogram of [^{3}H]PDBu binding in the same human eye as used for Fig. 26. Incubations with 20 nM [^{3}H]PDBu were carried out as described in Procedures of Chapter 6. Experiments were done in triplicate and in at least five different specimens all giving similar binding patterns of [^{3}H]PDBu. Note the high concentrations of binding in the retina and ciliary muscle. Abbrev.: r = retina, cm = ciliary muscle.

Panel B: Control sections were present in every [3H]PDBu in vitro autoradiography experiment by including 20 μm unlabelled PDBu, effectively competing for virtually all of the binding sites seen in Panel A.

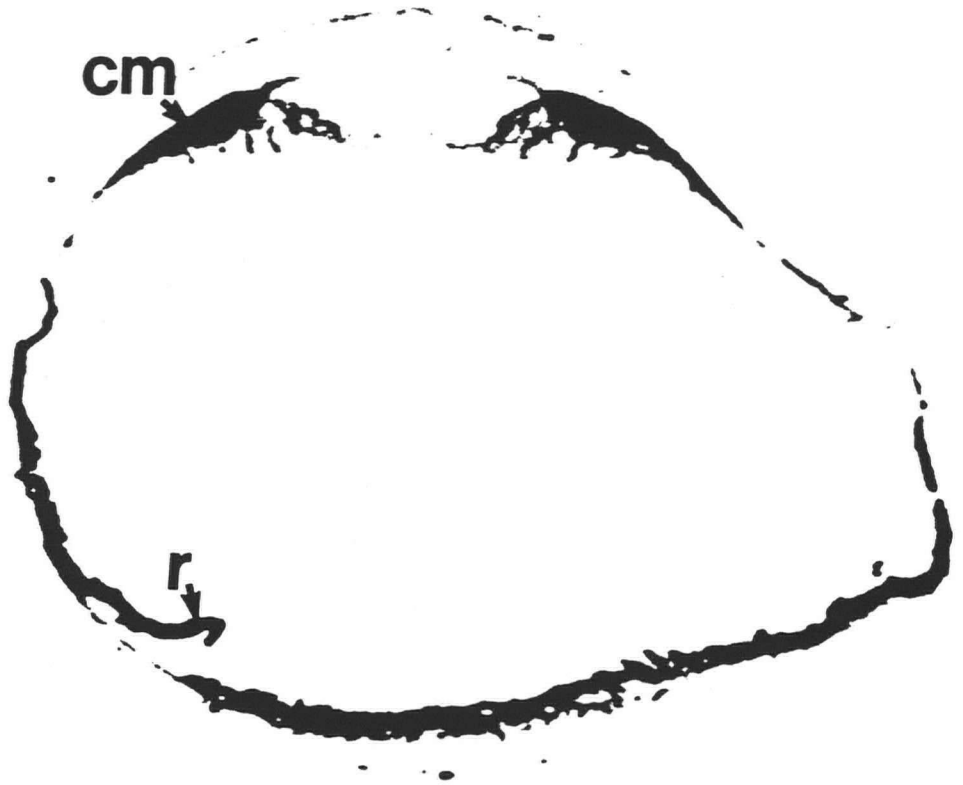

A

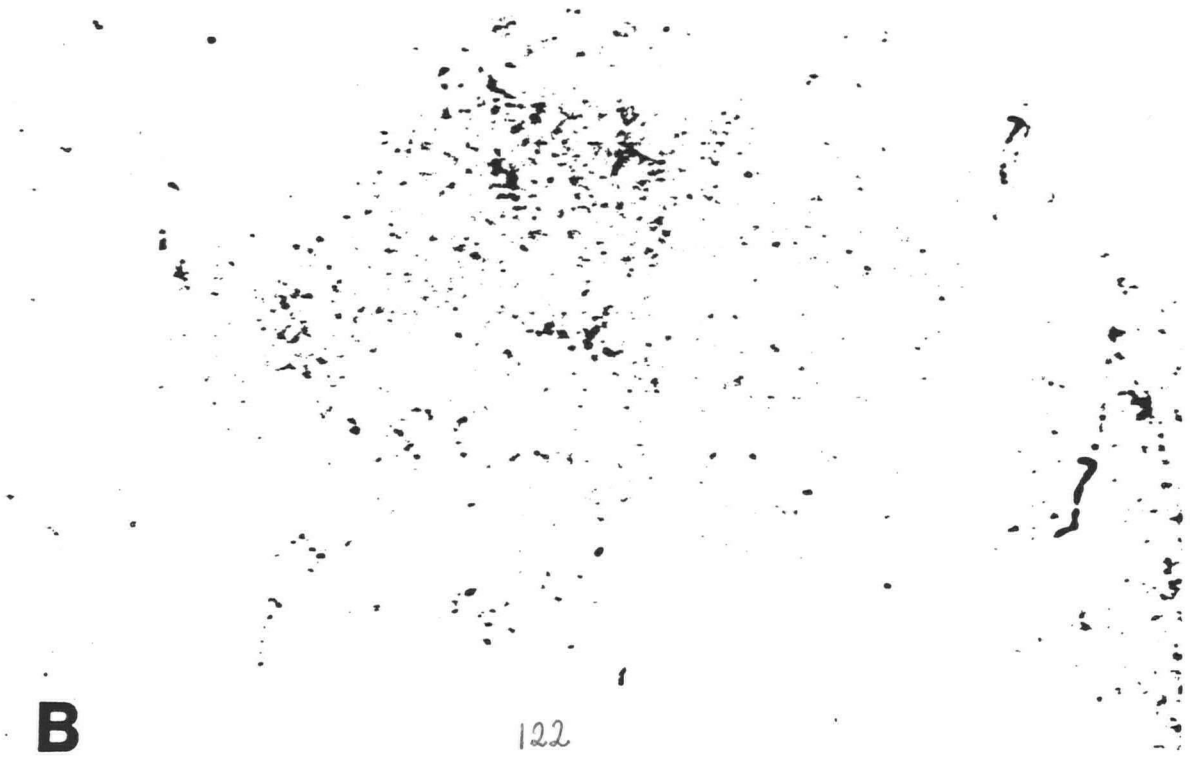

B

Figure 28

Panel A: High power view of the anterior segment angle of the [^{3}H]IP3 labelled autoradiogram seen in Figure 22 A. The highest density of silver grains is found in the ciliary muscle. [^{3}H]IP3 binding sites in the cornea are of higher density in the epithelial than the endothelial layer, where the peripheral margins corresponding to the trabecular endothelium have higher silver grain densities. The iris anterior stromal border and posterior epithelial layers are also labelled with more pronounced binding in the latter. Abbreviations: a = ciliary muscle, b = corneal epithelium, c = corneal endothelium, d = ciliary epithelium, e = trabecular endothelium, f = iris anterior stromal border, g = iris posterior epithelium,

Panel B: High power view of the anterior segment angle of the [^{3}H]PDBu labelled autoradiogram seen in Figure 23 A. [^{3}H]PDBU binding shows the highest concentration of silver grain densities in the ciliary muscle. Higher silver grain densities are noted in the corneal epithelium in contrast to the corneal endothelium. Moderate binding is seen in the trabecular meshwork, and peripheral corneal endothelium, with progressively lighter binding approaching the central endothelium area. In contrast to the density distribution of [^{3}H]IP3 seen in Panel A, the anterior stromal border of the iris is heavily and sharply distinguished from the lower levels of binding noted in the iris stroma and posterior epithelial layer. The ciliary epithelium shows moderate levels of silver grain density.

Abbreviations: a = ciliary muscle, b = corneal epithelium, c = corneal endothelium, d = ciliary epithelium, e = trabecular endothelium, f = iris anterior stromal border, g = iris posterior epithelium

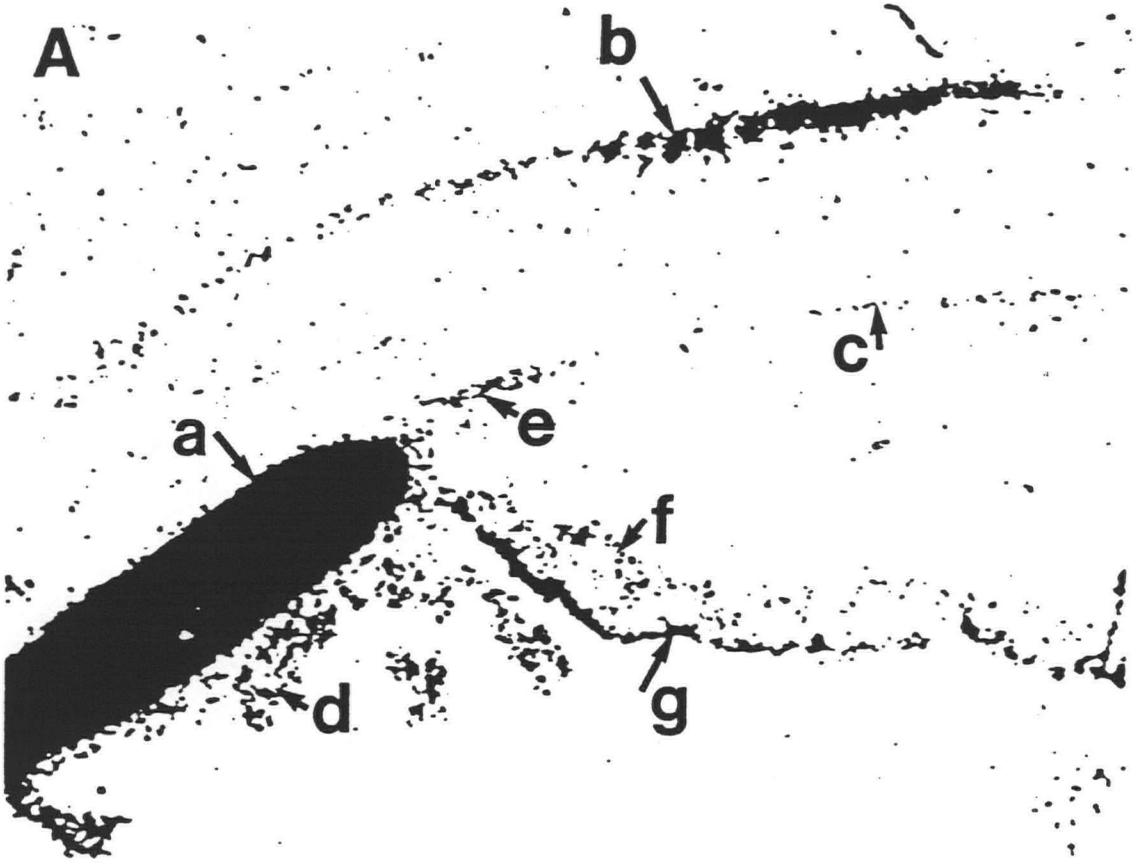
A
b
c
e
a
f
d
g

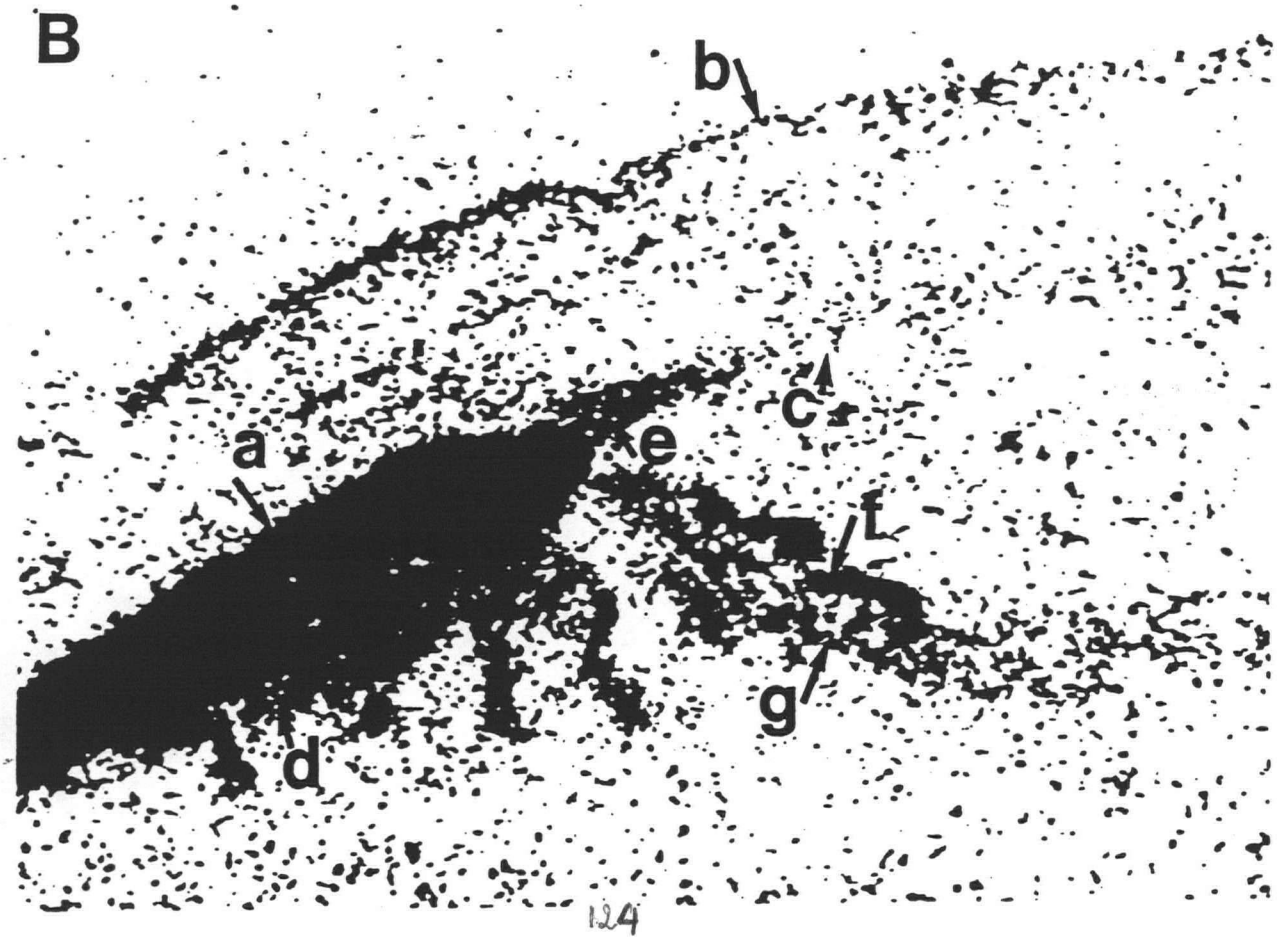
B
b
c
a
e
f
g
d

Figure 29

Panel A: High power view of a region of the posterior segment seen in the [^{3}H]IP3 labelled autoradiogram shown in Figure 26A. Three distinct bands of labelling can be discriminated. The heaviest [^{3}H]IP3 binding is seen in the retina, with moderate binding in the retinal pigment epithelium and choroid. Specific cell types within these structures are not identifiable. Abbreviations: r = retina, rpe = retinal pigment epithelium, ch = choroid.

Panel B: High power view of a region of the posterior segment seen in the [^{3}H]PDBu labelled autoradiogram shown in Figure 27A. PKC binding is heavy in the layers of the posterior segment with the most pronounced labelling throughout the layers of the retina. Heavy binding is also seen in both the retinal pigment epithelium and the choroid. Abbreviations: r = retina, rpe = retinal pigment epithelium, ch = choroid.

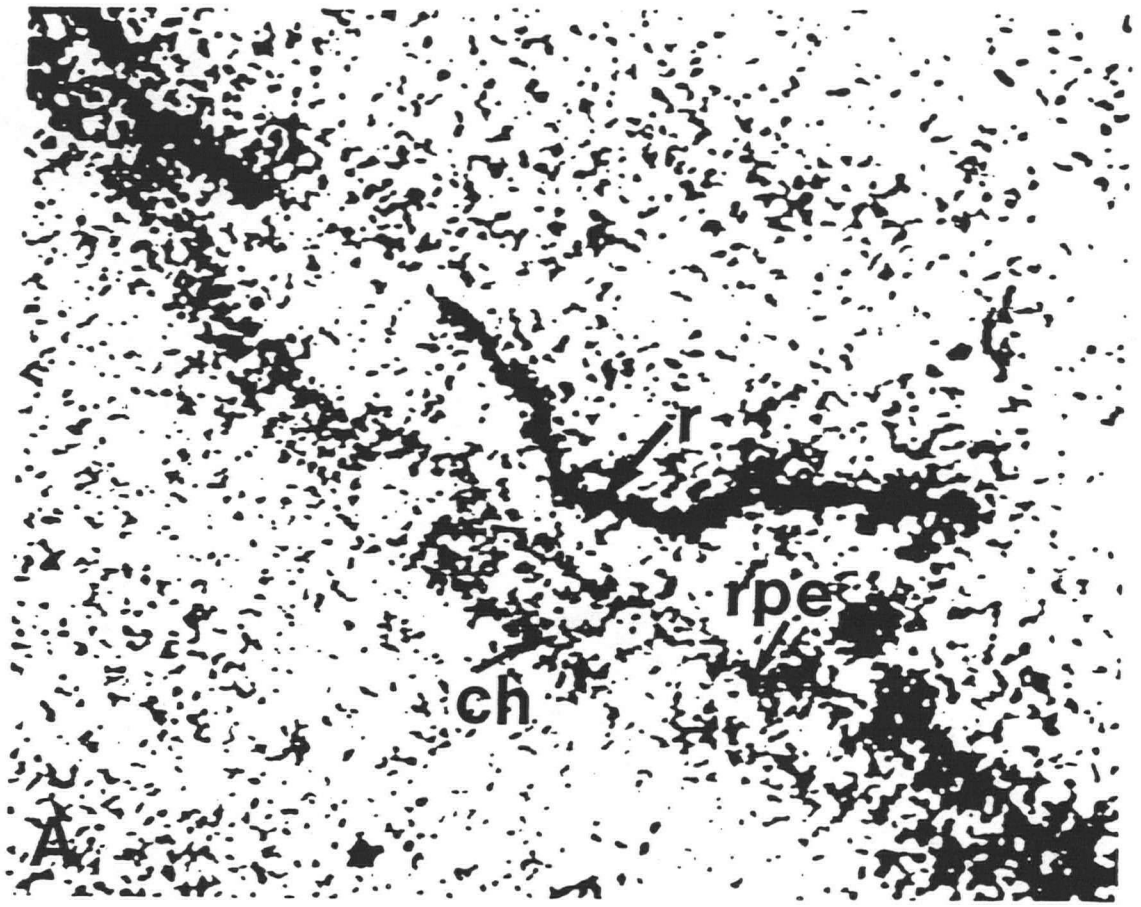
r
rpe
ch
A

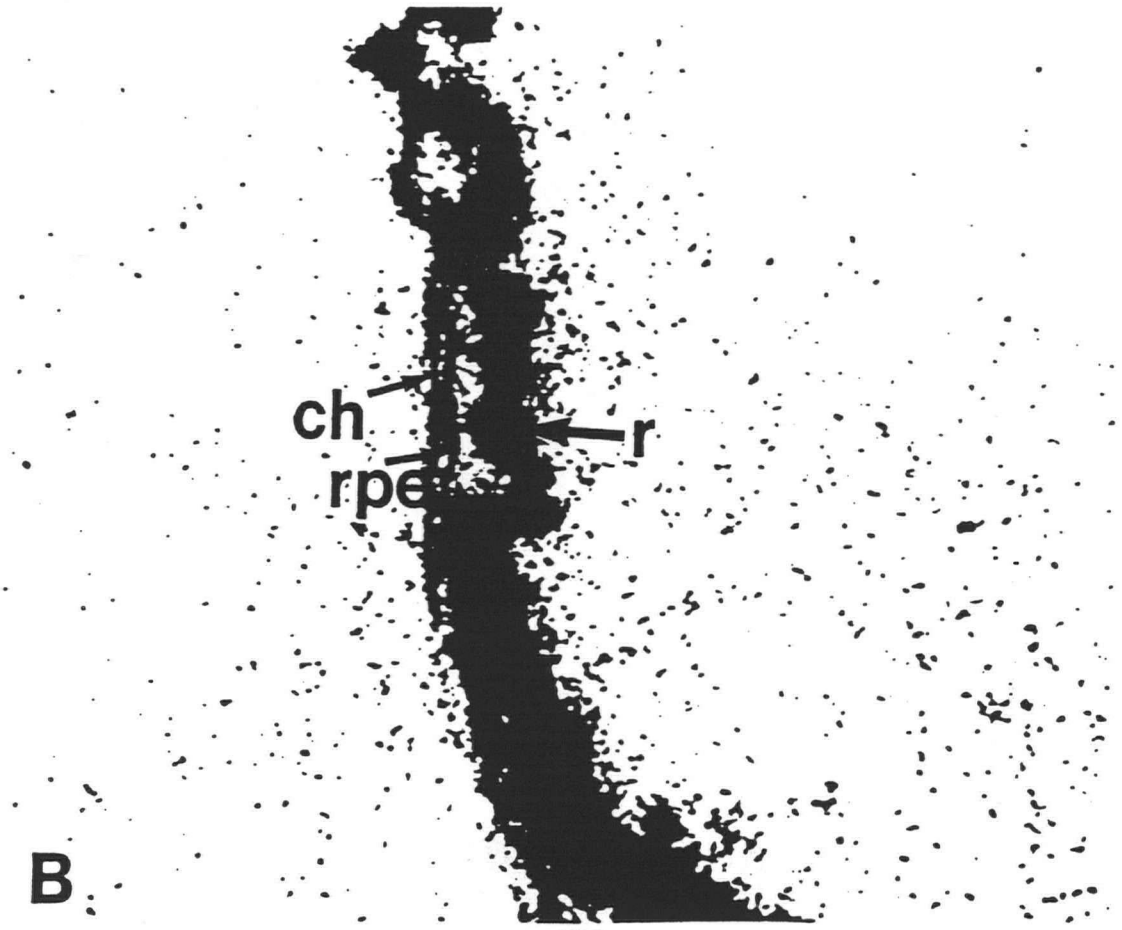
ch
r
rpe
B

prominent structure labelled was the ciliary muscle. Moderate binding was seen in the trabecular meshwork, with extension to the peripheral corneal endothelium, with lighter binding approaching the central endothelium area. Moderate to heavy binding is seen in the corneal epithelium. The anterior stromal border of the iris was sharply distinguished from the lower levels of binding noted in the iris stroma and posterior epithelial layer. The ciliary epithelium showed moderate levels of silver grain density.

PKC binding was heavy in the layers of the posterior segment, and corresponded specifically to the retina, retinal pigment epithelium and the choroid.(Fig. 29 *b*)

Quantitative Densitometry Of [^{3}H]IP3 And [^{3}H]PDBu Binding Sites

Quantitative analysis for each of [^{3}H]IP3 and [^{3}H]PDBu binding was performed in adjacent sections from a single specimen. Computerized densitometric measurements of the following structures labelled by autoradiography were performed: corneal epithelium, corneal endothelium, ciliary muscle, iris anterior stromal border, iris posterior layers, ciliary epithelium, trabecular meshwork, retina, retinal pigment epithelium, and choroid. The absolute values obtained are shown in Figure 30 *a*. What is most obvious from the figure is that the ciliary muscle contained the highest density of IP3 binding sites, and the retina showed the highest density of phorbol ester binding sites. The standardized graph shown in Figure 30 *b* facilitates examination of the densities in structures relative to the ciliary muscle, for both molecules, and allowed their relative

Figure 30A: Quantitation (nCi/mg) of mean grey levels in ocular structures by image analysis of autoradiograms showing [^{3}H]IP3 and [^{3}H]PDBu binding in adjacent sections within a single specimen. Following the calibration of autoradiograms with tritium standards containing known quantities of radiation, optical density readings of each of the structures shown were determined for each eye (See Chapter 2 for General Methods). [^{3}H]PDBu binding is highest in the retina, ciliary muscle, and iris anterior stromal border layers in decreasing order. [^{3}H]IP3 binding is highest in the ciliary muscle. Each value represents the mean of three independent measurements with standard errors ranging from 0.03 to 0.09.

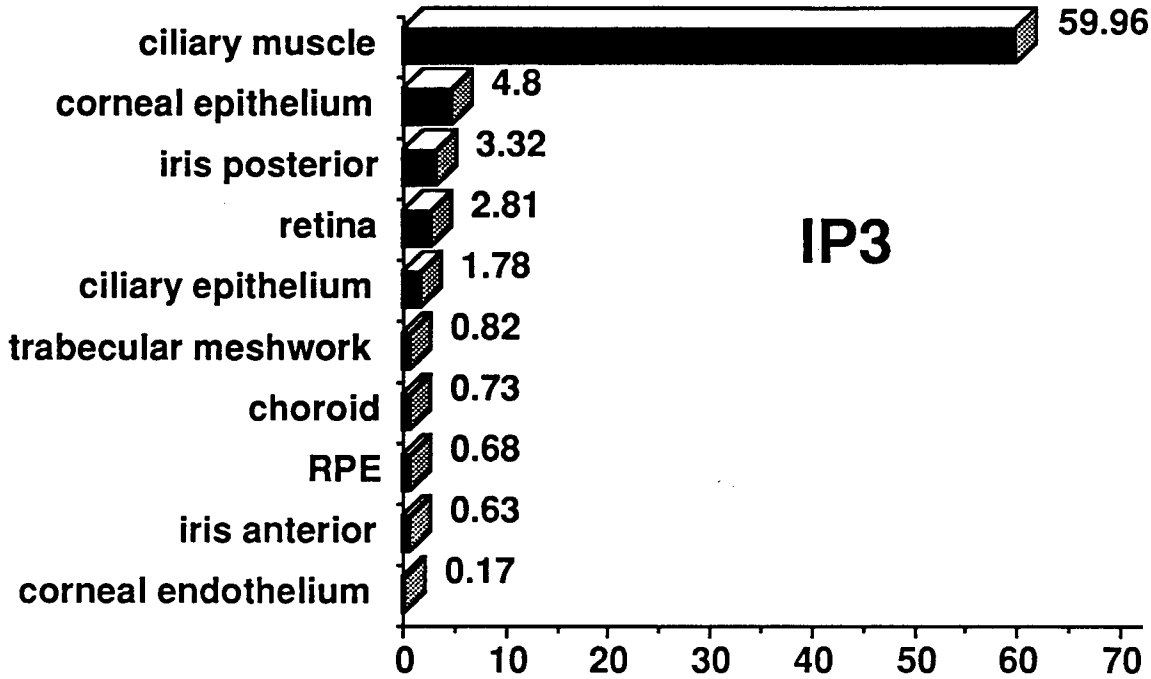
ciliary muscle
corneal epithelium
iris posterior
retina
ciliary epithelium
trabecular meshwork
choroid
RPE
iris anterior
corneal endothelium
59.96
4.8
3.32
2.81
1.78
0.82
0.73
0.68
0.63
0.17
IP3
0
10
20
30
40
50
60
70

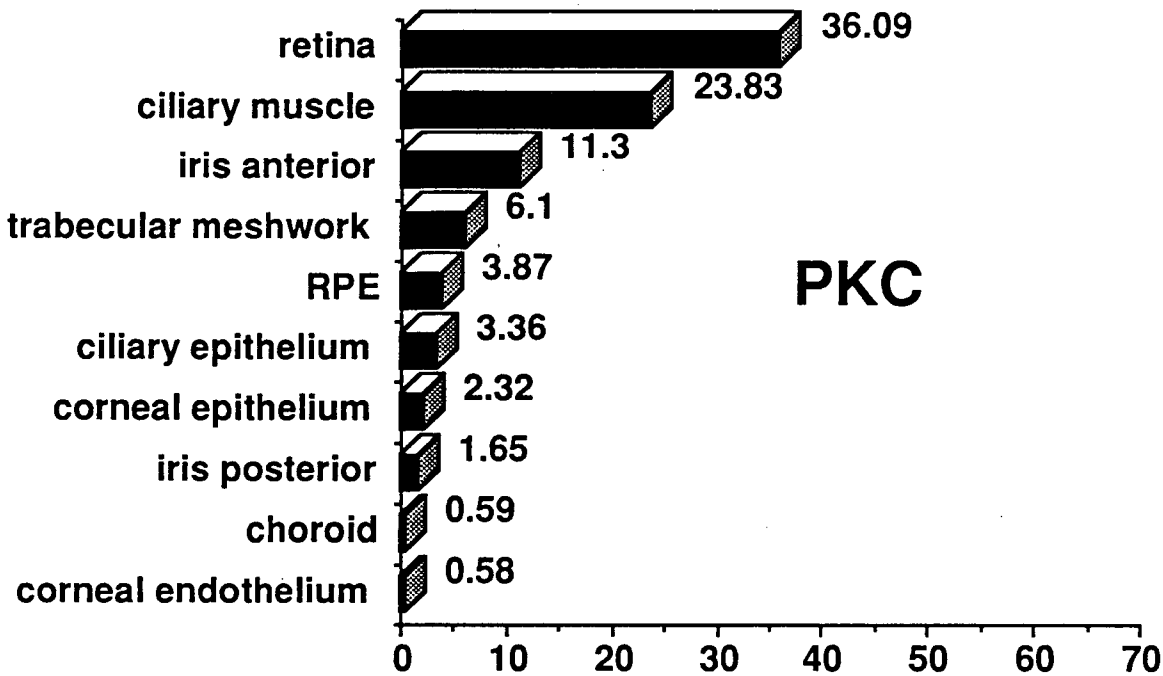
retina
ciliary muscle
iris anterior
trabecular meshwork
RPE
ciliary epithelium
corneal epithelium
iris posterior
choroid
corneal endothelium
36.09
23.83
11.3
6.1
3.87
3.36
2.32
1.65
0.59
0.58
PKC
0
10
20
30
40
50
60
70

Figure 30B: Panel B: Specific activity (nCi/mg) is expressed as a percentage of ciliary muscle activity, in the same structures within the adjacent eye sections examined for [^{3}H]IP3 and [^{3}H]PDBU binding seen in Panel A. Note that in every structure, the proportion of [^{3}H]PDBU binding relative to [^{3}H]IP3 binding in the same structures is higher. This discrepancy is most notable in the iris anterior stromal border, the retina, and the trabecular meshwork. In the iris, [^{3}H]PDBu binding is higher in the anterior stromal border than in the posterior border by a factor of greater than 6. [^{3}H]IP3 binding in the iris layers shows the inverse relationship with binding in the iris posterior epithelium higher than in the anterior stromal border by a factor of approximately 5. Abbreviations: iris anterior = iris anterior stromal border, iris posterior = iris posterior epithelium, RPE = retinal pigment epithelium.

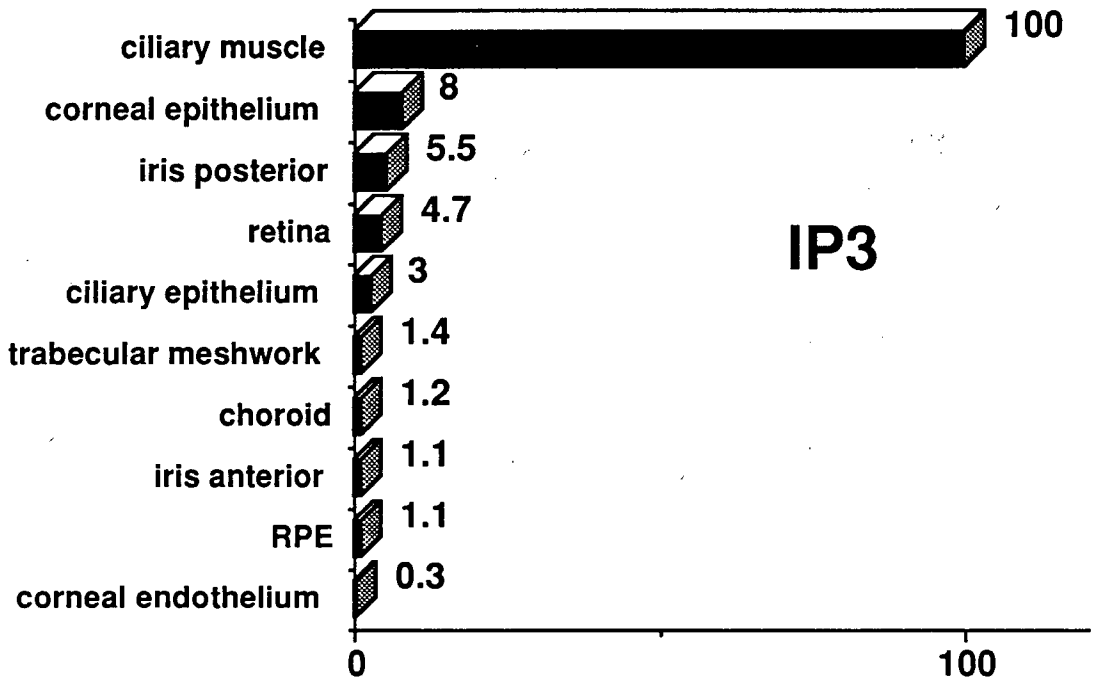
ciliary muscle
corneal epithelium
iris posterior
retina
ciliary epithelium
trabecular meshwork
choroid
iris anterior
RPE
corneal endothelium
100
8
5.5
4.7
3
1.4
1.2
1.1
1.1
0.3
IP3
0
100

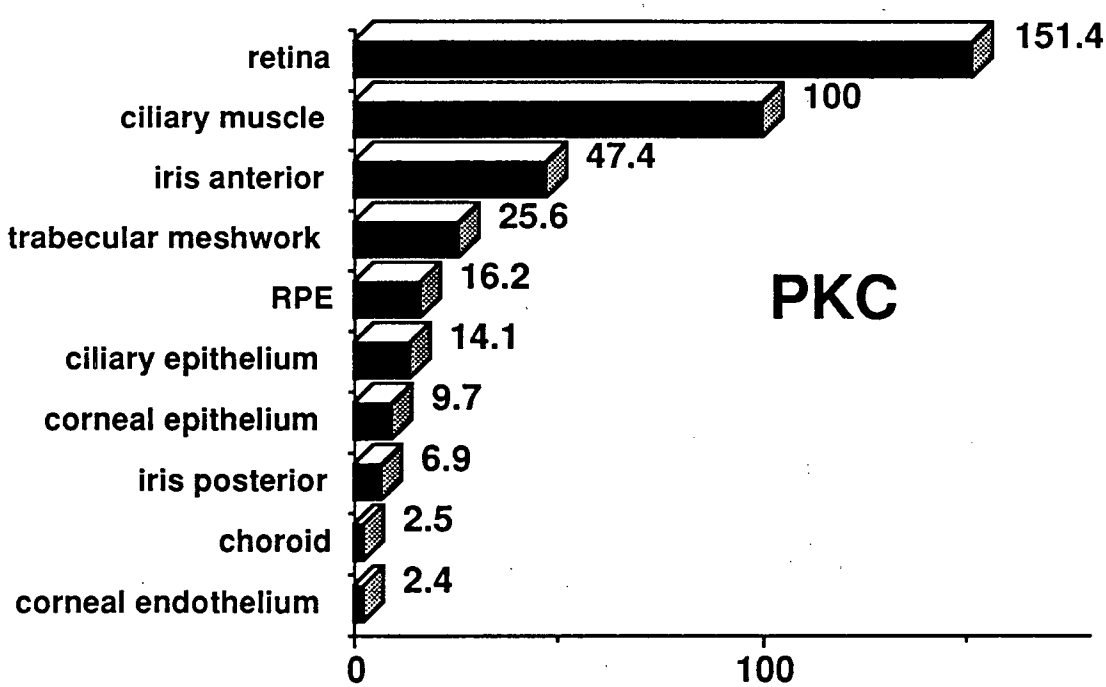
retina
ciliary muscle
iris anterior
trabecular meshwork
RPE
ciliary epithelium
corneal epithelium
iris posterior
choroid
corneal endothelium
151.4
100
47.4
25.6
16.2
14.1
9.7
6.9
2.5
2.4
PKC
0
100

quantitative comparison. The ratios of the bound activity in the ciliary muscle to that found in other structures consistently increased in the following order for IP3: iris and ciliary epithelium, retina, retinal pigment epithelium, and for PKC in the following order: corneal endothelium, choroid, iris posterior epithelial layer, corneal epithelium, ciliary epithelium, retinal pigment epithelium, trabecular meshwork, iris anterior stromal border, ciliary muscle, and retina. Each optical density value was calculated by averaging three independent measurements, each measurement made in adjacent sections of the same specimen.

SUMMARY

Employing the in vitro autoradiographic method previously used to effectively map muscarinic receptor populations in the human eye (Chapters 3, 4, 5), these studies report the distributions of the intracellular receptors for IP3 and phorbol-12, 13-dibutyrate (PDBu). In addition, their relative binding densities have been analyzed using quantitative densitometric analysis.

The results of these studies present several observations. In virtually every ocular structure examined, both [^{3}H]PDBu and [^{3}H]Ins(1,4,5) binding sites are present, suggesting the co-existance both limbs of the inositol hydrolysis pathway. Despite this co-localization however, the relative numbers of [^{3}H]PDBu and [^{3}H]Ins(1,4,5) sites vary widely in different ocular regions. This is evident from the densitometric study in which several structures such as the ciliary muscle and the retina showed

high concentrations of both molecules while other structures showed high concentrations of one or the other of IP3 or PKC. Whether this is in fact due to the localization of IP3 receptors and PKC in different cell populations within a tissue structure, or due to their localization in distinctly different subcellular regions within a single cell, is as yet uncertain. Evidence for each of these possibilities has been reported in the brain (110, 111). Molecular cloning analysis has established that protein kinase C represents a large family of proteins with multiple subspecies. In a variety of tissues, each of these isoenzymes, has been demonstrated to have distinct localization patterns, one being specific only to neuronal tissue (113). [^{3}H]PDBu is not isoenzyme specific. Collectively, this suggests that the PKC concentrations that we have measured in neural and non-neural ocular tissues likely reflect several PKC subtypes.

The ciliary muscle, unlike most other structures, showed co-localization of both IP3 and PKC with mutually high concentrations of each. On the other hand, while high levels of PKC binding sites were found in the retina, trabecular meshwork, and retinal pigment epithelium, in the same structures, there were relatively low numbers of [^{3}H]Ins(1,4,5) P3 binding sites. Evidence for both limbs of this pathway were noted in the human iris, however, within the confines of this single anatomically well-defined structure, further anatomical subdivisions were visualized by the preferential concentration of one effector molecule over the other, in highly specific regions.The iris anterior stromal border, rich in PKC binding sites, and low in IP3 sites, contrasted sharply with the iris posterior epithelial layer in which a high density of IP3 binding sites and relatively lower levels of PKC binding sites were found. Evidence in the bovine and

rabbit iris sphincter smooth muscle for PI turnover and protein kinase C respectively, has been demonstrated (114, 115, 116). The neuroanatomical evidence for effector system predominance in distinct regions of the iris may be important in understanding these regions from a functional perpective.

Both layers of the cornea demonstrated IP3 and phorbol ester binding sites; however, the corneal epithelium showed significantly higher concentrations of each of these molecules than does the corneal endothelium. The human ciliary epithelium demonstrated concentrations of both IP3 and PKC binding sites. Studies in the rabbit ciliary processes giving evidence for coupling to PI turnover , and protein kinase C activity, suggest that they are at least localized in the non-pigmented cell layer (117, 118). Products of the inositol pathway have been identified in the bovine rods (119). Our studies showed that the human retina contains both IP3 and phorbol ester binding sites.

The heterogeneous distribution of the [3H]IP3 and [3H]PDBu binding sites in human ocular structures raises the question of whether these products of phospholipase C activation act synergisically, independently, or with one limb ascending over the other to effect a particular cellular response. Mechanisms by which the latter may occur, may involve the capacity of the IP3 receptor to be phosphorylated into inositol 1,3,4,5-tetrakisphosphate (IP4), which in itself, can act as another second messenger in regulating extracellular Ca++ influx in various cell types.(120, 121,122, 123) The hydrolysis of phospholipid has been shown to occur in the absence of PKC activation in rat brain (124). On the other

hand, a mechanism by which more selective activation of PKC occurs, apart from DG regulation, and independent of IP3 receptor activation, may occur through the arachidonic acid cascade which can also regulate PKC (108,62). Based on the capacity of a cell to react to a multiplicity of changing external signals with which it is continually being presented, all of these alternatives may be possible.

The study of post-receptorial events is further complicated by the growing evidence for heterogeneity of the molecules involved in the second messenger cascades, including PLC (125, 126, 127), and PKC (113). As the distributions of these numerous ocular second messenger molecules in the human eye continue to be investigated, implications emerge for understandings of the way in which muscarinic cholinergic receptors and other receptors are regulated, and for targeting these intracellular molecules therapeutically.

CHAPTER 7: GENERAL DISCUSSION

In this thesis, the anatomical organization of general muscarinic receptors, 3 muscarinic receptor subtypes and 2 second messenger molecules have been described in the human eye. In this chapter, I would like to first discuss the importance of the *in vitro* autoradiographic approach, and the implications and importance of these studies in human eye tissue, keeping in mind several limitations. Finally, general conclusions and implications drawn from the specific distributions of the muscarinic receptor subtypes and second messenger molecules localized will be addressed.

These studies are the first to determine the distributions of muscarinic receptors in the anatomically intact human eye. The in vitro autoradiographic approach used in these experiments has numerous advantages. Through the visualization of the normal anatomical distributions of receptors in eye sections, the examination of many different ocular structures at once was possible, making it highly efficient as an approach. The practicality of this method is further emphasized by the need for very small quantities of eye tissue. In this way, it was possible to study the relative distributions of many different ligands in adjacent tissue sections from a single specimen. From a therapeutic standpoint, whether a drug is useful is crucially dependent upon its ability to produce its desired effects with tolerable or minimal undesired effects. Thus the *selectivity* of its effects is one of its most important characteristics.

The in vitro autoradiographic identification of anatomical targets highly specific for radioligands of high selectivity for a receptor subtype, permits hypothetical predictions regarding the effects of one pharmacological agent over the other in the eye. Traditionally, the pharmacokinetic analysis of ocular receptors has used the homogenate binding technique in which the ocular structure under examination is thoroughly disrupted before being subjected to ligand binding. Errors are more likely to occur by the homogenate technique due to measurements of small amounts of tissue that need to be handled, often from pooled specimens. By using in vitro autoradiography, this problem was circumvented by the high degree of control afforded by adjacent slide mounted sections within a single specimen, without the need for difficult dissections or the large amounts of tissue required by conventional binding methods. That this technique can also be applied to post-mortem human tissue is of particular importance.

Pharmacological evaluation in man is limited by technical, legal, and ethical considerations, thus choice of drugs must be based in part on their pharmacological evaluation in animals. Therefore, some knowledge of animal and comparative pharmacology is helpful in deciding the extent to which claims for drugs based upon studies in animals can be extrapolated to man. By examining and determining cholinergic drug targets first in human tissue, comparative anatomical studies in animals may follow, and a more rational basis for the pharmacological manipulations then to be performed in animals can be established. Of fundamental importance,

comparison of the results in human ocular tissue with those in animal ocular tissue, may be the first step in determining a suitable animal model for further investigations.

The studies in this thesis were performed on human eye specimens that were considered normal, having no documented history of acquired or hereditary eye disease. The success in applying in vitro autoradiographic techniques for the first time in the normal adult eye shows promise in the study of numerous other receptors. Furthermore, the localization of different receptors in normal eye specimens will provide the comparative means by which their localization in specimens with specifically well defined ocular pathologies can be examined.

Qualitatively, the results of in vitro autoradiography were consistent for each eye studied with a particular radioligand. The consistent anatomical distributions of muscarinic receptor binding sites in different specimens is in contrast to the considerable variations in density of muscarinic receptor binding sites measured by quantitative autoradiography in different donor eyes (Chapter 3). There are obviously many variables that may be affecting the muscarinic receptor pools in human donor eyes. To what extent the age or agonal state of the patient, post-mortem interval, other drug therapies, and many other complicating factors affect the human eye receptor pools, will be difficult to determine. Many more samples will need to be studied before any conclusions can be drawn about the significance of receptor binding densities. However, this study does suggest the potential for measuring the relative quantities of a

particular receptor in a controlled setting such as in an animal model. In this way, once the normal distributions and densities have been established, further studies may be undertaken to investigate the effect of experimental manipulation on previously defined patterns. Furthermore, a single animal specimen may be used to study the effects of an experimental condition on numerous different receptors.

The broken cell membrane preparation of the in vitro autoradiography technique precludes the selective identification of those muscarinic receptors that were cell membrane bound, and those that may have been internalized. Since the IP3 and PDBu binding site are both intracellular, this point is not relevant to their identification nor quantification. In addition, this technique which utilizes radio-isotope sensitive film instead of emulsion does not allow the visualization of receptors at the cellular level. As they are developed, monoclonal antibodies will be important immunocytochemical tools in the visualization of these receptors at cellular and ultrastructural levels by light and electron microscopy respectively.

The value of this powerful technique relies heavily on the specificity of the pharmacological agent employed to target a particular receptor population, and continues to increase with the growing availability of new receptor subtype - specific drugs. It should be kept in mind however, that the nomenclature used in identifying the various muscarinic receptor subtypes pharmacologically is likely to change as new information will need to be be accomodated.

In cases in which the results of receptor autoradiography with a specific radioligand are compared to the results of in situ hybridization with a

cDNA probe, we have assumed based on the available tools, that it is the transcript from which the protein is translated that is being identified. Interestingly, while both human trabecular meshwork and corneal endothelial structures were identified as having concentrations of m3 transcript, in vitro autoradiography did not detect the M3 receptor sites in either of these structures. When the results of in situ hybridization to localize a mRNA species are in conflict with the localization of the receptor protein, as in this case (Chapter 5), it is possible that the dissociation results from a rapid receptor turnover accompanied by its stable mRNA precursor. Thus the adjuctive use of in situ hybridization as a means with which to localize receptor populations and to support studies by in vitro autoradiography may also give information not provided by in vitro autoradiography.

GENERAL CONCLUSIONS AND IMPLICATIONS

This work provides direct anatomical evidence for the presence of multiple muscarinic receptor subtypes in the human eye. The ocular smooth muscles are the structures most functionally well defined and characterized with respect to cholinergic mechanisms. It has been clearly demonstrated by [^{3}H]QNB binding that ocular smooth muscles contain muscarinic receptors (Chapter 3), and it is well known that they mediate contraction. We have demonstrated M1, M2, and M3 muscarinic receptor

subtype binding sites and m3 transcript in the human ciliary muscle (Chapters 4 and 5). This is consistent with the information from the study of smooth muscles in other organ systems (6, 7) and high affinity profiles for receptor subtype selective antagonists by binding studies, suggesting that smooth muscle has both M2 and M3 receptor subtypes (128, 129) and also expresses m2 and m3 mRNA (130). The role for [^{3}H]pirenzipine labelled M1 sites in the human ciliary muscle is unclear, but they have also been identified pharmacologically in the rabbit iris/ciliary body (94). From the descriptions of muscarinic receptor subtypes in the ciliary muscle, several hypotheses will be presented.

M2 Muscarinic Receptor Subtype In The Longitudinal Ciliary Muscle

The conspicuous localization of [^{3}H]oxotremorine binding sites (M2) in only the longitudinal portion of the human ciliary muscle (Chapter 4) may be functionally very important for several reasons. The presence of a muscarinic receptor subtype in the ciliary muscle that is absent in the iris, may be of value in the design of therapy aimed at the dissociation of accomodation and miosis. In addition, this may be relevant to the mechanisms underlying improved aqueous humour drainage by cholinergic agonist therapy used in glaucoma. It is known that although contraction of the ciliary muscle controls accomodative mechanisms in the eye, it is the specific contraction of the longitudinal muscle of the ciliary muscle that is believed to contribute to outflow facility (Chapter 1). That different

portions of the ciliary muscle may be mediating functionally different roles, namely accomodation versus outflow was first suggested by Barany in 1965 (131). This hypothesis has since been supported by several physiological experiments in which the separation of accomodation from outflow has been demonstrated (132, 133). Recent histochemical studies suggest that the longitudinal ciliary muscle has characteristics of fast twitch muscle fibres, not found in the radial and circular portions of this muscle (134). Chapter 4 presents evidence for an anatomical-pharmacological basis supporting a unique function for the longitudinal ciliary muscle.

Pharmacological agents used to identify muscarinic receptor subtypes do not necessarily identify the same cloned receptor subtypes and [^{3}H]oxotremorine has been shown to bind to heterogeneous M2 sites (95). Whether the [^{3}H]oxotremorine (M2) labelled muscarinic receptor binding sites correspond to the m2 mRNA has not yet been determined. The m2 mRNA is known to be expressed in smooth muscle, and its most likely mechanism of action based on generally accepted literature, is through the inhibition of adenylate cyclase via the Gi protein. Through the stimulation of Gi, M2 muscarinic receptors can decrease levels of cAMP and close potassium channels (135). In addition, a sympathetic innervation has long been postulated to exist along with the well established cholinergic innervation in the ciliary muscle (136, 137), and relaxation of the monkey ciliary muscle has been demonstrated upon application of sympathomimetics (138). In our laboratory, preliminary experiments have shown beta adrenergic receptors in the ciliary muscle. Beta adrenergic

stimulated muscle relaxation occurs through an increase in cyclic AMP, and the opening of potassium channels. By this mechanism, it is possible that the M2 receptors which decrease cAMP and close potassium channels, negate the beta adrenergic induced muscle relaxation (135) maintaining a certain degree of ciliary muscular tone.

The state of tension of the ciliary muscle can significantly influence the resistance to outflow of aqueous fluid, and thus the intraocular pressure. In measuring the effects of ciliary muscle contraction and relaxation on intraocular pressure in young normal subjects, it was found that effortless accomodation in young normal subjects produced a significant reduction in intraocular pressure, whereas pressures during relaxation were higher (27). This is clinically exploited in the treatment of glaucoma through the use of muscarinic agonists to lower intraocular pressure (see Chapter 1). If such a mechanism by which M2 receptors antagonize beta adrenergic relaxation through negative coupling to adenylate cyclase, plays a role in the maintenance of normal ciliary muscle "tension", then it is conceivable that their influence on intraocular pressure is potentially significant. Alternatively, the M2 receptors may mediate some process within the muscle having nothing to do with contraction. In vivo pharmacological studies in an appropriate animal model will be an important step in clarifying the contributions of this muscarinic receptor subtype selectively found in the human longitudinal ciliary muscle portion, specifically in accomodation and in aqueous outflow.

M3 Receptors In The Human Ciliary Muscle

The localization of the M3 receptor subtype over the longitudinal, circular, and radial portions of the ciliary muscle (Chapter 5), in contrast to the selective M2 labelling in the longitudinal fibres, favours the hypothesis that the M3 receptors are at least partially responsible for smooth muscle contraction involved in the accomodative process of the entire ciliary muscle. This is supported by functional and ligand binding studies providing evidence for the M3 receptor subtype as the muscarinic receptor responsible for smooth muscle contraction (139). Studies in only the last few years indicate that M1 and M3 receptors can be coupled to PI turnover via PLC. The distribution of IP3 receptors and PKC over the entire ciliary muscle, in addition to, by quantitative analysis, their mutually abundant concentrations here relative to other ocular structures (Chapter 7), suggests that these molecules may be involved in the contraction process. Presumably, calcium is released from intracellular stores triggered by inositol triphosphate (IP3), which is formed by breakdown of phosphatidyinositol as a consequence to a muscarinic receptor stimulated phospholipase C (60). This is supported by studies of signal transduction pathways leading to the excitation of smooth muscle, demonstrating the existence of a muscarinic receptor mediated pathway involving a G protein stimulated increase in the turnover of phophatidylinositol, with a resulting increase in intracellular calcium. Experiments in human ciliary muscle cell cultures have recently demonstrated an acetylcholine induced intracellular

calcium rise in fura-2-loaded cells (140, 141). In addition, a direct increase in the nonselective conductance of cations, causing a calcium influx and leading to muscle contraction, has also been shown (7, 142). The M3 muscarinic receptor subtype is a prime candidate in mediating PLC activation, IP3 accumulation, and a rise in intracellular calcium, toward contraction. The abundant co-localization of PKC throughout the ciliary muscle, as demonstrated by in vitro autoradiography with [3H]PDBU (Chapter 7), supports the existence of a PLC mediated signal transduction pathway in the human ciliary muscle. The functional viability of this signal transduction pathway in the human ciliary muscle needs to be examined using physiological and biochemical approaches.

Muscarinic Receptor Subtypes In Non-Smooth Muscle Ocular Structures

Because the role of muscarinic receptors in non-smooth muscle ocular structures such as the cornea, trabecular meshwork, ciliary epithelium, and lens are either poorly defined or altogether unknown, it is difficult to hypothesize their functions. However, the localization of M3 muscarinic receptors and their transcripts in the corneal epithelium and anterior lens epithelium is particularly interesting (Chapter 5).

The outermost layer of the corneal epithelium, contains one of the highest concentrations of Ach of any mammalian tissue (19), even exceeding that found in sympathetic ganglion (143). Correspondingly, high activities of choline acetyltransferase (144), the enzyme responsible for its

synthesis, and acetylcholinesterase (145), the enzyme which hydrolyzes and inactivates Ach, are also found in the corneal epithelium. Most, if not all, of the Ach resides within the epithelial cells and not in the nerve endings (146, 147, 148), and although nerve processes have been demonstrated in the human corneal epithelium, they are found infrequently, and constitute a minor portion of the epithelial layer (149).

In trying to define a role for the presence of this neurotrasmitter, the results of searches for a muscarinic receptor component in the epithelial cells have been conflicting. The rabbit corneal epithelium is devoid of both muscarinic and nicotinic receptors by homogenate ligand binding (83). While other studies have also failed to detect epithelial receptors in broken cell preparations (84, 150), muscarinic receptors in epithelial cell cultures have been reported (151, 152). For the first time, direct evidence for a muscarinic receptor in the corneal epithelium, specifically the M3 muscarinic receptor subtype ligand binding site and m3 mRNA has been presented. Although no definitive physiologic role for the cholinergic system has been defined in the cornea, a number of functions have been suggested including the mediation of sensory impulses and pain (153), an adaptive developmental response to air and light (154), the regulation of ionic transport (155), and stromal hydration and corneal transparency (154, 156). In light of these results, the functional significance of M3 receptors in the corneal epithelium deserves further investigation.

Cataractogenesis, is a well known debilitating effect of cholinergic therapy in the eye, particularly anticholinesterase drugs, however at present there is no understanding of the mechanism by which this occurs.

Although the lenticular physiological roles played by Ach are unknown, acetylcholinesterase is present in human lens capsule/epithelium preparations, and echothiophate applied topically to the eye in vivo completely inhibits AChE activity (157). Direct evidence for M3 muscarinic receptors and the m3 transcript in the anterior lens epithelium (Chapter 5), the only mitotically active region of the lens has been shown. Further investigations of the M3 muscarinic receptor subtype may be of value in understanding the pathogenesis of lens opacities induced by cholinergic therapy.

Chapters 4 and 5 show that both M1 and M3 receptor subtypes are localized in the ciliary epithelium. Considering the clinical significance of this structure, the innervation of the ciliary process has been studied much less than expected, and the role of the parasympathetic system in regulating the production of aqueous humour is unclear. By acetylcholinesterase staining, cholinergic innervation has been demonstrated in the ciliary processes (158, 159). Muscarinic agonists have been found to both stimulate and inhibit the formation of aqueous humour (160). Administration of Ach alone has been shown to have no action on the formation rate (161). Recently however, muscarinic receptors in the bovine and primate non-pigmented ciliary epithelium of the ciliary process have been identified and characterized (80). The function of the muscarinic receptors in this tissue is unclear, however their further distinction into M1 and M3 subtypes may be helpful in examining their role.

Direct evidence for the m3 transcript in the human trabecular meshwork (Chapter 5) has also been presented. Whether there is a direct

parasympathetic control over outflow resistance in the trabecular meshwork exists is unknown. Studies have identified the angle as being acetylcholinesterase positive (159), and putative cholinergic nerve terminals in the trabecular meshwork of the cynomolgus monkey have been reported (162), although exactly which structures they innervate in the outflow region remains unclear (163, 164). Functional studies have also provided evidence for muscarinic receptors in the trabecular meshwork (102).

Supporting Evidence for Muscarinic Receptor Subtypes in the Human Eye: Tissue Specific Distributions and Second Messengers

Support for the notion that the muscarinic receptors are functionally diverse comes from studies in both the peripheral and central nervous systems, in which muscarinic receptor subtypes and mRNA species show distinct tissue specificity. The experiments presented in this thesis show that while many structures displayed overlapping distributions of the subtype-specific muscarinic ligands, several highly restricted and different patterns were noted. The presence of a single muscarinic receptor subtype in an ocular structure was demonstrated in both the corneal epithelium and the anterior lens epithelium which localized only the M3 subtype. The detection of a subtype unique to only one structure in the anterior segment was demonstrated by [^{3}H]Oxotremorine binding (M2) noted only in the longitudinal ciliary muscle. Furthermore, only one structure localized all three receptor subtypes in the anterior segment, specifically the M1, M2

and M3 receptor subtypes in the longitudinal ciliary muscle. Thus, evidence has been presented for tissue-specific muscarinic receptor subtypes in the human eye (for summary, see Table 2).

Further support for functional differences between the muscarinic subtypes comes from the predominant association of different muscarinic subtypes with specific biochemical effectors. Knowing that M1 and M3 receptors are coupled to PLC activation, one would expect that the ocular structures found to localize these muscarinic subtypes should also localize IP3 receptors and PKC. The distributions of these molecules were consistent with the combined distributions of the M1 and M3 muscarinic receptor binding sites and the m3 mRNA. Furthermore, quantitative analysis showed an abundance of both IP3 receptor binding sites and PKC in the ciliary muscle, consistent with the high density of muscarinic binding sites in the ciliary muscle (Chapters 4 and 6).

Cholinergic mechanisms are clearly of fundamental importance to many physiological control mechanisms in the eye. The muscarinic receptor subtypes and second messenger molecules that have been localized in the human eye should prove to be a useful adjunct to more directed receptor-related investigations at the biochemical and physiological level, and may provide the first rational step toward understanding the effects and side effects of ocular cholinergic drug therapy. A well-organized Eye Bank for the collection of human eye tissue of clinically well-described patients, taking into account pre-and post-mortem factors will be very important to the future use of in vitro and in situ autoradiographic methods in human

	M1	M2	M3	m3	IP3	PKC
corneal epithelium	-	-	✔	✔	+	+
corneal endothelium	-	-	-	✔	+	+
trabecular meshwork	-	-	-	✔	+	+
longitudinal ciliary muscle	✔	✔	✔	✔	+++	+++
circular and radial ciliary muscle	✔	-	✔	✔	+++	+++
ciliary epithelium	✔	-	✔	✔	+	+
iris	✔	-	✔	✔	+	++
anterior lens epithelium	-	-	✔	✔	+	+
retina	✔	✔	✔	✔	+	+++
retinal pigment epithelium	-	-	✔	✔	+	+
choroid	-	-	✔	✔	+	+

-	absent
✔	present
+	low
++	medium
+++	high

see figure 27

eye specimens. The approaches used in this thesis may be valuable to the future research of numerous other receptors in both normal and pathological human eye specimens, opening the door to new perpectives on ocular physiology, pathophysiology, and medical therapies.

References

1. Snyder, S. H. Drug and neurotransmitter receptors in the brain: Science.**224**: 22-31, 1984.

2. Yamamura, H. I., S. J. Enna and M. J. Kuhar. "Neurotransmitter Receptor Binding." Neurotransmitter Receptor Binding. Yamamura, Enna and Kuhar ed. 1978 Raven Press. New York.

3. Dale, H. H. The action of certain esters and ethers of choline, and their relation to muscarine. Journal of Pharmacology and Experimental Therapeutics. **6**: 147-190, 1914.

4. Giraldo, E., F. Martos and A. Gomez. Characterization of muscarinic receptor subtypes in human tissues. Life Sciences. **43**: 1507-1515, 1988.

5. Watson, M., H. I. Yamamura and W. R. Roeske. [3H]Pirenzipine and (-)-[3H]quinuclidinyl benzilate binding to rat cerebral cortical and cardiac muscarinic cholinergic sites. I. Characterization and regulation of agonist binding to putative muscarinic subtypes. Journal of Pharmacology and Experimental Therapeutics. **237**(2): 411-418, 1986.

6. Eglen, R. M. and R. L. Whiting. Muscarinic receptor subtypes: a critique of the current classification and a proposal for a working nomenclature. Journal of Autonomic Pharmacology. **6**(4): 323-346, 1986.

7. Moummi, C., R. Magous, D. Strosberg and J.-P. Bali. Muscarinic receptors in isolated smooth muscle cells from gastric antrum. Biochemical Pharmacology. **37**: 1363-1369, 1988.

8. Pappano, A. J., K. Matsumoto, T. Tajima, U. Agnarsson and W. Webb. Pertussis toxin-insensitive mechanism for carbachol-induced depolarization and positive inotropic effect in heart muscle.Trends in Pharmacological Science. **9**: 35-39, 1988.

9. McCann, S. M. and L. Krulich. "Role of transmitters in control of anterior pituitary hormone release." Endocrinology. De Groot ed. 1989 W.B. Saunders. Philadelphia.

10. Kuwahara, A., X. Y. Tien, L. J. Wallace and H. J. Cooke. Cholinergic receptors mediating secretion in guinea pig colon. Journal of Pharmacological Experimental Therapeutics. **242**: 600-606, 1987.

11. Louie, D. S. and C. Owyang. Muscarinic receptor subtypes on rat pancreatic acini: secretion and binding studies. American Journal of Physiology. **251**: G275-G279, 1986.

12. Bloom, J. W., M. Halonen and H. I. Yamamura. Characterization of muscarinic cholinergic receptor subtypes in human peripheral lung. Journal of Pharmacological Experimental Therapeutics. **240**: 51-58, 1987.

13. Kovacik, L. Acetylcholine des tissus du segment posterieur de l'oeil des bovides. Archives of Ophthalmology.(Paris) **32**(12): 837-842, 1972.

14. Kovacik, L., E. Mrazova and L. Jezek. Acetylcholine du corps ciliaire des bovins et action cholinergique de la pilocarpine. Archives of Ophthalmology.(Paris) **36**(3): 249-252, 1976.

15. Kovacik, L., L. Jezek and E. Mrazova. Acetylcholine de la choroide des bovins et effet cholinergique de la pilocarpine. Archives of Ophthalmology.(Paris) **36**(5): 425-428, 1976.

16. Kovacik, L., L. Jezek and E. Mrazova. Acetylcholine de l'iris de bovins et effet cholinergique de la pilocarpine. Archives of Ophthalmology (Paris). **36**(4): 341-346, 1976.

17. Kovacik, L., E. Mrazova and L. Jezek. Acetylcholine de la retine des bovins et effet parasympathicomimetique de la pilocarpine. Archives of Ophthalmology (Paris). **36**(8-9): 615-618, 1976.

18. Kovacik, L. Acetylcholine des tissus du segment posterieur de l'oeil des bovides. Archives of Ophthalmology (Paris). **33**(5): 429-437, 1973.

19. Williams, J. D. and J. R. Cooper. Acetylcholine in bovine corneal epithelium. Biochemical Pharmacology.**14**: 1286, 1965.

20. Amsler, M. and F. Verrey. Direct and instantaneous mydriasis and miosis by chemical mediators. Annual Ocular **32**: 936, 1949.

21. Schimek, R. A. The use of intraocular acetylcholine in anterior segment surgery. Annual Instituto Barraquer.**2**: 687, 1961.

22. Barany, E. H. "Relative importance of autonomic nervous tone and structure as determinants of outflow resistance in normal monkey eyes (Cercopithecus ethiops and Macaca irus)." Eye Structure - Second Symposium. Rohen ed. 1965 Schatthauer-Verlag. Stuttgart.

23. Moses, R. A. "Intraocular pressure." Physiology of the Eye: Clinical Application. Adler ed. 1981 The C.V. Mosby Company. Saint Louis.

24. Harris, L. S. Cycloplegic-induced intraocular pressure elevations. Archives of Ophthalmology. **79**: 242-246, 1968.

25. Galin, M. A. Mydriasis provocative test. Archives of Ophthalmology. **66**: 353-355, 1961.

26. Barany, E. H. and R. E. Christensen. Cycloplegia and outflow resistance. Archives of Ophthalmology. **77**: 757-760, 1967.

27. Armaly, M. F. and H. M. Burian. Changes in the tonogram during accommodation. Archives of Ophthalmology. **60**: 60-68, 1965.

28. Armaly, M. F. Studies on intraocular effects of the orbital parasympathetic pathway. 1. Technique and effects on morphology. Archives of Ophthalmology. **61**: 14-29, 1959.

29. Armaly, M. F. Studies on intraocular effects of the orbital parasympathetic pathway. 2. Effects on intraocular pressure. Archives of Ophthalmology. **62**: 117-124, 1959.

30. Kaufman, P. L. and E. Lutjen-Drecoll. Total iridectomy in the primate in vivo: surgical technique and postoperative anatomy. Investigative Ophthalmology. **14**: 766-771, 1975.

31. Kaufman, P. L. and E. H. Barany. Loss of acute pilocarpine effect on outflow facility following surgical disinsertion and retrodisplacement of the ciliary muscle from the scleral spur in the cynomolgus monkey. Investigative Ophthalmology. **15**(10): 793-807, 1976.

32. Kaufman, P. L. and E. H. Barany. Residual pilocarpine effects on outflow facility after ciliary muscle disinsertion in the cynomolgus monkey. Investigative Ophthalmology. **15**: 558-561, 1976.

33. Kaufman, P. L. Aqueous humor dynamics following total iridectomy in the cynomolgus monkey. Investigative Ophthalmology and Visual Science. **18**: 870-875, 1979.

34. Barany, E., C. P. Berriel, N. J. M. Birdsall, A. S. V. Burgen and E. C. Hulme. The binding properties of the muscarinic receptors of the cynomologus monkey ciliary body and the response to the induction of agonist subsensitivity. British Journal of Pharmacology. **77**: 731-739, 1982.

35. Yousufzai, S. Y. K., R. E. Honkanen and A. A. Abdel-Latif. Muscarinic cholinergic induced subsensitivity in rabbit iris-ciliary body. Investigative Ophthalmology and Visual Science. **27**(10): 1630-1638, 1987.

36. Hammer, R. and A. Giachetti. Muscarinic receptor subtype M1 and M2: biochemical and functional characterization. Life Sciences. **31**: 2991, 1982.

37. Hammer, R., C. P. Berrie, N. J. M. Birdsall, A. S. V. Burgen and E. C. Hulme. Pirenzipine distinguishes between different subclasses of muscarinic receptors. Nature. **283**: 90-92, 1980.

38. Mutschler, E., U. Moser, J. Wess and G. Lambrecht. "New approaches to the subclassification of muscarinic receptors." Recent Advances in Receptor Chemistry. Melchiorre and Giannella ed. 1988 Elsevier. Amsterdam.

39. Doods, H. N., M. J. Mathy, D. Davidesko, K. J. van Charldorp, A. de Jonge and P. A. van Zwieten. Selectivity of muscarinic antagonists in radioligand and in vivo experiments for the putative M1, M2, and M3 receptors. Journal of Pharmacology and Experimental Therapeutics. **242**: 257-62, 1987.

40. Peralta, E. G., A. Ashkenazi, J. W. Winslow, J. Ramachandran and D. J. Capon. Differential regulation of PI hydrolysis and adenyl cyclase by muscarinic receptor subtypes. Nature. **334**(4): 434-437, 1988.

41. Bonner, T. I., N. J. Buckley, A. C. Young and M. R. Brann. Identification of a family of muscarinic acetylcholine receptor genes. Science. **237**(4814): 527-532, 1987.

42. Bonner, T. I., A. C. Young, M. R. Brann and N. J. Buckley. Cloning and expression of the human and rat m5 muscarinic acetylcholine receptor genes. Neuron. **1**: 403-410, 1988.

43. Liao, C.-F., A. P. Themmen, R. Joho, C. Barberis, M. Birnbaumer and L. Birnbaumer. Molecular cloning and expression of a fifth muscarinic acetylcholine receptor. Journal of Biological Chemistry. **264**: 7328-7337, 1989.

44. Zuker, C., A. Cowman and G. Rubin. Isolation and structure of a rhodopsin gene from D. melanogaster. Cell. **40**: 851-858, 1985.

45. Dixon, R., B. Kobilka, d. Strader, J. Bonovic, H. Dolhman, T. Frielle, M. Bolanowski, C. Bennett, E. Rands, R. Diehl, R. Mumford, E. Slater, I. Sigal, M. Caron, R. Lefkowitz and C. Strader. Cloning of the gene and cDNA for mammalian B-adrenergic receptor and homology with rhodopsin. Nature. **321**: 75-79, 1986.

46. Nathans, J., D. Thomas and D. Hogness. Molecular genetics of human colour vision: The genes encoding red, blue and green pigments. Science. **232**: 193-200, 1986.

47. Yarden, Y., H. Rodriguez, S. Wong, D. Brandt, D. May, J. Burnier, P. Harkins, E. Chen, J. Ramachandran, A. Ullrich and E. Ross. The avian B-adrenergic receptor: Primary structure and membrane topology. Proceedings of the National Academy of Science USA. **83**: 6795-6799, 1986.

48. Peralta, E. G., A. Ashkenazi, J. W. Winslow, D. H. Smith, J. Ramachandran and D. J. Capon. Distinct primary structures, ligand-binding properties and tissue-specific expression of four human muscarinic acetylcholine receptors. The EMBO Journal. **6**(13): 3923-3929, 1987.

49. Gilman, A. G. G proteins: transducers of receptor-generated signals. Annual Review of Biochemistry. **56**: 615-649, 1987.

50. Kyte, J. and J. Doolittle. A simple method for displaying the hydropathic character of a protein. Journal of Molecular Biology. **57**: 105, 1982.

51. Allard, W. J., I. S. Sigal and R. A. F. Dixon. Sequence of the gene encoding the human M1 muscarinic acetylcholine receptor. Nucleic Acids Research. **15**(24): 10604, 1987.

52. Peralta, E., J. Winslow, G. Peterson, D. Smith, A. Ashkenazi, J. Ramachandran, M. Schimerlik and D. Capon. Primary structure and biochemical properties of an M2 muscarinic receptor. Science. **236**: 600-605, 1987.

53. Nathanson, N. M. Molecular properties of the muscarinic acetylcholine receptor. Annual Review of Neuroscience. **10**: 195-236, 1987.

54. Kubo, T., H. Bujo, I. Akiba, J. Nakai, M. Mishina and S. Numa. Location of a region of the muscarinic acetylcholine receptor involved in selective effector coupling. FEBS letter. **241**: 119-125, 1988.

55. Buckley, N. J., T. I. Bonner, C. M. Buckley and M. R. Brann. Antagonist binding properties of five cloned muscarinic receptors expressed in CHO-k1 cells. Molecular Pharmacology. **35**(4): 469-476, 1989.

56. Northup, J. K., P. C. Sternweis, M. D. Smigel, L. S. Schleifer, E. M. Ross and A. G. Gilman. Purification of the regulatory component of adenylate cyclase. Proceedings of the National Academy of Science, USA. **77**(11): 6516, 1980.

57. Katada, T., J. K. Northup, G. M. Bokoch, M. Ui and A. G. Gilman. The inhibitory guanine nucleotide-binding regulatory component of adenylate cyclase. Journal of Biological Chemistry. **259(6)**: 3578-3585, 1984.

58. Itoh, H., T. Kozasa and S. Nagata. Molecular cloning and sequence determination of cDNA's for alpha subunits of the guanine nucleotide-binding proteins Gs, Gi, and Go from rat brain. Proceedings of the National Academy of Science, USA.**83**: 3776-3780, 1986.

59. Nishizuka, Y. The role of protein kinase C on cell surface signal transduction and tumour promotion. Nature. **308**(5961): 693-698, 1984.

60. Berridge, M. J. and R. F. Irvine. Inositol trisphosphate, a novel second messenger in cellular signal transduction. Nature. **312**: 315, 1984.

61. Ullrich, A., L. Coussens, J. S. Hayflick, T. J. Dull, A. Gray, A. W. Tam, J. Lee, Y. Yarden, T. A. Libermann, J. Schlessinger, J. Downward, E. L. V. Mayes, N. Whittle, M. D. Waterfield and P. H. Seeburg. Human epidermal growth factor receptor cDNA sequence and aberrant expression of the amplified gene in A431 epidermoid carcinoma cells. Nature. **309**: 418-425, 1984.

62. Nishizuka, Y. Studies and perspectives on protein kinase C. Science. **233**: 305-312, 1986.

63. Fukuda, K., T. Kubo, A. Maeda, I. Akiba, H. Bugo, J. Nakai, M. Mishina, H. Higashida, E. Neher, A. Marty and S. Numa. Selective effector coupling of muscarinic acetylcholine receptor subtypes. Trends in Pharmacological Science (Supplement - Subtypes Muscarinic Receptors IV)**10**: 4-10, 1989.

64. Ashkenazi, A., E. G. Peralta, J. W. Winslow, J. Ramachandran and D. J. Capon. Functional diversity of muscarinic receptor subtypes in cellular signal transduction and growth. Trends in Pharmacological Science (Supplement - Subtypes Muscarinic Receptors IV)**10**: 16-22, 1989.

65. Bonner, T. I. The molecular basis of muscarinic receptor diversity. Trends in Neuroscience. **12**: 148-151, 1989.

66. Conklin, B. R., M. R. Brann, N. J. Buckley, A. L. Ma, T. I. Bonner and J. Axelrod. Stimulation of arachnidonic acid release and inhibition of mitogenesis by cloned genes for muscarinic receptor subtypes stably expressed in A9 L cells. Proceedings of the National Academy of Science USA. **85**(22): 8698-8702, 1988.

67. Berridge, M. J. Inositol triphosphate and diacylglycerol: Two interacting second messengers. Annual Review of Biochemistry. **56**: 159-193, 1987.

68. Yoshimasa, T., D. R. Sibley, M. Bouvier, R. J. Lefkowitz and M. G. Caron. Cross-talk between cellular signalling pathways suggested by phorbol-ester-induced adenylate cyclase phosphorylation. Nature. **327**(6117): 67-70, 1987.

69. Salter, R. S., M. H. Krinks, C. B. Klee and E. J. Neer. Calmodulin activates the isolated catalytic unit of brain adenylate cyclase. Journal of Biological Chemistry. **256**(19): 9830-9833, 1981.

70. Zivin, J. A. and D. R. Waud. How to analyse binding, enzyme and uptake data: simplest case, a single phase. Life Science. **30**(17): 1407-22, 1982.

71. Munson, P. J. and D. Robard. LIGAND: A versatile computerized approach for characterization of ligand-binding systems. Analytical Biochemistry. **107**: 220-239, 1980.

72. Lowry, O. H., N. J. Rosebrough, A. L. Farr and R. J. Randall. Protein measurement with the folin phenol reagent. Journal of Biological Chemistry. 265-275, 1951.

73. Young, W. S. I. and M. J. Kuhar. A new method for receptor autoradiography: [3H]opioid receptors in rat brain. Brain Research **179**: 255-270, 1979.

74. Stumpf, W. E. and L. G. Roth. High resolution autoradiography with dry mounted, freeze dried frozen sections. Journal of Histochemical Cytochemistry. **14**: 274, 1966.

75. Palacios, J. M., D. L. Niehoff and M. J. Kuhar. Receptor autoradiography with tritium-sensitive film: Potential for computerized densitometry. Neuroscience Letters. **25**: 101-105, 1981.

76. Bylund, D. B. "Analysis of receptor binding data." Receptor binding techniques. 1980 Society for Neuroscience. Bethesda.

77. Limbird, L. E. "Identification of neurotransmitter receptors using radioligand binding techniques." Chemical and functional assays of receptor binding. B.J. Hoffer ed. 1986 Society for Neuroscience. Washington.

78. Zlock, D., A. Zumbrun, J. Alvarado, M. Drake and J. Polansky. Cholinergic receptors and acetylcholinesterase in ciliary muscle. ARVO abstracts. **53**: 92, 1982.

79. Hutchins, J. B. and J. G. Hollyfield. Autoradiographic identification of muscarinic receptors in human iris smooth muscle. Experimental Eye Research.**38**: 515-521, 1984.

80. Polansky, J. R., D. Zlock, A. Brasier and E. Bloom. Adrenergic and cholinergic receptors in isolated non-pigmented ciliary epithelial cells. Current Eye Research. **4**(4): 517-522, 1985.

81. Zarbin, M. A., J. K. Wamsley, J. M. Palacios and M. J. Kuhar. Autoradiographic localization of high affinity GABA, benzodiazepine, dopaminergic, adrenergic and muscarinic cholinergic receptors in the rat, monkey, and human retina. Brain Research. **374**: 75-92, 1986.

82. Friedman, Z., S. F. Hackett and P. A. Campochiaro. Human retinal pigment epithelial cells possess muscarinic receptors coupled to calcium mobilization. Brain Research.**446**(1): 11-16, 1988.

83. Olsen, J. S. and A. H. Neufeld. The rabbit cornea lacks cholinergic receptors. Investigative Ophthalmology and Visual Science. **18**: 1216, 1979.

84. Fogle, J. A. and A. H. Neufeld. The adrenergic and cholinergic corneal epithelium. Investigative Ophthalmology and Visual Science. **18**: 1212, 1979.

85. Walkenbach, R. J. and G.-S. Ye. Muscarinic receptors and their regulation of cyclic GMP in corneal endothelial cells. Investigative Ophthalmology and Visual Science. **31**(4): 702-707, 1990.

86. Watson, M., H. I. Yamamura and W. R. Roeske. A unique regulatory profile and regional distribution of [3H]pirenzipine binding in the rat provide evidence for distinct M1 and M2 muscarinic receptor subtypes. Life Sciences. **32**: 3001-3011, 1983.

87. Goyal, R. K. and S. Rattan. Neurohumoral, hormonal and drug receptors for the lower esophageal sphincter. Gastroenterology. **74**: 598-619, 1978.

88. Gilbert, R., S. Rattan and R. K. Goyal. Pharmacologic identification, activation and antagonism of two muscarine receptor subtypes in the lower esophageal sphincter. Journal of Pharmacology and Experimental Therapeutics. **230**(2): 284-291, 1984.

89. Birdsall, N. J. M., A. S. V. Burgen and E. C. Hulme. The binding of agonists to brain muscarinic receptors. Molecular Pharmacology. **14**: 723-736, 1978.

90. Spencer Jr., D. G., E. Horvath and J. Traber. Direct autoradiographic determination of M1 and M2 muscarinic acetylcholine receptor distribution in the rat brain: relation to cholinergic nuclei and projections. Brain Research. **380**: 59-68, 1986.

91. Prusky, G. and M. C. Cynader. The distribution of the M1 and M2 muscarinic acetylcholine receptor subtypes in the developing cat visual cortex. Developmental Brain Research.**56**: 1-12, 1990.

92. Vanderheyden, P., G. Ebinger and G. Vauquelin. Characterization of M1 and M2 muscarinic receptors in calf retina membranes. Vision Research. **28**(2): 247-250, 1988.

93. Gremo, F., A. M. Marchisio and A. Vernadakis. Muscarinic receptor subclasses in the chick embryo retina: influence of corticosterone treatment. Journal of Neurochemistry. **45**: 345-351, 1985.

94. Tobin, A. B. and N. N. Osborne. Evidence for the presence of cholinergic muscarinic receptors negatively linked to adenylate cyclase in the iris-ciliary body. Neurochemistry International. **13**(4): 517-523, 1988.

95. Gillard, M., M. Wailbroeck and J. Christophe. Muscarinic receptor heterogeneity in rat central nervous system. II. Brain receptors labeled by [3H]Oxotremorine-M correspond to heterogeneous M2 receptors with very high affinity for agonists. Molecular Pharmacology. **32**: 100-108, 1987.

96. De Jonge, A., H. N. Doods, J. Riezebos and P. A. Van Zwieten. Heterogeneity of muscarinic receptor binding sites in rat brain, submandibular gland and atrium. British Journal of Pharmacology.**89**: 551P, 1986.

97. Hammer, R., E. Monferini, L. DeConti, E. Giraldo, G. B. Schiavi and H. Ladinsky. "Distinct muscarinic receptor subtypes in the heart and in exocrine glands." Cellular and Molecular Basis of Cholinergic Function. W.J. Dowall ed. 1987 Ellis Horwood Series in Biomedicine.

98. Michel, A. D., E. Stefanich and R. L. Whiting. Direct labeling of rat M3-muscarinic receptors by [3H]4-DAMP. European Journal of Pharmacology. **166**: 459-466, 1989.

99. Honkanen, R. E., E. F. Howard and A. A. Abdel-Latif. M3 muscarinic receptor subtype predominates in the bovine iris sphincter smooth muscle and ciliary processes. Investigative Ophthalmology and Visual Science. **31**: 590-593, 1990.

100. Chen, J. and E. WoldeMussie. Similarities of muscarinic receptor subtypes in smooth muscles of cat iris sphincter, ciliary and guinea pig ilium. Federation of American Societies for Experimental Biology. **2**(2): A788, 1988.

101. Woldemussie, E. and B. Feldmann. Characterization of muscarinic receptors in human ciliary and iris smooth muscle cells by ligand binding and biochemical response studies. FASEB Journal.**2**(2): A364, 1988.

102. Woldemussie, E., G. Ruiz and B. Feldmann. Muscarinic receptor subtype involved in signalling mechanisms in cultured human trabecular meshwork cells. Investigative Ophthalmology and Visual Science supplement: **31**:338, 1990.

103. Wax, M. B. and M. Coca-Prados. Receptor-mediated phosphoinositide hydrolysis in human ocular ciliary epithelial cells. Investigative Ophthalmology and Visual Science supplement.**30**: 1675-1679, 1989.

104. Michell, R. H., C. J. Kirk, L. M. Jones and J. A. Creba. The stimulation of inositol lipid metabolism that accompanies calcium mobilization in stimulated cells: defined characteristics and unanswered questions. Philosophical Transactions of the Royal Society of London - Series B: Biological Sciences. **296**: 123-137, 1981.

105. Cutliffe, N. and N. N. Osborne. Serotonergic and cholinergic stimulation of inositol phophate formation in the rabbit retina. Evidence for the presence of 5HT-2 and muscarinic receptors. Brain Research. **421**: 95-104, 1987.

106. Osborne, N. N. Muscarinic stimulation of inositol phosphates formation in rat retina. Developmental changes. Vision Research. **28**: 875-881, 1988.

107. Berridge, M. J. and R. F. Irvine. Inositol phophates and cell signalling. Nature. **341**: 197-205, 1989.

108. Farooqui, A. A., T. Farooqui, A. J. Yates and L. A. Horrocks. Regulation of protein kinase C activity by various lipids. Neurochemical Research. **13**(6): 499-511, 1988.

109. Worley, P. F., J. M. Baraban and S. H. Snyder. Heterogenous location of protein kinase C in rat brain: Autoradiographic analysis of phorbol ester receptor binding. Journal of Neuroscience.**6**: 199-207, 1986.

110. Worley, P. F., J. M. Baraban, E. B. De Souza and S. H. Snyder. Mapping second messenger systems in the brain: Differential localizations of adenylate cyclase and protein kinase C. Proceedings of the National Academy of Science USA. **83**: 4053-4057, 1986.

111. Worley, P. F., J. M. Baraban, J. S. Colvin and S. H. Snyder. Inositol triphosphate receptor localization in brain: variable stoichiometry with protein kinase C. Nature. **325**(8): 159-161, 1987.

112. Akhtar, R. A. and A. A. Abdel-Latif. Specific binding of [3H]inositol 1,4,5-triphosphate to bovine iris sphincter microsomal membranes. Current Eye Research. **9**(4): 387-392, 1990.

113. Nishizuka, Y. The molecular heterogeneity of protein kinase C and its implications for cellular regulation. Nature. **334**(25): 6610-665, 1988.

114. Abdel-Latif, A. A., P. H. Howe and R. A. Akhtar. Muscarinic-receptor induced myo-inositol trisphosphate accumulation, myosin light chain phosphorylation and contraction in the rabbit iris sphincter smooth muscle. Progress in Clinical and Biological Research. **249**(119): 119-32, 1987.

115. Abdel-Latif, A. Polyphosphoinositides, generation of second messengers, myosin light chain phosphorylation and contraction in rabbit iris sphincter smooth muscle. Molecular and Cellular Biochemistry.**82**(1-2): 125-30, 1988.

116. Howe, P. H. and A. A. Abdel-Latif. Purification and characterization of protein kinase C from rabbit iris smooth muscle. Journal of Biochemistry. **255**: 423-429, 1988.

117. Mallorga, P., S. Buisson and M. F. Sugrue. Pharmacological characterization of receptors coupled to phosphoinositide metabolism in the albino rabbit ciliary process. Investigative Ophthalmology and Visual Science supplement.**28**(3): 10, 1987.

118. Mittag, T. W., N. Yoshimura and S. M. Podos. Phorbol ester: Effect on intraocular pressure, adenylate cyclase, and protein kinase in the rabbit eye. Investigative Ophthalmology and Visual Science. **28**(12): 2057-2066, 1987.

119. Gehm, B. D. and D. G. McConnell. Phosphatidylinositol-4,5-biphosphate phospholipase C in bovine rod outer segments. Biochemistry **29**: 5447-5452, 1990.

120. Changya, L., D. V. Gallacher, R. F. Irvine and O. H. Peterson. Inositol 1,3,4,5-tetrakisphosphate and inositol 1,4,5-triphosphate act by different mechanisms when controlling Ca+2 in mouse lacrimal acinar cells. Federation of European Biochemical Societies. **251**(1,2): 43-48, 1989.

121. Ely, J. A., L. Hunyady, A. J. Baukal and K. J. Catt. Inositol 1,3,4,5-tetrakisphosphate stimulates calcium release from bovine adrental microsomes by a mechanism independent of the inositol 1,4,5-trisphosphate receptor. Biochemistry Journal. **268**: 333-338, 1990.

122. Sawada, M., M. Ichinose and T. Maeno. Protein kinase C activators reduce the inositol trisphosphate-induced outward current and the Ca++ activated outward current in identified neurons of Aplysia. Journal of Neuroscience Research. **22**: 158-166, 1989.

123. Fink, L. and L. K. Kaczmarek. Inositol polyphosphates regulate excitability. Trends in Neurosciences. **11**(8): 338-339, 1988.

124. Zatz, M. Translocation of protein kinase C in rat hippocampal slices. Brain Research. **385**: 174-178, 1986.

125. Bennet, C. F., J. M. Balcauk and A. Varrichio et al. Molecular cloning and complete sequence of form-I phosphoinositide-specific phospholipase C. Nature. **334**: 268-270, 1988.

126. Suh, P., S. H. Ryu and K. H. Moon. Cloning and sequencing of multiple forms of phospholipase C. Cell. **54**: 161-169, 1988.

127. Suh, P., S. H. Ryu and K. H. Moon. Inositol phospholipid-specific phospholipase C: complete cDNA and protein sequences and sequence homology to tyrosine kinase-related oncogene products. Proceedings of the National Academy of Science USA. **85**: 5419-5423, 1988.

128. Mitchelson, F. Muscarinic receptor differentiation. Pharmacological Therapeutics. **37**: 357-423, 1988.

129. Ladinsky, H., E. Giraldo and E. Monferini. Muscarinic receptor heterogeneity in smooth muscle: binding and functional studies with AF-DX 116. Trends in Pharmacological Science. **9**: 44-48, 1988.

130. Maeda, A., T. Kubo, M. Mishina and S. Numa. Tissue distribution of mRNA's encoding muscarinic acetylcholine receptor subtypes. FEBS Letter. **239**: 339-342, 1988.

131. Barany, E. H. and J. W. Rohen. Localized contraction and relaxation within the ciliary muscle of the Vervet monkey, Cercopithecus ethiops. Eye Structure. **11**: 287-311, 1965.

132. Erickson-Lamy, K. and A. Schroeder. Dissociation between the effect of aceclidine on outflow facility and accomodation. Experimental Eye Research. **50**: 143-147, 1990.

133. Erickson-Lamy, K. A. and P. L. Kaufman. Cholinergic reinnervation of the ciliary muscle following ciliary ganglionectomy in the cynomolgus monkey. Investigative Ophthalmology and Vision Research supplemental **27**: 288, 1986.

134. Elugel, C., E. Lutjen-Drecoll and E. H. Barany. Morphological and histochemical differences within the ciliary muscle portions. Investigative Ophthalmology and Vision Research supplemental **31**(4): 169, 1990.

135. Sims, S. M., J. J. Singer and J. V. J. Walsh. Antagonistic adrenergic-muscarinic regulation of M current in smooth muscle cells. Science. **239**: 190-193, 1988.

136. Adler, F. H. "Physiology of the eye." 1965 The C.V. Mosby Company. St. Louis.

137. Duke-Elder, W. S. and K. C. Wybar. " The anatomy of the visual system." System of Ophthalmology: The anatomy of the visual system. Duke-Elder and Wybar ed. 1961 Henry Kimpton. London.

138. van Alphen, G. W. H. M., S. L. Robinette and F. J. Macri. Drug effects on ciliary muscle and choroid preparations in vitro. Archives of Ophthalmology. **68**: 81-93, 1962.

139. Collins, S. M. and D. J. Crankshaw. Dissociation of contraction and muscarinic receptor binding to isolated smooth muscle cells from gastric antrum. American Journal of Physiology. **251**: G546-G552, 1986.

140. Stahl, F., A. Lepple-Wienhues, C. Korbmacher, H. Haller and M. Wiederholt. Acetylcholine increases intracellular calcium in single cells of cultured human ciliary muscle cells. Pflugers Archives.**415**: R281, 1990.

141. Korbmacher, C., H. Helbig, M. Coroneo, K. A. Erickson-Lamy, B. Stiemer, E. Tamm, E. Lutjen-Drecoll and M. Wiederholt. Membrane voltage recordings in a cell line derived from human ciliary muscle. Investigative Ophthalmology and Visual Science. **31**(11): 2420-2430, 1990.

142. Christie, M. J. and R. A. North. Control of ion conductances by muscarinic receptors. Trends in Pharmacological Science.**9**: 30-34, 1988.

143. Macintosh, F. C. The distribution of acetylcholine in the peripheral and central nervous system. Journal of Physiology. **99**: 436, 1941.

144. Van Alphen, G. W. H. M. Acetylcholine synthesis in corneal epithelium. Archives of Ophthalmology. **58**: 449, 1957.

145. Peterson, R. A., K.-J. Lee and A. Donn. Acetylcholinesterase in the rabbit cornea. Archives of Ophthalmology.**73**: 370, 1965.

146. Gnadinger, M. C., E. Heimann and R. Markstein. Choline acetyltransferase in corneal epithelium. Experimental Eye Research. **15**: 395, 1973.

147. Stevenson, R. W. and W. S. Wilson. Drug-induced depletion of acetylcholine in the rabbit corneal epithelium. Biochemical Pharmacology. **23**: 3449, 1974.

148. Mindel, J. S. and T. W. Mittag. Variability of choline acetyltransferase in ocular tissues of rabbits, cats, cattle, and humans. Experimental Eye Research. **24**: 25, 1977.

149. Hogan, M. J., J. A. Alvarado and J. E. Weddell. "Histology of human eye." 1971 W.B. Saunders Co. Philadelphia.

150. Mittag, T. W. On the presence of acetylcholine receptors in ocular structures of the rabbit. Investigative Ophthalmology and Visual Science supplemental.**19**: 189, 1979.

151. Colley, A. M. and H. D. Cavanagh. Binding of [3H]dihydroalprenolol and [^{3}H]quinuclidinyl benzilate to intact cells of cultured corneal epithelium. Metabolic, Pediatric and Systemic Ophthalmology. **6**: 75, 1982.

152. Cavanagh, H. D. and A. M. Colley. Cholinergic, adrenergic and PGE1 effects on cyclic nucleotides and growth in cultured corneal epithelium. Metabolic, Pediatric and Systemic Ophthalmology. **6**: 63, 1982.

153. Fitzgerald, G. G. and J. R. Cooper. Acetylcholine as a possible sensory mediator in rabbit corneal epithelium. Biochemical Pharmacology. **20**: 2741, 1971.

154. Howard, R. O., W. S. Wilson and B. J. Dunn. Quantitative determination of choline acetylase, acetylcholine, and acetylcholinesterase in the developing rabbit cornea. Investigative Ophthalmology. **12**: 418, 1973.

155. Stevenson, R. W. and W. S. Wilson. The effect of acetylcholine and eserine on the movement of Na+ across the corneal epithelium. Experimental Eye Research. **21**: 235, 1975.

156. Pesin, S. R. and O. A. Candia. Acetylcholine concentration and its role in ionic transport by the corneal epithelium. Investigative Ophthalmology and Visual Science. **22**: 651, 1982.

157. de Roetth, A. J. Lens opacities in glaucoma patients on phospholine iodide therapy. American Journal of Ophthalmology. **62**: 619-628, 1966.

158. Koelle, G. B. and J. S. Friedenwald. The histochemical localization of cholinesterase in ocular tissues. American Journal of Opthalmology. **33**: 253, 1950.

159. Laties, A. and D. Jacobowitz. A histochemical study of the adrenergic and cholinergic innervation of the anterior segment of the rabbit eye. Investigative Ophthalmology. **3**(6): 592-600, 1964.

160. Macri, F. J. and S. J. Cevario. The dual nature of pilocarpine to stimulate or inhibit the formation of aqueous humour. Investigative Ophthalmology. **13**(8): 617-619, 1974.

161. Macri, F. J. and S. J. Cevario. The induction of aqueous humor formation by the use of Ach + eserine. Investigative Ophthalmology. **12**(12): 911-916, 1973.

162. Nomura, T. and G. K. Smelser. The identification of adrenergic and cholinergic nerve endings in the trabecular meshwork. Investigative Ophthalmology. **13**: 525-532, 1974.

163. Rohen, J. W., R. Futa and E. Lutjen-Drecoll. The fine structure of the cribriform meshwork in normal and glaucomatous eyes as seen in tangential sections. Investigative Ophthalmology and Visual Science. **21**: 574-585, 1981.

164. Lutjen-Drecoll, E., R. Futa and J. W. Rohen. Ultrahistochemical studies on tangential sections of the trabecular meshwork in normal and glaucomatous eyes. Investigative Ophthalmology and Visual Science. **21**: 563-573, 1981.

165. Gabelt, B.T., Kaufman, P.L., and Polansky, J.R. Ciliary muscle muscarinic binding sites, choline acetyltransferase, and acetylcholinesterase in aging rhesus monkeys. Investigative Opthalmology and Visual Science. **31**:2431-2436, 1990.